Holocene Evolution of the Ocracoke Inlet Flood-tide Delta Region, Outer Banks, North Carolina

by

Caroline Faulkner Smith

August, 2015

Directors of Thesis: Drs. Mallinson and Culver

Major Department: Geological Sciences

ABSTRACT

Numerous studies have been conducted along the Outer Banks (OBX) barrier islands of North Carolina to address Holocene climatic change using a combination of lithological, micropaleontological, stratigraphical, and geochronological data to reconstruct Holocene paleoenvironmental reconstructions. These data reveal the importance of inlet formation in the evolution of the modern barrier island chain. However, few studies have been conducted within the Ocracoke Inlet and its associated flood-tide delta (OFTD), which has been proposed to be the most stable inlet along the OBX. Detailed knowledge of the anatomy of the modern, active OFTD is necessary to further elucidate the origin and geologic evolution of Ocracoke Inlet and the OFTD region during the Holocene. Five vibracores, and ca. 100 km of seismic data (boomer and chirp) were collected from the Ocracoke Inlet flood-tide delta (OFTD). Twenty-six age estimates were obtained from the five vibracores (13 AMS radiocarbon age estimates, and 13 Optically Stimulated Luminescence-OSL age estimates). Sediments recovered are all Holocene, except a blue clay interpreted to be Pleistocene that is overlain by a basal peat (core VC1) interpreted to have formed in a freshwater riverine swamp forest (EF VI) environment at ca. 7200 cal yr BP. Sediments are predominantly fine-to-medium grained quartz sand, and contain foraminiferal assemblages composed of 41 taxa dominated by *Elphidium excavatum* and *Ammonia parkinsoniana*. Foraminiferal assemblages were used to define four biofacies. The geographical distribution of bio- and lithofacies is related to salinity and to distance from the inlet. Six environmental facies (EFs) were determined by correlating bio-, litho-, and seismic facies.

Using the six EFs, three transects and five evolutionary time intervals were produced to reconstruct paleoenvironmental changes recorded in the OFTD region during the Holocene. From ca. 7200–6900 cal yr BP rising sea level caused the initial flooding of the paleo-Pamlico Creek drainage system that was characterized by a freshwater swamp environment (EF VI). Between ca. 6900–6600 cal yr BP EF VI transitioned to a high salinity estuarine environment (EF III). EF IV (undetermined, likely mid-to high salinity) estuarine environments characterized the OFTD region ca. 3400 cal yr BP. Flood-tide delta deposits (core VC3B) occurred in the study area ca. 1100 cal yr BP (during the Medieval Climate Anomaly-MCA) and Royal Shoal began to form ca. 500 cal yr BP (during the Little Ice Age-LIA), when Ocracoke Inlet was first documented in historical maps. EF V represents a sand flat/ shoal environment typical of surficial sediments, specifically near Royal Shoal (core VC2B). OFTD deposits (cores VC3B, VC5A, and VC8A) are characterized by two normal marine salinity FTD depositional environments (EF II-low energy and EF I-high energy). The OFTD region probably existed to the south of the study area when estuarine deposits characterized the study area and migrated northwards as sea-level rose.

Holocene Evolution of the Ocracoke Inlet Flood-tide Delta Region, Outer Banks, North Carolina

A Thesis

Presented to

The Faculty of the Department of Geological Sciences

East Carolina University

In Partial Fulfillment

Of the Requirements of the Degree

Master of Science in Geology

by

Caroline Faulkner Smith

August, 2015

Holocene Evolution of the Ocracoke Inlet Flood-tide Delta Region, Outer Banks, North Carolina

by: Caroline Smith

Director of Thesis: _____

Dr. David Mallinson

Co-Director of Thesis: _____

Dr. Stephen Culver

Committee Member: _____

Dr. Eduardo Leorri

External Committee Member: _____

Dr. Regina DeWitt

Chair of Geological Sciences: _____

Dr. Stephen Culver

Dean of Graduate School _____

Dr. Paul Gemperline

DEDICATION

To My Dog, Junior.

ACKNOWLEDGEMENTS

I would first like to thank my family, especially my mother and my dog Junior, for all their support, guidance, encouragement, and patience during this challenging time of my life. I would like to thank my advisors and committee members for all of their guidance and support. A special thanks to Drs. Mallinson, and Culver for reading my thesis numerous times and for being patient with me. Dr. Mallinson, thank you for hiring me as an undergraduate and showing me the ropes regarding geology lab and field work. The initial work I did for you as an undergraduate is what really grabbed my attention and passion to go forward with my coastal geology education. Also, a special thanks to Dr. DeWitt for all your support and patience with me while processing OSL samples at ECU. Thanks to Dr. Terri Woods and Dr. Stephen Harper for their guidance throughout my geology career, I would not be writing this without their care. Of course I have a special thanks to Dr. Stan Riggs and Dorothea Ames for always having an open door policy and listening to me ramble about my thesis ideas, as well as providing me with valuable feedback. Jim Watson and John Woods, thank you both for everything, if I listed the whole shebang this thesis would be twice as long. Thank you to the NSF grant (OCE1130843) and the Department of Geological Sciences at ECU for funding. Finally, thank you to my fellow graduate students for their friendship, assistance, and guidance. I would especially like to thank Mark Akland, David Hawkins, Devon Reed, Jessi Strand, and Nick Zaremba for all of their support and suggestions.

TABLE OF CONTENTS

LIST OF TABLES

LIST OF FIGURES

Holocene Evolution of the Ocracoke Inlet Flood-tide Delta Region, Outer Banks, North Carolina

by

Caroline Faulkner Smith

1.0 Introduction

Climate change has affected eustatic sea level, geomorphological, biological, as well as meteorological conditions along the North American Atlantic Coast (Riggs and Ames, 2003; Horton et al., 2009). The northeast North Carolina barrier islands, also known as the Outer Banks, are located along the passive southeast U.S. continental margin and extend for more than 270 km between the North Carolina/Virginia border and Cape Lookout (Fig.1) (Riggs et al., 1995; Mallinson et al., 2011). Geomorphic evolution of this coastal system is attributed to dynamic processes, including changes in climate, sediment flux, and sea level, all of which affect the environmental components of this complex system (Culver et al., 2006; Smith et al., 2009; Mallinson et al., 2010b; Ames et al., 2011; Peek et al., 2013). The evolution of the coastal area of North Carolina produced a distinct stratigraphic framework, which provides a record of the geologic history and paleoclimate of the area (Riggs et al., 1995; Culver et al., 2007; Peek et al., 2013).

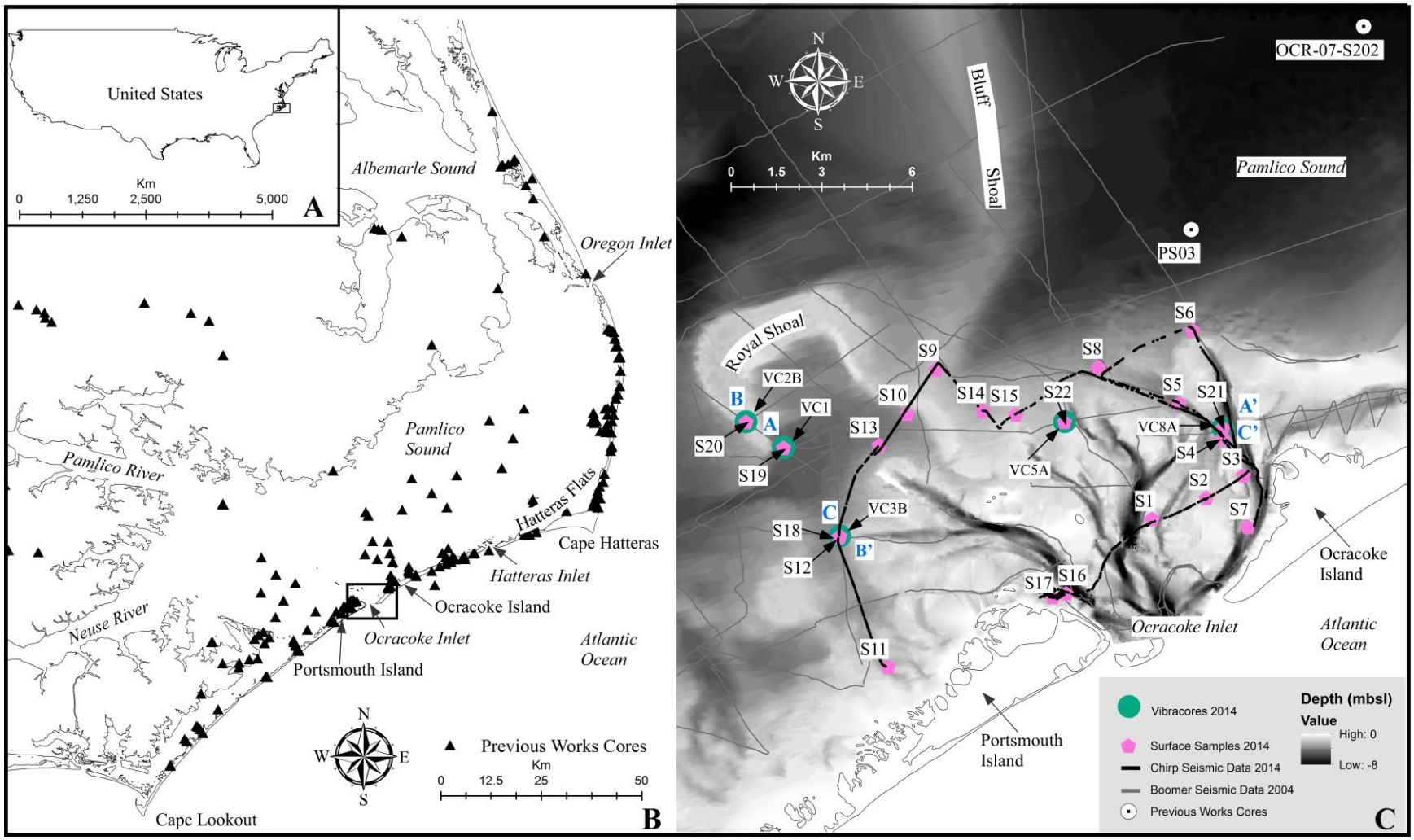

Figure 1. (A) Location of the study area is boxed in on the east coast of North America. **(B)** Location of the Pamlico Sound region with the study area boxed in, as well as vibracores (black triangles) collected for previous studies. **(C)** Location map of the study area, Ocracoke Inlet flood-tide delta, NC, and a map of Pamlico Sound indicating location of seismic lines (chirp-black; boomer-gray), transect lines (blue text), surface samples (pink pentagons), and vibracores (green circles) used in this study. Vibracores used in other studies (circle with a dot) (OCR 07 S202-Metger, 2009, and PS03 (Grand Pre et al., 2011) are located to the northwest of the OFTD region in Pamlico Sound.

Recent multidisciplinary investigations (Fig. 1) have focused on the geologic evolution of the Outer Banks to understand the relationship between the islands' history, geology, geomorphology, inlet formations, and the potential for erosion (Riggs et al., 1995; Riggs and Ames, 2003; Culver et al., 2006; Culver et al., 2007; Horton et al., 2009; Kemp et al., 2009a; Smith et al., 2009; Grand Pre et al., 2011; Mallinson et al., 2010b; Mallinson et al., 2011; Peek et al., 2013). This research project complements previous studies by investigating the Holocene geologic evolution and coastal processes of the Ocracoke Inlet flood-tide delta (OFTD) region. Data from this study aid in understanding how the natural system responds to changes in sea level and climate by utilizing a multi-faceted approach to assess the variability of the processes occurring within the barrier islands and Ocracoke Inlet during the Holocene. The Ocracoke Inlet is considered to be one of the most stable and oldest inlet along the OBX (Mallinson et al., 2011), and may have formed when the barrier islands initially formed ca. 7000 cal yr BP (Culver et al., 2007; Grand Pre et al., 2011) when paleovalleys were flooded. The Pamlico Sound experienced five major time intervals of evolution during the Holocene (Culver et al., 2007; Grand Pre et al., 2011). Two major events, characterized by widespread inlet formation and barrier island erosion and segmentation, highlight sudden environmental changes that occurred ca. 4,000 and 1,100 cal yr BP (Culver et al., 2007; Grand Pre et al., 2011). Of particular interest is how this system responded to climate and sea-level change during the Medieval Climate Anomaly (MCA; ca. 1000 to 700 cal yr BP; Lamb, 1979; Briffa et al., 1990; Keigwin, 1996; Trouet et al., 2009), the Little Ice Age (LIA; ca. 550 to 250 cal yr BP; Lamb, 1979; Briffa et al., 1990; Keigwin, 1996; Cronin et al., 2003), and from 1900 to present.

Records of FTD deposits provide clear evidence for large and small-scale barrier island collapse events. FTDs form as a result of barrier breaching followed by inlet development (Hubbard et al., 1978; Boothroyd, 1978; Moslow and Heron, 1978; Hayes, 1980; Moslow and Tye, 1985). Ocracoke Inlet carries sediment acquired from longshore transport and current erosion to the OFTD region from the Atlantic Ocean via ebb-and flood-tidal current flow. As a result of the location of FTD deposits in the barrier island system, they are more likely to be preserved than the barrier islands themselves during

transgression, as FTDs and overwash deposits represent the dominant mode of landward migration (Hubbard et al., 1978; Hayes, 1980; Moslow and Tye, 1985). These OFTD deposits are essential for determining the mode of landward migration for the barrier islands development in the future.

1.1 Objectives

The main objective of this study is to understand the record of coastal change contained within the sediments of the OFTD region, and the response to geomorphic and environmental changes associated with Holocene climatic events (e.g., the MCA and the LIA). This objective and the following scientific questions were addressed by defining the lithostratigraphic and seismic stratigraphic framework, as well as biofacies occurring in Holocene sediments within the OFTD region.

Specific scientific questions addressed in this study include:

1. When did the OFTD form?
2. Does the stratigraphic framework record regional climatic patterns?
3. Does the OFTD region contain a record of paleoenvironmental changes as indicated by modern and down-core foraminiferal assemblages?
4. Is Royal Shoal part of the current FTD, or is it an antecedent FTD or other shoal?
5. What is the relationship between the OFTD and the Hatteras Flats?

1.2 Geologic Setting and Study Area

Atlantic US East Coast passive margin coastlines have a limited sand supply and are influenced by the underlying geologic framework of older stratigraphic units (Riggs et al., 1995). The morphology, as well as the sediment composition and beach dynamics, of the barrier islands are often determined by the paleo-topographic surface that was inundated during the sea-level rise following the Last Glacial Maximum (LGM, ca. 20 ka) (Riggs et al., 1995; Mallinson et al., 2010a). During the LGM, fluvial systems incised into Quaternary sediments, forming interstream divides and paleovalleys associated with the Roanoke, Neuse, Tar/Pamlico Rivers and Pamlico Creek (Fig. 2) (Riggs and Ames, 2003; Culver et

al., 2007, 2011; Mallinson et al., 2010a, 2010b, 2011; Grand Pre et al., 2011). The Pamlico Sound and OFTD region occupy these drowned river systems (Riggs and Ames, 2003; Culver et al., 2007; Mallinson et al., 2010a; Grand Pre et al., 2011; Peek et al., 2013). Much of the modern geomorphology and hydrodynamics is controlled by the antecedent topography associated with the paleo-drainage system (Mallinson et al., 2005, 2010a). For example, the modern northern barrier islands (larger northern basin of Pamlico Sound) occur on a late Pleistocene interstream divide known as the Hatteras Flats (HFID) which separates Pamlico Creek from the Atlantic Ocean (Fig. 1) (Culver et al., 2007; Mallinson et al., 2010b; Riggs et al., 2011). Likewise, Bluff Shoal (depth ca. 3 m) extends NNW from Ocracoke Inlet which separates Pamlico Sound into two basins (the northern and southern basin). The shallower southern basin southwest of Bluff Shoal is penetrated by shoals projecting from the western shore and the OFTD region (Luettich et al., 2002). The OFTD region is positioned near the paleo-valley of Pamlico Creek with the Pamlico Sound (Fig. 2).

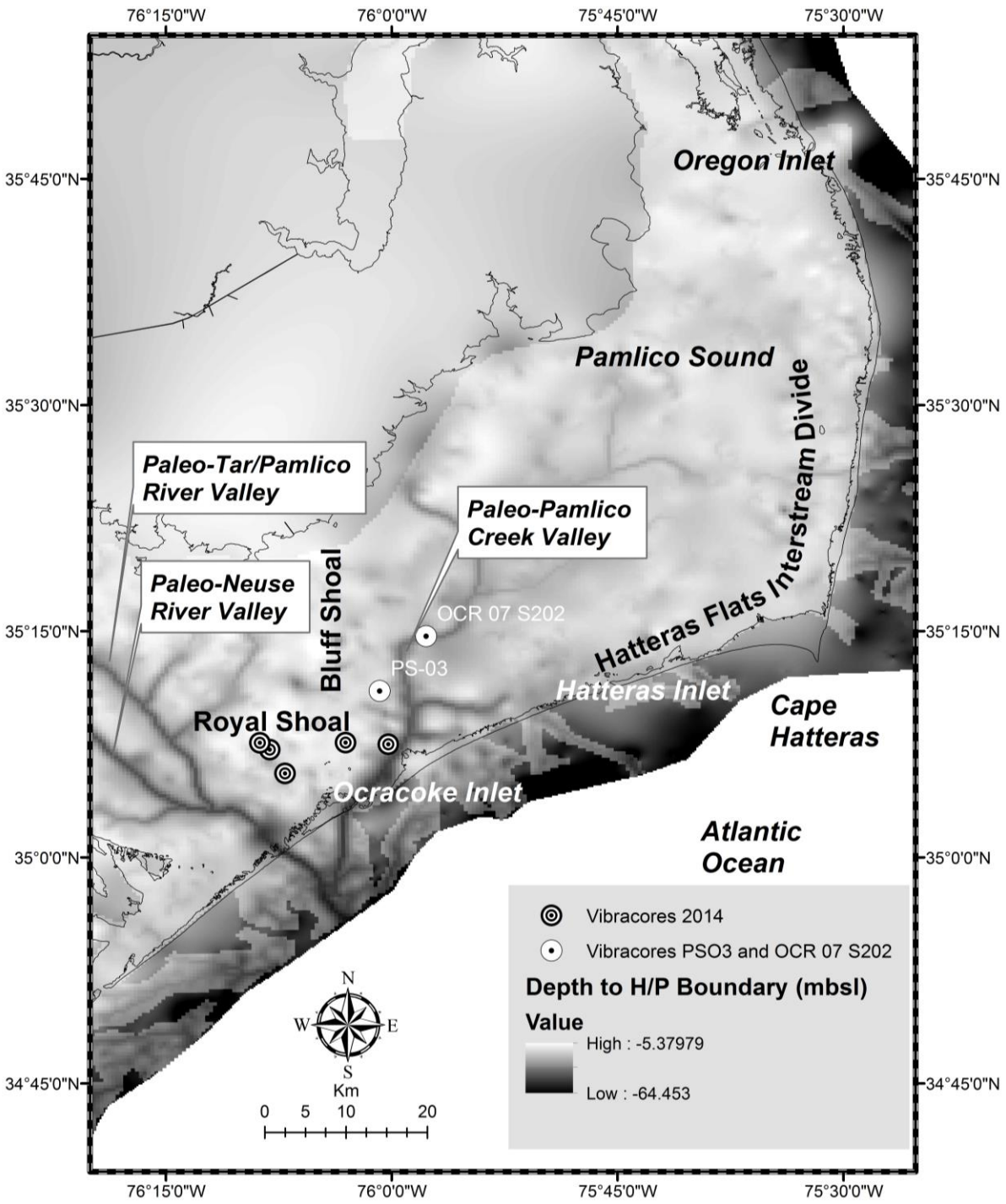

Figure 2. Map of paleo-drainages in the southern Pamlico Sound region of North Carolina during the last glacial maximum based on seismic data. Vibracores in this study (OFTD-14-) are represented as circles. Vibracores used in other studies (PS03- Grand Pre et al., 2011, and OCR 07 S202-Metger, 2009) are represented as a white circle with a dot.

The Pamlico Sound is part of the second largest estuarine complex and is the largest lagoonal estuary in the United States covering ca. 6,600 km^2 (Pietrafesa et al., 1986; Wells and Kim, 1989; Luettich et al., 2002). Hatteras, Portsmouth, and Ocracoke Islands separate the Atlantic Ocean from the eastern side of the Pamlico Sound. Currently, three inlets (Oregon, Hatteras, and Ocracoke Inlets) connect the Pamlico Sound to the Atlantic Ocean, and three low-salinity estuaries (Neuse, Tar, Pamlico; Fig. 1) drain into the sound (Riggs and Ames, 2003; Luettich et al., 2002; Culver et al., 2007; Grand Pre et al., 2011). Within the OFTD region, wave action and tidal currents are the dominant driving forces of circulation and vertical mixing which both determine the thickness of the diffusive bottom boundary layer, the sediment budget of this coastal system, and the position and strength of the salt-water wedge that affects the sediments and fauna (Wells and Kim, 1989; Dalrymple et al., 1992; Luettich et al., 2002). The salinity within the OFTD region decreases to the west with increased distance from the inlets (Marshall, 1951; Wells and Kim, 1989; Luettich et al., 2002; Riggs and Ames, 2003; Abbene et al., 2006), and ranges from 17–38 with an average of 25 based on data from this study.

Historical and geological records show many more inlets existed along the Outer Banks in the past than there are today (Fisher, 1962, Moslow and Tye, 1985; Smith, 2004; Culver et al., 2006; Mallinson et al., 2010b; 2011). The longevity and stability of Ocracoke Inlet (at least 1590 A.D. to present) is likely due to the fact that it occupies the paleo-Pamlico Creek drowned river valley (Riggs and Ames, 2003; Mallinson et al., 2010a; Theiler et al., 2014). Modern tidal inlets may become situated in paleovalleys as a result of tidal currents more easily removing the unconsolidated sediment filling the valley as compared to the more indurated sediments composing the interstream divides. Chemical and physical conditions (e.g., hurricanes, storm impacts, sea-level change, sediment budget, current patterns, and fauna distributions) in the Pamlico Sound and OFTD region fluctuate as inlets migrate, open, and close through time.

New FTDs are formed at laterally migrating inlets as these inlets move along the coast and encounter large back barrier open water areas (Moslow and Tye, 1985; Smith et al., 2009; Mallinson et

al., 2011). Contrastingly, the sand that composes most stable inlets is recirculated within the FTD, such as around the OFTD. The transport of sand on FTDs is controlled by the tidal range, and the strength and direction of the tidal currents. Most FTDs exhibit a characteristic lobate-shaped morphology which generally consists of the following morphological components: (1) flood ramp, (2) flood channel, (3) ebb shield, (4) ebb spits, and (5) spillover lobes (Boothroyd, 1978). Changes in depositional patterns within FTDs produce a multi-lobate morphology (Boothroyd, 1978) that are characterized by sand bars. FTDs are common along microtidal and mesotidal coasts in which there is sufficient open-water area for sand to accumulate landward of a tidal inlet. The OFTD is located along a microtidal coast, and this coastline generally has larger FTDs and smaller ebb tide deltas as compared to mesotidal coastlines (Hayes, 1980). Sedimentation rates and accommodation space control the intertidal exposure and thickness of FTD deposits. Sediments of the OFTD are typically composed of medium-to-fine sand with shell layers that form a sharp gradational contact with muddy estuarine sediments, which is typical for FTD sediments (Hubbard et al., 1978; Boothroyd, 1978; Moslow and Heron, 1978; Hayes, 1980; Moslow and Tye, 1985).

2.0 Previous Works

The geologic evolution of the North Carolina coastal system has been extensively studied by using a combination of litho-, bio-, and seismic-facies analyses, historical inlet activity, and geochronological data (Fig. 1) (Riggs et al., 1992, 1995; Abbene et al., 2006; Pruitt et al., 2010; Foley, 2006; Vance et al., 2006; Mallinson et al., 2005, 2010a, 2010b, 2011; Rosenberger, 2006; Robinson and McBride, 2006, 2008; Culver et al., 2006, 2007, 2008, 2011; Hale, 2008; Metger, 2009; Smith et al., 2009; Grand Pre et al., 2011; Peek et al., 2013; Moran et al., 2015 in review; Zaremba et al., in review). An integration of various methodologies (e.g., litho-, bio-, and seismic- stratigraphical analyses, and dating techniques) has proved useful in understanding the evolution of this complex coastal system and its stratigraphic components.

2.1 Historical Inlet Activity and Climatic Changes

Inlet activity along the barrier islands is recorded in historical documents back to at least 1590 CE when the first European map of the area was created (White-deBry map). Pre-historic (i.e., pre-1590 CE) inlet activity (Smith et al., 2008, 2009; Mallinson et al., 2010b) has been documented using ground penetrating radar data, lithostratigraphic and biofacies analyses (Robinson and McBride, 2003; 2006) coupled with Optically Stimulated Luminescence (OSL) and radiocarbon age analyses of paleo-inlet and FTD facies (Mallinson et al., 2008; Mallinson et al., 2010b; Mallinson et al., 2011). At least two periods of widespread paleo-inlet activity are supported by OSL (Mallinson et al., 2008, 2011) and radiocarbon dating estimates, these periods correspond to the MCA and the LIA. OSL dating of inlet facies corroborates historical data (maps), and supports the interpretation of large scale barrier island segmentation occurring between Avon and Hatteras during the MCA (Culver et al., 2007; Grand Pre et al., 2011; Mallinson et al., 2011; Peek et al., 2013). As many as 20 inlets may have been open during the LIA peak as a product of intensified storms, whereas today there are only three main inlets (Fisher, 1962; Culver et al., 2006; Smith et al., 2009; Mallinson et al., 2011).

Behind the barrier islands from Oregon Inlet to Hatteras Inlet is The Hatteras Flats (Fig. 1), which is a sandy Holocene shoal (ca. 0–3 m depth) that extends up to 8 km into the Pamlico Sound. This shoal is hypothesized to be composed of coalesced relict FTDs which appear to have formed primarily during the MCA (Peek et al., 2013). Beneath the Hatteras Flats, the erosional base of the Holocene is characterized by a marine ravinement or a bay ravinement surface, depending on location, and is at a depth of ca. 9 m below sea level (Culver et al., 2007; Mallinson et al., 2010a). Active shoals and shallow channels characterize this shallow-water platform today (Peek et al., 2013).

Tidal inlet-related sedimentary environments, such as FTD's and spit platforms, represent important components in the barrier island depositional system (Fisher, 1962; Boothroyd, 1978; Hubbard et al., 1979; Sexton, 1981; Moslow and Tye, 1985; Smith et al., 2009). According to Moslow and Tye (1985) inlet processes erase previous stratigraphic records and leave relatively thick units of coarse-grained channel-fill and FTD deposits that represent a brief interval of time (10–10^2 yr). Inlet-fill deposits have high preservation potential, and represent ca. 15% of Holocene sediments beneath Core Sound (Moslow and Heron, 1978) and up to ca. 62% of the record beneath the Outer Banks (Mallinson et al., 2010b). Inlet and FTD processes have proven to be important in maintaining barrier islands width and elevation as they experience sea-level rise (Fisher, 1962; Riggs and Ames, 2003; Mallinson et al., 2010b).

As sea level rises and storms occur more frequently, new inlets could possibly form creating a more segmented barrier islands system (Mallinson et al., 2010b). Segments of the barrier islands could disappear during the next several decades if one or more category 4 or 5 hurricanes directly impacts the area (Riggs et al., 2011). Severe erosion that has mainly occurred during the past century on the oceanic side, as well as on the estuarine side of the barrier islands, indicates that destructive climatic events could possibly be repeated (e.g., MCA and LIA) (Riggs et al., 1995; Culver et al., 2006, 2007; Mann et al., 2009). Barrier island destruction may also be accelerated by anthropogenic interruption of natural sedimentation processes (Culver et al., 2006; Mallinson et al., 2011).

2.2 Shelf, Estuary, and Flood-tide Delta Environments

Holocene paleoenvironmental reconstructions commonly involve the use of foraminifera which complement geochronological, sedimentological, and geophysical data. Benthic foraminifera live in a wide range of shallow marginal marine to open marine environments (Grossman and Benson, 1967; Scott and Medioli, 1977, 1980; Scott et al., 2001; Murray, 1969, 1982, 1991, 2006; Culver and Buzas, 1980, 1981; Woo et al., 1997; Murray, 1991). Thus, their assemblages are very useful in reconstructing paleoenvironments recorded in cored sediments (Scott et al., 2001). Normal marine salinity refers to salinity typical of an inner shelf environment off North Carolina (ca. 34).

Estuarine foraminifera in North Carolina have been well documented. Grossman and Benson (1967) were the first to describe the distribution of foraminifera in Core Sound and in the southern part of Pamlico Sound. A saltwater lagoon biofacies dominated by *Elphidium* species occurred in Core Sound and the southern part of Pamlico Sound. A tidal delta facies identified by the same authors near inlets was similar to the salt water lagoon assemblages except for the presence of *Hanzawaia strattoni* in the former.

Modern shelf foraminiferal assemblages off the coast of North Carolina on the continental shelf were described by Murray (1969), Schnitker (1971), and Workman (1981). Murray (1969) recognized a major assemblage change at Cape Hatteras with higher diversity assemblages occurring south of the Cape.

The shelf off North Carolina was subdivided by foraminiferal assemblages into nearshore, central shelf, and shelf edge environments by Schnitker (1971). *Elphidium clavatum* (= E. excavatum in this study*)* dominated the inner shelf environment. The central shelf assemblage was characterized by *Hanzawaia concentrica* (= H. strattoni in this study), *Reophax atlantica*, *Peneroplis proteus*, *Quinqueloculina seminula*, and *Asterigerina carinata* (Schnitker, 1971). *Lenticulina orbicularis*,

Cibicides pseudoungerianus, and *Amphistegina carinata* were characteristic of the shelf edge assemblage (Schnitker, 1971).

Workman (1981) studied shallow inner shelf (water depth < 21 m) foraminiferal assemblages at two locations in North Carolina: north of Cape Hatteras off Nags Head, and in southern Onslow Bay off Wilmington. Low diversity assemblages dominated by *Elphidium excavatum*, with secondary and rare species such as *Elphidium gunteri*, *Eggerella advena*, *Quinqueloculina seminula*, *Ammonia tepida*, and *Rosalina floridina* characterized the inner shelf off Nags Head. High diversity assemblages characterized Onslow Bay and were dominated by several species of *Quinqueloculina*, and secondary species *Elphidium excavatum*, *Elphidium gunteri*, *Elphidium limatulum*, and *Ammonia beccarii* (= A. parkinsoniana in this study) (Workman, 1981).

The distribution of modern foraminifera in Pamlico Sound was documented by Abbene et al. (2006). Four Biofacies were distinguished by cluster analysis of dead foraminiferal assemblages: marsh biofacies, low salinity estuarine biofacies A, high salinity estuarine biofacies B, and marine biofacies. *Ammonia parkinsoniana* (33%), *Ammotium salsum* (13%), and typical agglutinated marsh species (*Trochammina inflata* and *Haplophragmoides wilberti*) characterized the marsh biofacies. *Ammotium salsum* (83%) dominated low salinity estuarine biofacies A. High salinity biofacies B was dominated by *Elphidium excavatum* (65%), *Ammotium salsum* (15%), and *Ammonia parkinsoniana* (12%). The marine biofacies included samples from Ocracoke and Hatteras Inlets and included many species (not present in the other three biofacies) characteristic of normal marine salinity and open shelf environments (e.g., *Cibicides lobatulus*, *Cibicides refulgens*, *Elphidium subarcticum*, *Quinqueloculina lamarckiana*, and *Quinqueloculina seminula*) (Schnitker, 1971; Workman, 1981). The calcareous species *Elphidium excavatum* (70%) dominated the marine biofacies.

Vance et al. (2006) studied the distribution of modern foraminifera in Albemarle Sound. A cluster analysis of dead foraminiferal assemblages yielded five biofacies. Biofacies A was dominated by

calcareous foraminifera characteristic of nearshore marine and inlet environments (e.g., *Elphidium excavatum*, *Hanzawaia strattoni*, *Ammobaculites crassus*, *Elphidium subarcticum*, and *Ammonia parkinsoniana*). Agglutinated foraminifera (e.g., *Ammobaculites crassus, Ammotium salsum, Ammobaculites subcatenulatus,* and *Miliammina fusca,* respectively) dominated Biofacies B, C, D, and E, characteristic of estuarine shoal (B), estuarine (C), inner estuarine (D), and marsh (E) environments.

In Core Sound, Pruitt et al. (2008) identified three estuarine biofacies representing different salinities. Biofacies A and B were interpreted as high salinity and C as low salinity. Biofacies B, located in the central sound and the western mainland shoreline, was dominated by *Ammonia parkinsoniana* (53%), *Elphidium excavatum* (26%), and contained few *Quinqueloculina* species (<1%). Biofacies A, generally located along the eastern margin of Core Sound, was dominated by *Ammonia parkinsoniana* (24%), *Elphidium mexicanum* (22%), and *Quinqueloculina* species (9%). The agglutinated species *Ammotium salsum* (49%) dominated the low salinity estuarine Biofacies C adjacent to the mainland.

Foraminiferal assemblages of FTDs vary in diversity, abundance, and composition as a result of the dynamic nature of these coastal geomorphic features. Vance et al. (2006) and Smith et al. (2009) found that modern FTDs in the Outer Banks region north of Cape Hatteras have low species richness and abundance. In contrast, Grossman and Benson (1967) and Abbene et al. (2006) found that FTD deposits from Hatteras, Ocracoke, and Drum Inlets (south of Cape Hatteras) have higher species richness (Rosenberger, 2006; Hale, 2008; Metger, 2009). This pattern is not, however, completely related to the major biogeographic boundary at Cape Hatteras (Murray, 1969; Culver and Buzas, 1981) because Old Currituck Inlet in the northern Outer Banks has FTD deposits with high species richness (Robinson and McBride, 2006). Some of the most dominant foraminifera found within FTD deposits behind the Outer Banks are *Elphidium excavatum*, *Quinqueloculina seminula*, *Cibicides lobatulus*, and *Hanzawaia strattoni* (Grossman and Benson, 1967; Robinson and McBride, 2006; Abbene et al., 2006; Vance et al., 2006; Smith et al., 2009; Peek et al., 2013). These species all occur in normal salinity, marine conditions (Murray, 1969; Schnitker, 1971; Workman, 1981; Abbene et al., 2006; Vance et al., 2006; Robinson and

McBride, 2006; Rosenberger, 2006; Hale, 2008; Metger, 2009; Smith et al., 2009, Peek et al., 2013). However as a result of transportation processes, some of these species (e.g., *Elphidium excavatum* and *Quinqueloculina seminula*) also live in brackish environments and others do not (e.g. *Cibicides lobatulus*).

3.0 Materials and Methods

3.1 Field

Using the R/V Stanley Riggs, chirp seismic reflection surveys were conducted during the summer of 2014 to complement boomer data collected in 2004 (Mallinson et al., 2010a). Approximately 50 km of chirp data (Fig.1) were collected using an EdgeTech Chirp 2–16 kHz subbottom profiling system. All data were acquired with a WAAS-enabled Trimble GPS for navigation (Mallinson et al., 2010a). The chirp towfish was towed at ca. 1 m depth and the survey was conducted at ca. 3–4 knots.

Five 7-cm diameter vibracores were collected in the summer of 2014 within the Ocracoke Inlet FTD area (Fig. 1; Table 1; Appendix A). Cores were positioned on seismic lines to facilitate correlation of lithofacies and biofacies to the seismic stratigraphic and geochronologic framework. Latitude, longitude, recovery length, and water depth were recorded for each of the five vibracores (Table 1). Cores were split in half lengthwise, photographed, and visually logged for sediment grain size (Appendices A, B, C), mineralogy, sedimentary structures, fossils, etc. using the general technique of Farrell et al. (2012, 2013).

Table 1. Vibracore (VC) and surface (S) sample metadata listed by increasing distance from the inlet, with vibracores listed first. Mbsl- meters below sea level, and mbsf-meters below seafloor.

Sample ID	Latitude	Longitude	mbsf	mbsl	Distance from the Inlet (m)	Salinity
OFTD-14-VC-5A	35.1268	76.0511	1.14	2.64	6878	24
OFTD-14-VC-8A	35.1250	76.0039	2.21	5.21	7625	25
OFTD-14-VC-3B	35.0928	76.1181	4.10	7.40	9731	23
OFTD-14-VC-1	35.1191	76.1349	5.64	9.64	12354	23
OFTD-14-VC-2B	35.1268	76.1461	1.72	2.92	13953	24
OC-14-S16	35.0757	76.0506		3.23	3360	35
OC-14-S17	35.0746	76.0546		2.29	3496	38
OC-14-S1	35.0979	76.0250		1.22	3812	28
OC-14-S7	35.0956	75.9964		1.83	4009	35
OC-14-S2	35.1042	76.0089		1.16	4528	27
OC-14-S3	35.1109	75.9978		1.83	5728	27
OC-14-S4	35.1219	76.0040		1.83	6559	27
OC-14-S21	35.1250	76.0039		3.00	6878	25
OC-14-S5	35.1323	76.0170		4.88	7467	24
OC-14-S22	35.1268	76.0511		1.50	7625	24
OC-14-S11	35.0539	76.1037		1.58	7827	20
OC-14-S15	35.1290	76.0656		1.77	8420	20
OC-14-S8	35.1431	76.0410		2.47	8985	24
OC-14-S14	35.1301	76.0754		2.13	9007	18
OC-14-S12	35.0925	76.1184		2.74	9632	17
OC-14-S18	35.0928	76.1181		3.30	9731	23
OC-14-S6	35.1541	76.0129		2.74	9990	23
OC-14-S13	35.1198	76.1064		2.96	10171	17
OC-14-S10	35.1292	76.0981		1.62	10182	21
OC-14-S9	35.1424	76.0894		1.71	10899	23
OC-14-S19	35.1191	76.1349		4.00	12354	23
OC-14-S20	35.1268	76.1461		1.20	13953	24

A Wildco grab sampler was used to collect 17 surface samples for foraminiferal studies along the chirp data transects (Fig. 1; Appendices E, F). Approximately 60 ml of the top 1 cm of sediment was placed into 100 ml plastic bottles. At the same sites where five vibracores were taken, five additional (Fig. 1) 60 ml surface samples were collected by divers by scooping the top 1 cm of sediment into 100 ml plastic bottles. Immediately after sampling, a marble chip (for a buffer) and 70% alcohol with rose Bengal were added. Rose Bengal stains cytoplasm pink in live foraminifera which allows for discrimination of live and dead specimens (Walton, 1955). Latitude, longitude, salinity, and water depth were recorded for each sample (Table 1).

3.2 Foraminiferal Sample Processing

Samples were washed over a nest of 710 micron and 63 micron sieves to separate coarse material, sand, and mud. The 63 to 710 micron and > 710 micron size fractions were weighed after drying at 40°C. The 63 to 710 micron fraction was floated using sodium polytungstate to separate the foraminifera from the sand grains (Munsterman and Kerstholt, 1996). "Floats" and "sinks" were dried at 40°C and weighed. For surface samples, known fractions of the float portion were spread evenly onto a 45 square gridded picking tray and ca. 100 foraminifera were picked from each sample and placed upon micropaleontological slides.

Thirty-three down-core samples were dried, weighed, and, where necessary, disaggregated by soaking overnight in water with ca. 1 mg of sodium hexametaphosphate and 0.2 mg caustic soda (Appendices G, H). Core samples were wet sieved, dried, weighed, floated when necessary, and dried again. Floats were split into manageable aliquots using a microsplitter. Approximately one hundred specimens were picked (Cronin et al., 2000; Karlson et al., 2000; Grand Pre et al., 2011) from a known fraction of the float using a random numbers table when necessary to select squares on the picking tray.

Forty-one species were identified through comparison with illustrations in the published literature on modern benthic foraminifera of the U.S. Atlantic Coast and identifications were confirmed through comparison type and comparative specimens lodged in the Cushman Collection, Smithsonian Institution, Washington, D.C (Appendix D). Foraminiferal biofacies of surface and down-core samples were defined via Q-mode cluster analysis (Mello and Buzas, 1968; Abbene et al., 2006). The analysis included benthic species (28) except for those (13) represented by only one specimen in the entire study (Appendices I, J), thus planktonic and indeterminate rotaliid species were excluded. Ten of 55 samples with ≤ 15 specimens were excluded from the analysis. Percent abundance data were transformed using the following equation: $2\arcsin\sqrt{p}$ (p = abundance) (Appendices H, F) (Buzas, 1979). The transformed data were run through a cluster analysis (using Wards Linkage at Euclidian distances) in SYSTAT 12.

3.3 Sedimentological Sample Processing

Vibracores were sampled at lithologic contacts, and then grain size sample bags were placed in a 40°C oven until dry (Appendix A). To determine % gravel, % sand, and % mud, samples were weighed and then wet sieved using a 63 micron sieve to separate the mud from the sand and gravel (Appendix C). Sieved samples were placed in weigh boats, dried again in a 40°C oven, and weighed. The > 63 micron fraction was sieved using Rotap machines, and grain size statistics were calculated using the GRADISTAT Excel Spreadsheet (Appendix B) (Blott and Pye, 2001). Sedimentological data were used to define lithofacies based on the method of Farrell et al. (2012, 2013).

3.4 Geophysical Data Processing

Seismic data (SEG-Y data) were processed, integrated, and digitized using the Seismic Micro-Technology Kingdom Suite Software (v. 8.8). Both types of surveys (chirp and boomer) were analyzed to define the regional subsurface characteristics and the stratigraphic framework (Mallinson et al., 2010a; Peek et al., 2013; Zaremba et al., in review).

3.5 Optically Stimulated Luminescence Sample Processing

3.5.1 Sampling and Laboratory Procedures

Thirteen samples for OSL dating were derived under dark room conditions from the sediments within the five vibracores after they were split. Two types of samples were obtained to measure OSL ages: (1) Gamma Spectrometry: used to measure the radiation dose rate that the sample was exposed to, and (2) OSL: used to measure the equivalent Dose (D_e). The sampling process included the removal of the top ½ cm (ca. 100 g) which was used for gamma spectrometry to calculate dose rates. Sampling for D_e determination included scooping ca. 100 g of sandy sediments (ca. 5 –7 cm depth interval) from aluminum vibracore halves, bagging it, and sealing it in an opaque bag. OSL samples were derived from the center of the cores to avoid contamination of potential light exposed material, or disturbed sediment stuck to the wall of the aluminum cores. Remaining sediment, and some sediments below and above (ca. 30 cm) the OSL sample were also sampled for gamma spectrometry.

All OSL samples were processed and analyzed under red light conditions. All thirteen samples were wet sieved to separate sand grains, and the >125 micron fraction was used for processing, except for VC2B samples which used the >150 micron fraction. Chemical treatments began with dissolving carbonate material using two different concentration levels of HCL: (1) 3.7% HCL, and (2) 10% HCL. Organic material was removed by using 27% H_2O_2. The quartz grains were then etched by applying 48%–51% HF for 40 minutes. Samples were etched with HF to remove feldspars, and the outer rinds of quartz grains to assure they were not damaged by alpha particles. To ensure all carbonate material was removed, as well as fluorite precipitates that might have formed during HF etching, samples were treated with 3.7% HCl again. After each chemical treatment, all samples were rinsed with distilled water three times. Each sample was then floated using lithium polytungstate to separate the quartz fractions from heavy (magnetite, titanium, etc.) and light minerals (feldspars). A density of 2.75 g/ml was used to separate the heavy minerals, and a density of 2.62 g/ml was used to separate light materials from quartz grains.

3.5.2 Evaluating the Dose Rate

The concentrations of ^{40}K, ^{238}U, and ^{232}Th used for dose rate determination were determined by gamma spectrometry using a high resolution Canberra germanium detector. Concentrations were determined by comparing gamma emission intensities of the samples with those of standard samples (e.g., IAEA-300). Gamma and beta dose-rates were calculated using the conversion factors by Adamiec and Aitken (1998). Cosmic radiation contributions were calculated based on the geographic position of the core as well as individual sample depths (Prescott and Stephan, 1982; Barbouti and Rastin, 1983). A gamma sample was acquired for every OSL sample that was derived from a different lithology in each core, therefore, a total of 16 gamma samples were used for the 13 OSL samples in this study. Two samples, (VC1 0.30–0.37 mbsf, 4.30–4.37 mbsl; and VC3B 2.94–2.99 mbsf, 6.24–6.29 mbsl), were derived from a generally sand/mud lithological contact. Both of these samples required three different gamma spectrometry measurements (six total for the two samples) from the three different lithologies present (the position of the OSL sample itself, and the layers above and below the OSL sample) to obtain the accurate dose rate associated with gamma radiation emitted from the varying sediments.

3.5.3 Evaluating the Equivalent Dose (De)

A Risø TL/OSL DA-20 reader was used to obtain D_e measurements using the single-aliquot regenerative-dose (SAR) protocol on a minimum of 16 aliquots per sample (Murray and Wintle, 2000, 2003; Wintle and Murray, 2006). OSL was stimulated at 125°C (60 s). A Sr^{90}/Y^{90} source for beta irradiation and blue LEDs (470 nm at 125°C for 60 s) for OSL stimulation were used. OSL emission was filtered through a U340 filter. The dating procedure included four measurement sequences using the Risø TL/OSL DA-20 reader for each OSL sample: (1) dose test, (2) plateau test, (3) dose recovery test, and (4) dating measurement. The dose test is used to get a rough estimate for the laboratory D_e compared to the natural D_e by giving known amounts of increased radiation. The plateau test is performed to get a rough estimate of the best preheat temperature for each sample, as well as to check the signal stability over a temperature range (180–280 °C). Dose recovery tests were performed to further test the applicability of

the plateau test to confirm the preheat temperature for each sample, which supported the validity of the chosen protocol. Dose recovery tests include bleaching the sample, giving the sample a known (laboratory produced) dose, and measuring the dose with a full SAR procedure at two to three preheat temperatures. Plateau test results yielded preheat and cutheat temperatures for samples, and in most samples these were 240 °C (10 s) and 160 °C (0 s), respectively (depending on the sample and its depositional environmental characteristics). OSL was stimulated at 125°C (60 s). After each cycle a high temperature OSL measurement was performed at a temperature 20 °C above the preheat temperature. During the dating test, the natural signal is measured, and then laboratory doses are added to construct a luminescence signal vs. dose growth curve. The natural signal is then compared to this regenerated growth curve to calculate the D_e for each individual aliquot. Aliquots were rejected following the criteria suggested by Wintle and Murray (2006), i.e. if (1) recycling ratios differed more than 10% from 1 (ratios between 0.9 and 1.1 are ideal), (2) recuperation exceeded 5% of natural signals or was significantly above background, (3) dose recovery errors exceeded 10%, and (4) if signal depletion by IR stimulation was larger than 10%.

When the dating sequence measurement results yielded ≥ 16 aliquots that did not fail the protocol, the final D_e was calculated following the procedure suggested by Galbraith et al. (1999) who apply the common age model to D_e distributions to estimate the mean D_e and the associated error, along with overdispersion for each sample. Thus the D_e of each sample is represented by the weighted average of many aliquots per sample (≥ 16). OSL ages were calculated by dividing the D_e by the dose rate and are reported in quartz years as well as cal yr BP.

Measurements were run on surficial (modern) samples (ca. 0–0.2 mbsf) to ensure the D_e was zero, or close to zero to detect for incomplete bleaching, mixing of grains, and to test the methodology. To detect and account for incomplete bleaching and mixing of grains, we used the decision process suggested by Murray and Wintle (2000, 2003) and Wintle and Murray (2006). For this process we calculated the overdispersion value (as %) using the standard deviation and weighted mean derived from all aliquots

used for calculation of the D_e. The overdispersion value expresses variations caused by luminescence properties (e.g. recuperation) as well as differences between natural beta dose rates to individual grains (Nathan et al., 2003). Older samples fell within an estimated overdispersion value of < 20%. Overdispersion values of the modern samples were disregarded (even though they were high) as the D_e values were reliable when considering the OFTD depositional environment, which is further supported by ^{14}C ages and sedimentation rates. According to Rhodes (2011), a high overdispersion value (>10%) may indicate incomplete bleaching or grain mixing, however, no particular threshold value exists as a result of variations in grain sensitivity distributions.

3.6 Radiocarbon Sample Processing

Samples for radiocarbon (^{14}C) age estimates were collected from two vibracores, VC1 and VC3B. Thirteen radiocarbon ages were determined using Accelerator Mass Spectrometry (AMS) analysis of mollusc shells (mostly articulated) and peat. Samples were analyzed at BETA Analytic and National Ocean Sciences Accelerator Mass Spectrometry Facility (NOSAMS), and calibrated using CALIB 7.0 software (Stuiver and Reimer, 1988). Shell samples were calibrated using the marine-calibration curve (MARINE13) (Stuiver and Reimer, 1998) and Delta-R correction of 102 ± 70 years to correct for the ocean reservoir effect (Thomas, 2008). The peat sample was calibrated using the terrestrial-calibration (INTCAL13) database (Stuiver and Reimer, 1998).

4.0 Results

4.1 Geochronologic Data

Four radiocarbon (^{14}C) dates were received from Beta Analytic and nine additional ^{14}C dates were received from the National Ocean Sciences Accelerator Mass Spectrometry Facility (NOSAMS) (Table 3). The thirteen ^{14}C dates were obtained from two out of five cores, VC1 and VC3 (Table 2). All ^{14}C sampling material consisted of bivalve shells, except for one peat sample in core VC1 (Table 2). The oldest age measured was 7160–6940 cal yr BP from the peat at the base of VC1. Ages decrease up-section in all cores, except for a reversal in VC3B at 1124–777 cal yr BP, likely indicating upward reworking of older material. All ^{14}C and OSL ages agree except for the one age reversal obtained from a ^{14}C age date (Tables 2, 3; Appendix A).

Table 2. Accelerated Mass Spectrometry (AMS) radiocarbon (^{14}C) age estimates for thirteen samples from the OFTD, with the associated calibration measurements. Mbsl- meters below sea level, and mbsf-meters below seafloor.

Core ID	mbsl	mbsf	Material	$\delta^{13}C$	$\Delta^{14}C$	Conventional ^{14}C age yr BP	2 σ Cal. yr BP	Laboratory	Laboratory Code
OFTD-14-VC1	4.57	0.57	*Tonna galea*	*	*	435 +/- 20	n/a	NOSAMS	125381
OFTD-14-VC1	5.28	1.28	*Spisula solidissima*	*	*	815 +/- 20	500—228	NOSAMS	125382
OFTD-14-VC1	5.52	1.52	*Spisula solidissima*	*	*	1180 +/- 15	766—520	NOSAMS	125383
OFTD-14-VC1	6.44	2.44	*Tellina sybaritica*	*	*	1410 +/- 15	914—783	NOSAMS	125384
OFTD-14-VC1	8.43	4.43	*Mulina lateralis*	*	*	3790 +/- 15	3810—3430	NOSAMS	125385
OFTD-14-VC1	8.5	4.50	*Crassostrea virginica*	-2.9	-408.6 +/- 2.2	4220 +/- 30	4400—3960	BETA	389331
OFTD-14-VC1	9.43	5.43	*Mactra fragilis*	-5.1	-532.6 +/- 1.7	6110 +/- 30	6610—6275	BETA	389332
OFTD-14-VC1	9.62	5.62	Woody peat	-26.7	-533.8 +/- 1.7	6130 +/- 30	7160—6940	BETA	389333
OFTD-14-VC3B	4.48	1.18	*Tellina nuculoides*	*	*	800 +/- 15	489—223	NOSAMS	125386
OFTD-14-VC3B	4.90	1.60	*Divaricella quadrisulcata*	*	*	1030 +/- 20	651—428	NOSAMS	125387
OFTD-14-VC3B	5.76	2.46	*Mulina lateralis*	*	*	1500 +/- 20	1124—777	NOSAMS	125388
OFTD-14-VC3B	6.63	3.33	Barnacles	*	*	1360 +/- 15	932—665	NOSAMS	125389
OFTD-14-VC3B	6.70	3.40	*Anomia simplex*	0.3	-161.0 +/- 3.1	1410 +/- 30	995—690	BETA	389334

* $\delta^{13}C$ and $\Delta^{14}C$ values were not provided by NOSAMS

* The NOSAM results were corrected for isotopic fractionation using unreported $\delta^{13}C$ values measured on the accelerator.

* The stable isotope $\delta^{13}C$ results reported should not be used to post-correct.

Table 3. OSL age estimates and associated data derived from the five vibracores. Mbsl- meters below sea level, and mbsf-meters below seafloor.

Core ID	mbsl	mbsf	Total Dose Rate (mGy/a)	Equivalent Dose (Gy)	Quartz Age (a)	Age (a) (cal yr BP)	Gamma dose rate (mGy/year)	Beta dose rate (mGy/year)	Cosmic dose rate (mGy/year)	Water Content (%)	Overdispersion Value (%)
OFTD-14-VC-1	4.0–4.05	0.0–0.05	1.1436 +/- 0.0748	0.0120 +/ -0.0013	11 +/ - 1	-53	0.314 +/- 0.028	0.804 +/- 0.035	0.1564 +/- 0.011	31.441	73.868
OFTD-14-VC-1 (OSL)	4.30–4.37	0.3–0.37	1.4361 +/- 0.0586	0.0753 +/- 0.0027	52 +/- 3	-12	0.474 +/- 0.035	0.816 +/- 0.047	0.1530 +/- 0.010	72.000	11.994
above OSL	4.30–4.37	0.3–0.37					0.314 +/- 0.028				
below OSL	4.30–4.37	0.3–0.37					0.433 +/- 0.024				
OFTD-14-VC-2B	1.34–1.40	0.14–0.20	0.6580 +/- 0.0222	0.0197 +/- 0.0010	30 +/- 2	-34	0.167 +/- 0.008	0.326 +/- 0.015	0.187 +/- 0.013	18.113	54.223
OFTD-14-VC-2B	2.01–2.06	0.81–0.86	0.5546 +/- 0.1154	0.2415 +/- 0.0079	435 +/- 21	371	0.114 +/- 0.005	0.262 +/- 0.014	0.179 +/- 0.012	16.867	16.525
OFTD-14-VC-2B	2.70–2.75	1.50–1.55	0.6243 +/- 0.1394	0.2992 +/- 0.0099	479 +/- 26	415	0.137 +/- 0.010	0.317 +/- 0.023	0.171 +/- 0.012	16.000	9.583
OFTD-14-VC-3B	3.30–3.35	0.0–0.05	1.6770 +/- 0.1244	0.0292 +/-0.0012	17 +/-1	-47	0.622 +/- 0.007	1.155 +/- 0.121	0.164 +/- 0.012	24.762	38.103
OFTD-14-VC-3B	4.27-4.32	0.97–1.02	1.5393 +/-0.4758	0.5968 +/- 0.0189	388 +/- 27	324	0.468 +/- 0.042	0.918 +/- 0.082	0.153 +/- 0.011	23.333	8.836
OFTD-14-VC-3B (OSL)	6.24–6.29	2.94–2.99	1.803 +/- 0.1701	1.8833 +/- 0.0601	1044 +/- 104	980	0.581 +/- 0.049	1.056 +/- 0.076	0.134 +/- 0.009	27.193	5.556
above OSL	6.24–6.29	2.94–2.99					0.465 +/- 0.038				
below OSL	6.24–6.29	2.94–2.99					0.676 +/- 0.035				
OFTD-14-VC-5A	1.50–1.60	0.0–0.10	1.2472 +/- 0.0353	0.0498 +/- 0.0019	40 +/- 2	-24	0.219 +/- 0.008	0.511 +/- 0.024	0.185 +/- 0.013	22.115	64.631
OFTD-14-VC-5A	2.45–2.55	0.95–1.05	0.7938 +/- 0.1869	0.2592 +/- 0.0083	327 +/- 15	263	0.185 +/- 0.008	0.435 +/- 0.020	0.173 +/- 0.012	20.879	13.890
OFTD-14-VC-8A	3.00–3.05	0.0–0.05	1.2038 +/- 0.0248	0.0306 +/- 0.0012	25 +/- 1	-39	0.231 +/- 0.007	0.529 +/- 0.019	0.156 +/- 0.011	22.667	88.485
OFTD-14-VC-8A	4.31–4.36	1.31–1.36	0.9206 +/- 0.2447	0.4072 +/- 0.0132	442 +/- 26	378	0.241 +/- 2.019	0.527 +/- 0.041	0.153 +/- 0.011	18.269	19.995
OFTD-14-VC-8A	4.97-5.02	1.97–2.02	0.6883 +/- 0.1667	0.3557 +/- 0.0113	517 +/- 23	453	0.166 +/- 0.007	0.377 +/- 0.017	0.146 +/- 0.010	20.000	9.521

*Averages of three gamma measurements were used. A total of 16 gamma samples and 13 OSL samples were processed and analyzed in this study.

4.1.1 Reliability of OSL Data

Thirteen OSL samples were obtained from the five OFTD cores: VC1, VC2B, VC3B, VC5A, and VC8A (Table 3; Appendix A). All ages are reported in cal yr BP and quartz years (Table 3). Sediments that were dated generally consisted of fine-to-medium grained quartz sand, with a few samples collected from muddy sand or sandy mud (e.g., VC1 0.30–0.37 mbsf, 4.30–4.37 mbsl; and VC3B 2.94–2.99 mbsf, 6.24–6.29 mbsl). The bleaching of OSL samples derived from within the dynamic environment of the OFTD region, as well as other areas with similar depositional environments, is an area of increasing research within the OSL dating community (Murray and Wintle 2000, 2003; Wintle and Murray, 2006; Lian and Roberts., 2006; Rodnight et al., 2006). Results presented here suggest the OSL dating method is reliable and works well within dynamic modern (and paleo) FTD deposits of the OFTD region.

It has been speculated by previous works that modern ages (recently deposited) can be significantly overestimated as a result of (1) partial bleaching prior to final deposition and (2) post-depositional mixing of grains (Murray and Wintle 2000, 2003; Wintle and Murray, 2006). More recent studies have focused on the applicability of using the OSL method to date sediments of dynamic environments and have proved this method to be useful (Olley et al., 1998; Rodnight et al., 2006; Madsen and Murray, 2009; Mallinson et al., 2010b). This study concludes that the modern samples derived from the OFTD region have D_e values that are near zero (Fig. 3). However, the overdispersion values for the OFTD samples range from ca. 5.5% to 88.5% (Fig. 3; Table 3) suggesting reworking and mixing of sediments (likely during high energy events). Nevertheless, near surface samples (upper ca. 10 cm of the sedimentary section) yielded young ages ($\leq$ 52 quartz years ($\pm$ 3)) and the deeper samples are consistent with underlying ^{14}C ages (Tables 2, 3; Appendix A). This further demonstrates that OSL is an appropriate method to date sediments at varying depths within sedimentary sections such as within active FTD depositional environments.

Overdispersion values for samples derived from depths greater than ca. 0.37 mbsf were < 20%, which represent the older samples (Fig. 3). This overdispersion value represents a common spread in

well-bleached samples analyzed using the SAR protocol (Murray and Wintle 2000, 2003; Wintle and Murray, 2006; Madsen and Murray, 2009). Even though some deeper samples exhibited a D_e distribution pattern that was more scattered and positively skewed than shallow samples, the overdispersion values were < 20 % (Fig. 3; Table 3).

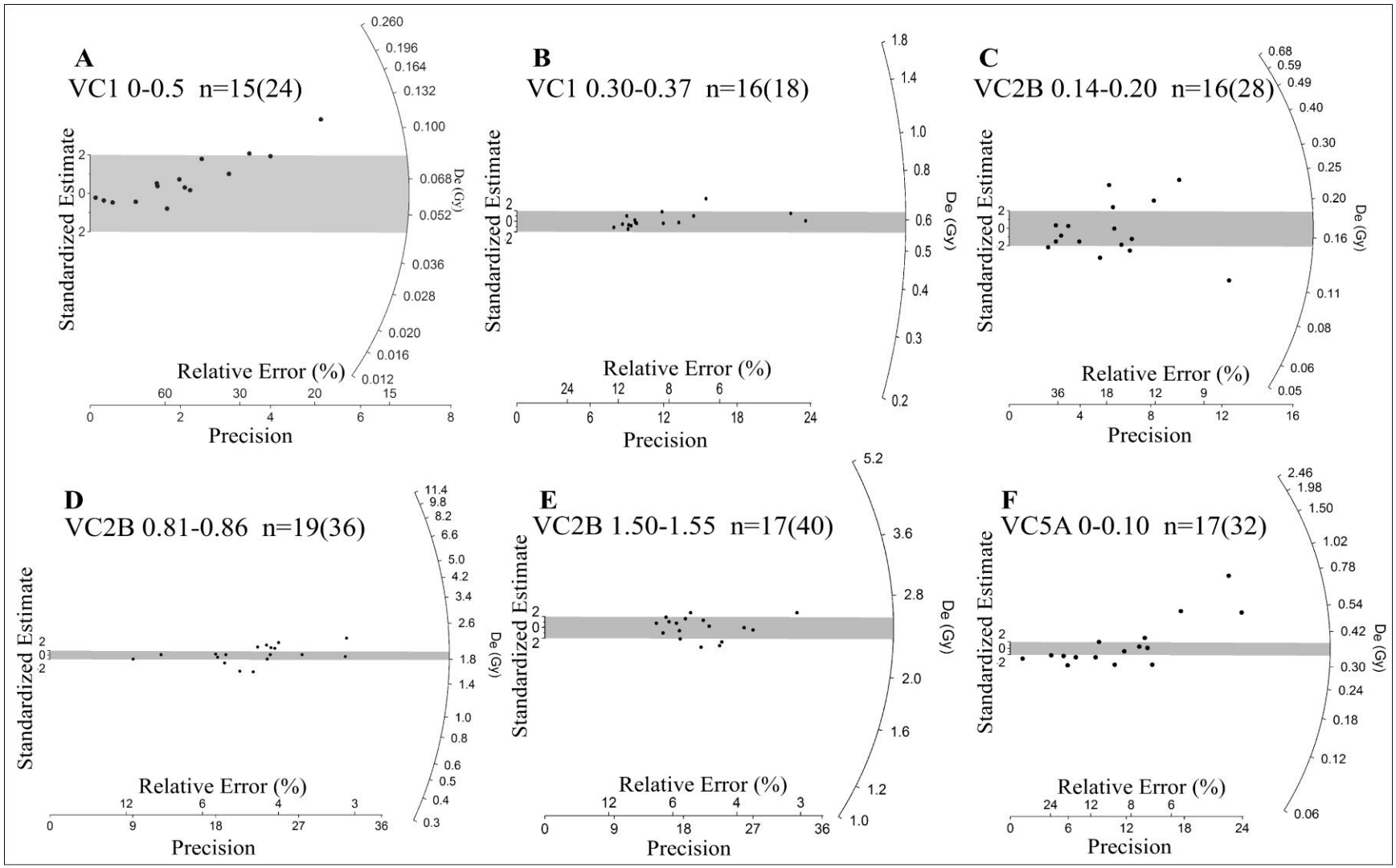
A
VC1 0-0.5 n=15(24)
B
VC1 0.30-0.37 n=16(18)
C
VC2B 0.14-0.20 n=16(28)
D
VC2B 0.81-0.86 n=19(36)
E
VC2B 1.50-1.55 n=17(40)
F
VC5A 0-0.10 n=17(32)
Standardized Estimate
Relative Error (%)
Precision
De (Gy)

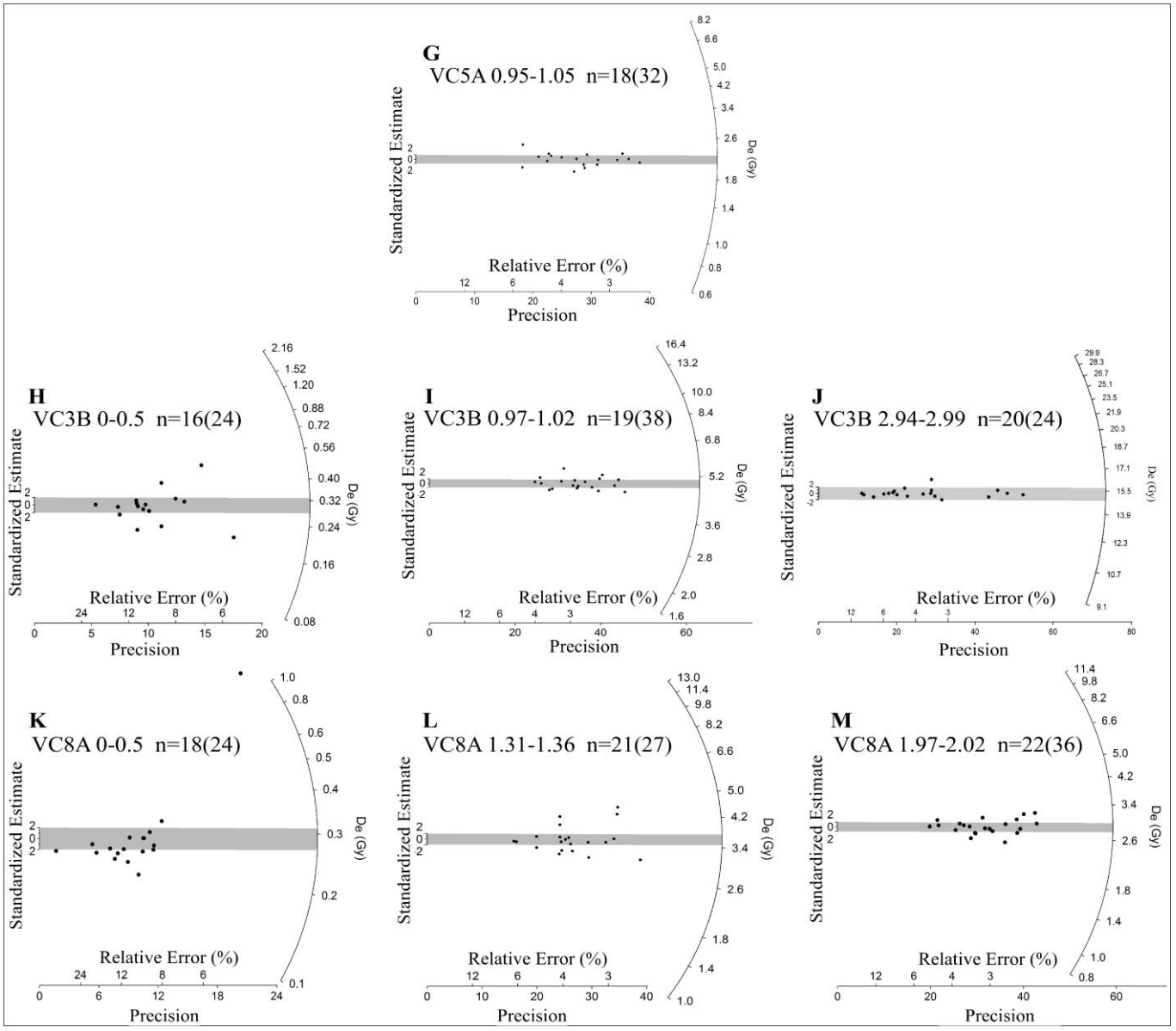
G
VC5A 0.95-1.05 n=18(32)
H
VC3B 0-0.5 n=16(24)
I
VC3B 0.97-1.02 n=19(38)
J
VC3B 2.94-2.99 n=20(24)
K
VC8A 0-0.5 n=18(24)
L
VC8A 1.31-1.36 n=21(27)
M
VC8A 1.97-2.02 n=22(36)
Standardized Estimate
Relative Error (%)
Precision
De (Gy)

Figure 3. Radial plots of OSL samples and the precision of their associated equivalent doses calculated using overdispersion values and standard deviation of each aliquot. Left axis is standardized estimate within 2 sigma. Right axis is equivalent dose measured (Gy). The bottom axis is the relative error (%) and the precision of the equivalent dose for each sample. Included in each sample label is: n= number of aliquots used to calculate the equivalent dose, and (#) = the total number of aliquots measured. All 13 samples processed in this study are represented in each plot as the core name and depth interval (mbsf-meters below sea-floor): **(A)** VC1 0–0.5 mbsf, **(B)** VC1 0.30–0.37 mbsf, **(C)** VC3B 0.14–0.20 mbsf, **(D)** VC2B 0.81–0.86 mbsf, **(E)** VC2B 1.50–1.55 mbsf, **(F)** VC5A 0–0.10 mbsf, **(G)** VC5A 0.95–1.05 mbsf, **(H)** VC3B 0–0.5 mbsf, **(I)** VC3B 0.97–1.02 mbsf, **(J)** VC3B 2.94–2.99 mbsf, **(K)** VC8A 0–0.5 mbsf, **(L)** VC8A 1.31-1.36 mbsf, and **(M)** VC8A 1.97–2.02 mbsf.

The oldest age measured was 980 cal yr BP (1044 ± 104 quartz years) in VC3B at 6.24–6.29 mbsl (Table 3; Appendix A). The youngest ages, derived from surficial sediments range from -12 to -53 cal yr BP, which are also reported in quartz years as 52 (± 3) to 11 (± 3) (Table 3; Appendix A). All other OSL ages range from 453 to 263 cal yr BP, also reported in quartz years as 517 (± 23) to 327 (± 15) (Table 3; Appendix A). All ages obtained are in agreement with the accepted relative sea-level curves for this region (Horton et al., 2009; Kemp et al., 2009; Zaremba et al., in review).

Data from this study indicate that in active FTD environments such as the OFTD region, OSL is likely a reliable dating tool. Sediments are constantly being altered, reworked, and re-deposited by physical processes (e.g. waves, tides, currents) associated with transport in the littoral zone, during which grains are bleached (Fig. 3) (Rink and Forest, 2005). Sand grains deposited on an FTD are derived from longshore transport, up drift of the inlet, and only begin to acquire a D_e signal once they are buried below a zone of reworking.

4.2 Geophysical Data

Multiple Quaternary incised small- and large-scale channel- and valley-fill seismic facies and reflections lie unconformably on top of Pliocene deposits in the OFTD area. The six seismic stratigraphic units (SU) defined by the eight reflections (Fig. 5; Table 4) contain multiple lithofacies and characteristics that represent many different coastal environments. Reflections (R) defined include four Pleistocene (P) reflections (P/P, P1, P2, and P3) and three Holocene (H) reflections (H1, Hftd, and Hmsf). Seismic stratigraphic units generally thicken from Royal Shoal towards the mouth of the Ocracoke Inlet. Not all SUs have been validated with core data as a result of: (1) transgressive processes eroding seismic units and sedimentological units, and (2) coring techniques limiting core data to the upper ca. 9 m of sediments. As a result of the lack of cores in the OFTD region, the sediment type in most areas cannot be determined directly. However, seismic characteristics are useful for inferring lithologies in some areas.

Table 4. Seismic reflections (R) and units (SU) with their associated age, characteristics, and interpretation.

Reflection (R)	Unit (SU)	Interpreted Age	Characteristics	Interpretation and Correlated Reflections (Mallinson et al., 2010a; Zaremba, 2014; Zaremba et al., in review)
Hmsf		Late Holocene	Low to High amplitude	Modern day seafloor
	6		Bounded by Hftd and Hmsf	Holocene estuarine and marine sediments
Hftd		Late Holocene	High amplitude, thin parallel reflection that pinches out in some areas	Tidal ravinement surface; Basal flood-tide delta; H_{1000}
			Bounded by H1 and Hftd	Holocene estuarine and marine sediments
H1		Late Holocene	High amplitude	Bay Ravinement surface
	5		Bounded by Plgm and H1	Holocene fluvial, estuarine, and shallow shelf sediments
Plgm		Pleistocene LGM (ca. 20000 ka)	Medium to high amplitude, base of paleo-fluvial valleys	Incised paleo-valleys; subaerial unconformity; Q99
	4		Bounded by P3 and Plgm	Channel-and valley-fill estuarine and shelf MIS 5 deposits; a transgressive ravinement surface associated with MIS 6 to 5 sea-level rise
P3		Late Pleistocene	Medium amplitude reflection, dipping clinoforms	Subaerial unconformity; Q50
	3		Bounded by P2 and P3	Pleistocene fluvial and estuarine sediments
P2		Middle Pleistocene	High amplitude, semi-parallel reflection	Marine transgressive ravinement surface
	2		Bounded by P1 and P2	Pleistocene fluvial and estuarine sediments
P1		Early Pleistocene	High amplitude, semi-parallel reflection	Ravinement surface; Q10b
	1		Bounded by PP and P1	Pleistocene fluvial and estuarine sediments
P/P		Pliocene/Pleistocene Boundary	High amplitude, parallel reflection	Submarine unconformity; Q0

4.2.1. Reflection P/P

The P/P reflection occurs at ca. 32–42 mbsl, is medium-to-high amplitude, and dips gently to the northeast. This reflection corresponds to the Q0 reflection defined by Mallinson et al. (2010a) and represents the Pleistocene/Pliocene Boundary based on core data (Mallinson et al., 2010a) and serves as the acoustic basement (Table 4). P/P is interpreted to represent a regional-scale submarine unconformity.

4.2.2. SU 1

Seismic Unit 1 is constrained by reflection P/P at the base and reflection P1 at the top and ranges from ca. 8–10 m in thickness. The basal reflector (P/P) and top reflector (P1) of SU 1 are planar and horizontal. SU 1 is characterized by chaotic-distorted reflection configurations (Table 4).

4.2.3 Reflection P1

The P1 reflection occurs at ca. 22–34 mbsl, and is a medium-to-high amplitude, horizontal, semi-continuous surface that is sub-parallel to the Pleistocene/Pliocene Boundary (Table 4). The Q10b reflection defined by Mallinson et al. (2010a) correlates to this P1 reflection. P1 displays relatively low relief is interpreted to represent a ravinement surface.

4.2.4. SU 2

Seismic Unit 2 is constrained by reflection P1 at the base and reflection P2 at the top. SU 2 ranges from ca. 8–14 m in thickness and is characterized by sub-horizontal beds at the base of the unit. The top of this unit is characterized by sub-horizontal beds that are truncated in some areas by small-scale (ca. 100 m wide) and large-scale (ca. 1000 m wide) channels. Overall, the bedding characteristics of SU 2 are sub-horizontal except where local incisions occur (Table 4).

4.2.5 Reflection P2

The P2 reflection occurs at ca. 12–16 mbsl and is a semi-continuous, sub-horizontal, medium-to-high amplitude reflection sub-parallel to the Pleistocene/Pliocene Boundary (Table 4). P2 is

discontinuous as a result of truncation by an incised channel (reflection P3) and the associated cut-and-fill deposits. P2 is interpreted as a marine transgressive ravinement surface (TRS).

4.2.6 SU 3

Seismic Unit 3 is bounded by reflection P2 at the base and reflection P3 at the top and ranges from ca. 8–28 m in thickness. SU 3 is characterized by horizontal beds at the base of the unit that are generally traceable throughout the study area and are overlain by clinoform packages that generally dip towards the southwest in the middle of the unit. The clinoform terminations at the top of the unit are overlain by a set of semi-parallel, relatively discontinuous, and semi-horizontal beds (Table 4).

4.2.7 Reflection P3

Seismic reflection P3 occurs from ca. 9–32 mbsl and is characterized by a discontinuous medium amplitude reflection with high relief (ca. 20 m) (Figs. 5A–C; Table 4). P3 defines a prominent Pleistocene channel that incised into underlying Pleistocene sediments (SU 3) and thus represents a subaerial unconformity. This P3 channel reflection is overlain by multiple cut-and-fill deposits comprising clinoform packages in SU 4 that dip to the southwest and are overlain by horizontal parallel beds in SU 4. This channel-fill is interpreted to represent fluvial-fill overlain by estuarine deposits. The horizontal beds, interpreted as estuarine deposits, are truncated by a TRS which correlates to Q50 of Mallinson et al. (2010a), the TRS associated with Termination II (MIS 6 to 5 transition). This P3 channel appears to represent two channels superimposed upon each other with varying degrees of preservation, however the data are discontinuous, and therefore, somewhat ambiguous (Figs. 4A, 5; Table 4).

In the gridded P3 reflection bathymetry map, the depth of the channel base occurs from ca. 9–32 mbsl complementing the digitized surface, and the width ranges from ca. 500–1400 m (Fig. 4A). The surface has variable relief and depths suddenly shallow to ca. 15 mbsl as the channel approaches the modern distal OFTD (Royal Shoal arcuate feature) (Figs. 5A–C, 6A).

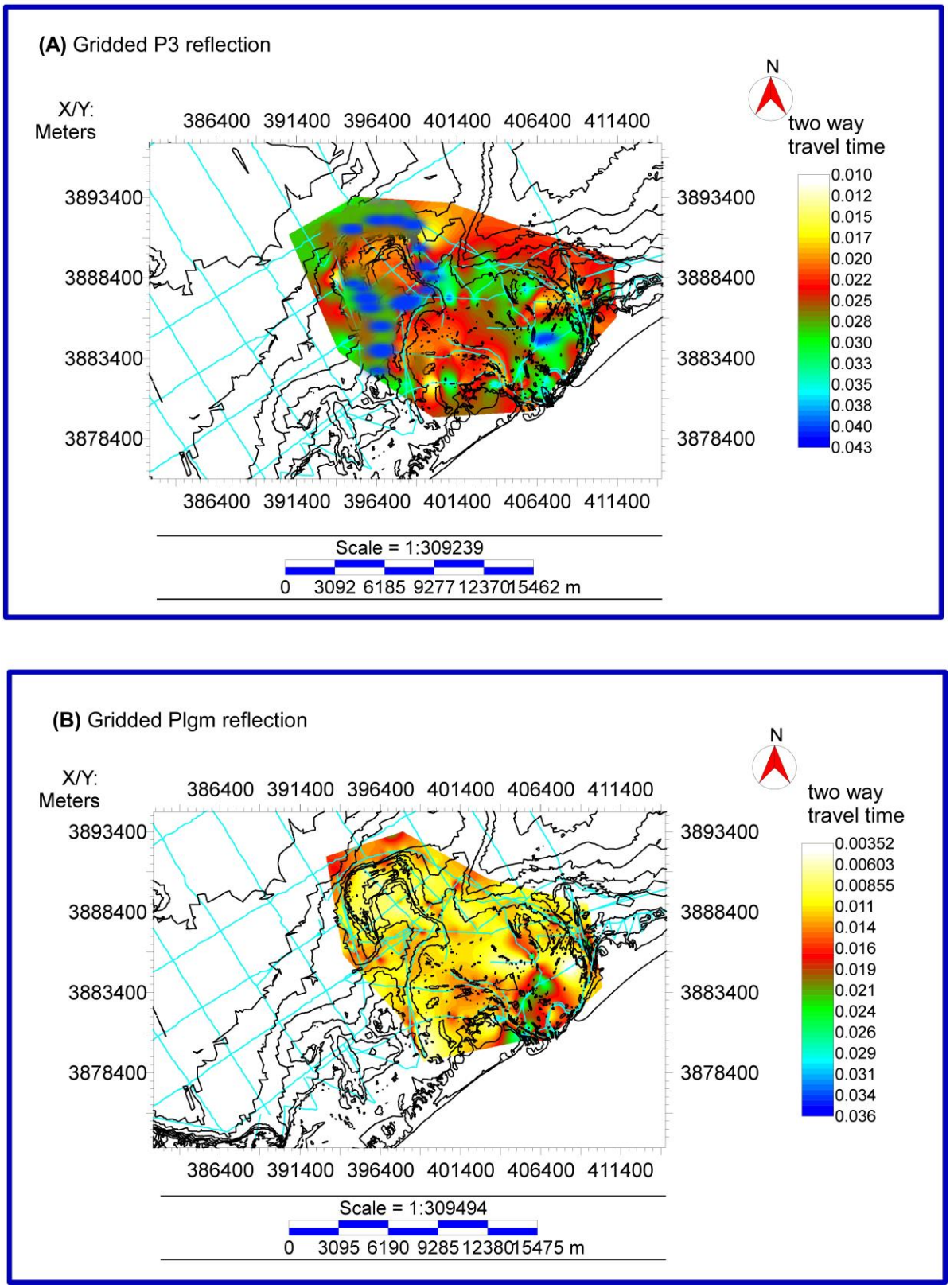

Figure 4. Maps showing the depth of seismic reflections discussed in text: **(A)** P3; **(B)** Plgm.

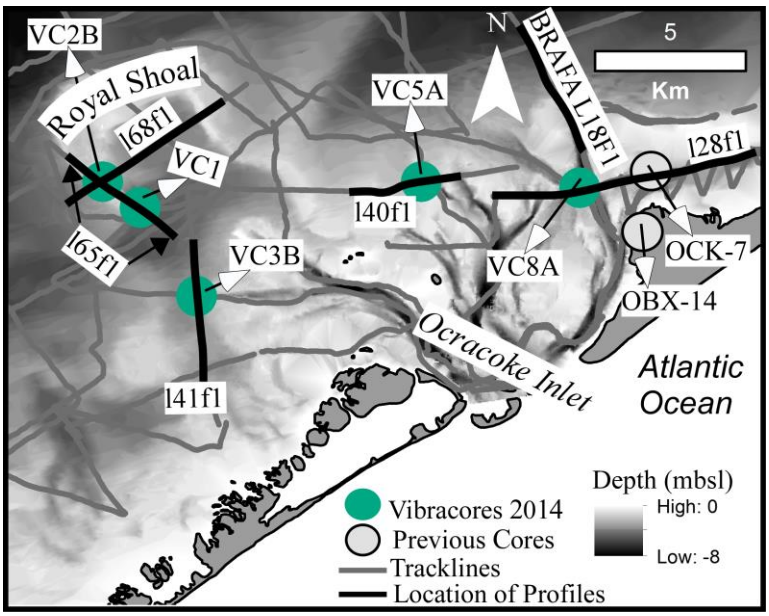

Figure 5. Interpretations of seismic survey profile data (black lines), seismic tracklines (gray lines), and location map of cores (green circles) used in this study. The names of seismic lines that intersect with the interpreted seismic lines shown are illustrated as gray text above the meters and shotpoint horizontal scale bar for each seismic line in figures **A**–**F**. **(A)** Line L65f1 is oriented from the northwest to the southeast and is located on and at the base of Royal Shoal (distal OFTD area), which shows a prominent Pleistocene valley (P3). The line crosses over the location of cores VC1 and VC2B. **(B)** Line L68f1 is oriented form the southwest to the northeast and shows a cross sectional view of the subsurface characteristics associated with Royal Shoal (distal OFTD area). The line crosses over the location of core VC2B. **(C)** Line l41f1 is oriented from the northwest to the southeast and is located within the western intermediate OFTD area, and shows how the P3 channel extends to the southwest of the OFTD area. The line crosses over the location of core VC3B. **(D)** Line l40f1 is oriented from the northeast to the southwest and is located within the eastern intermediate OFTD area. The line crosses over the location of core VC5A. **(E)** Line BRAFA_L18f1 is oriented from the northwest to the southeast and is located within the eastern intermediate OFTD area. The line crosses over core VC8A. **(F)** Line l128f1 is oriented from the southwest to the northeast and is located within the eastern intermediate OFTD area. The line crosses over vibracores VC8A and OCK-7 (Metger, 2009), and the line is near rotasonic core OBX-14 (Mallinson et al., 2010a) located on the northwest end of Ocracoke Island. Both lines presented in figures E and F illustrate how the paleo-Pamlico Creek drainage system affects the modern day morphology.

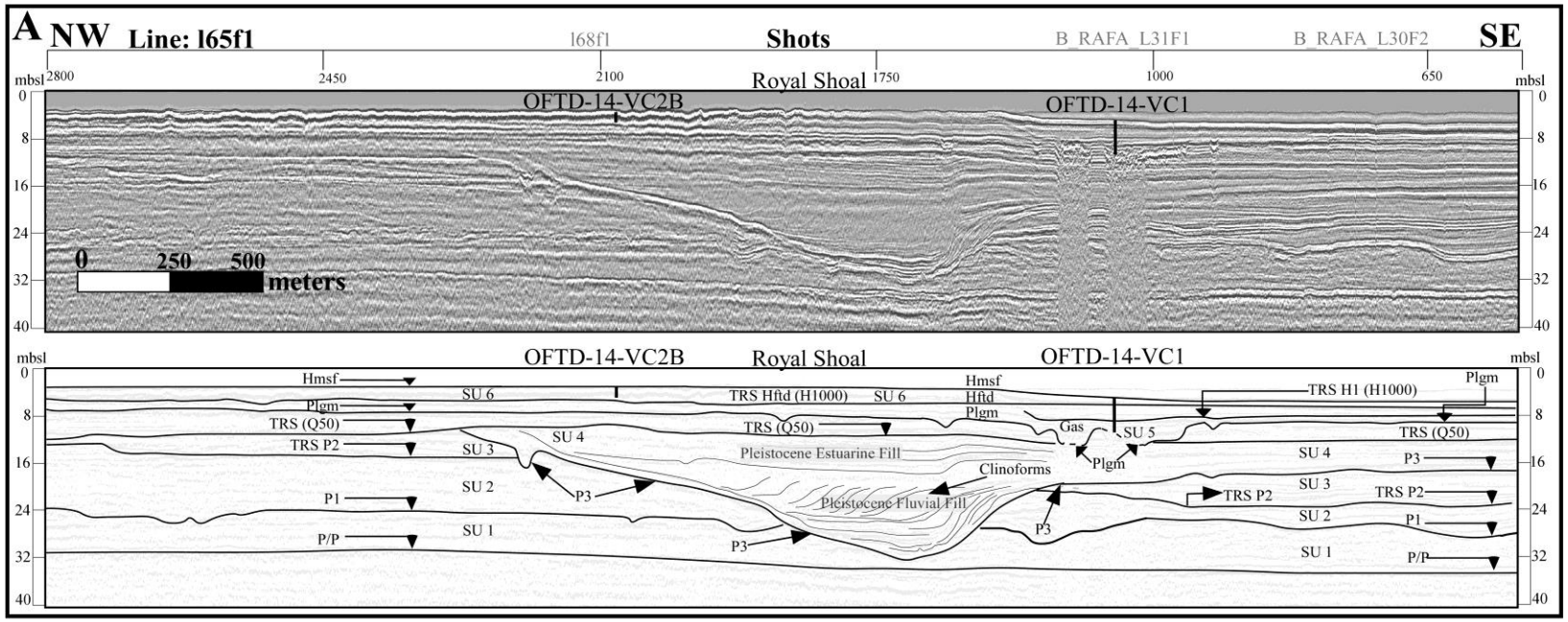
A
NW
Line: l65f1
l68f1
Shots
B_RAFA_L31F1
B_RAFA_L30F2
SE
mbsl
2800
2450
2100
Royal Shoal
1750
1000
650
OFTD-14-VC2B
OFTD-14-VC1
0
250
500
meters
Hmsf
Plgm
TRS (Q50)
TRS P2
P1
P/P
SU 6
SU 4
SU 3
SU 2
SU 1
P3
TRS Hftd (H1000)
Pleistocene Estuarine Fill
Pleistocene Fluvial Fill
Clinoforms
Hftd
Gas
SU 5
TRS H1 (H1000)

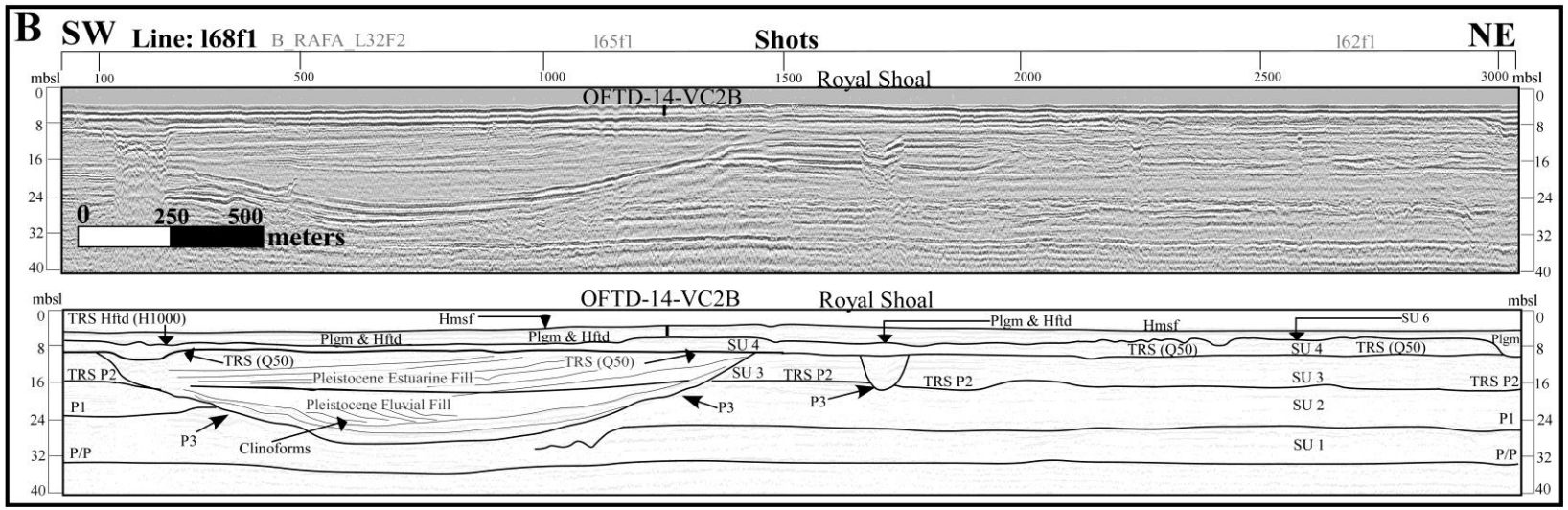
B
SW
Line: l68f1
B_RAFA_L32F2
l65f1
Shots
l62f1
NE
mbsl
100
500
1000
1500
Royal Shoal
2000
2500
3000
OFTD-14-VC2B
0
250
500
meters
TRS Hftd (H1000)
Hmsf
Plgm & Hftd
TRS (Q50)
TRS P2
P1
P/P
SU 4
SU 3
SU 2
SU 1
P3
Pleistocene Estuarine Fill
Pleistocene Fluvial Fill
Clinoforms
SU 6
Plgm

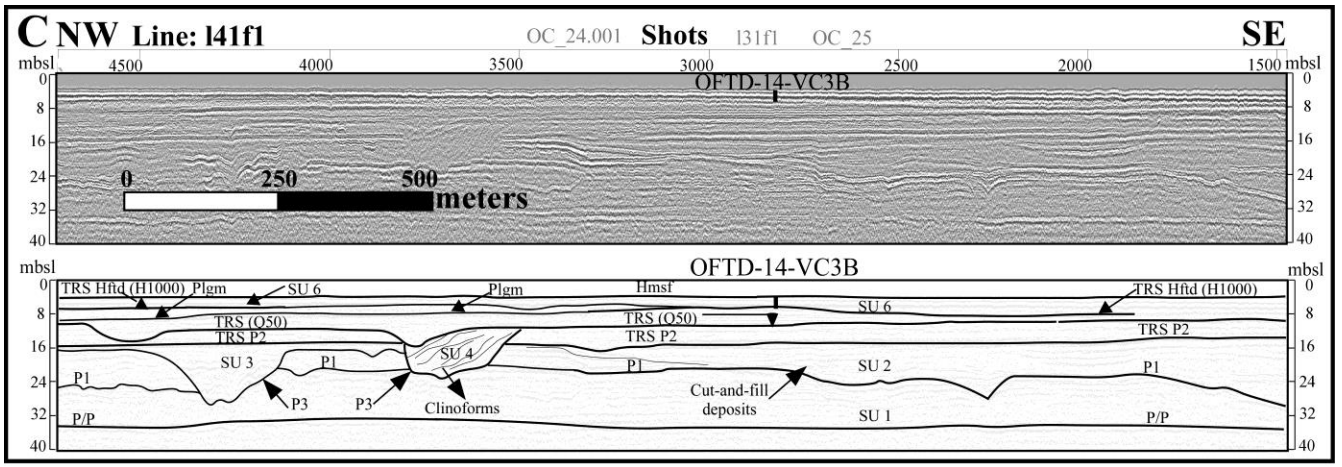
C NW Line: l41f1
OC_24.001
Shots
l31f1
OC_25
SE
mbsl
4500
4000
3500
3000
2500
2000
1500 mbsl
OFTD-14-VC3B
0
250
500
meters
OFTD-14-VC3B
TRS Hftd (H1000)
Plgm
SU 6
Plgm
Hmsf
TRS (Q50)
TRS P2
SU 3
P1
SU 4
P3
P3
Clinoforms
Cut-and-fill deposits
SU 2
SU 1
P/P

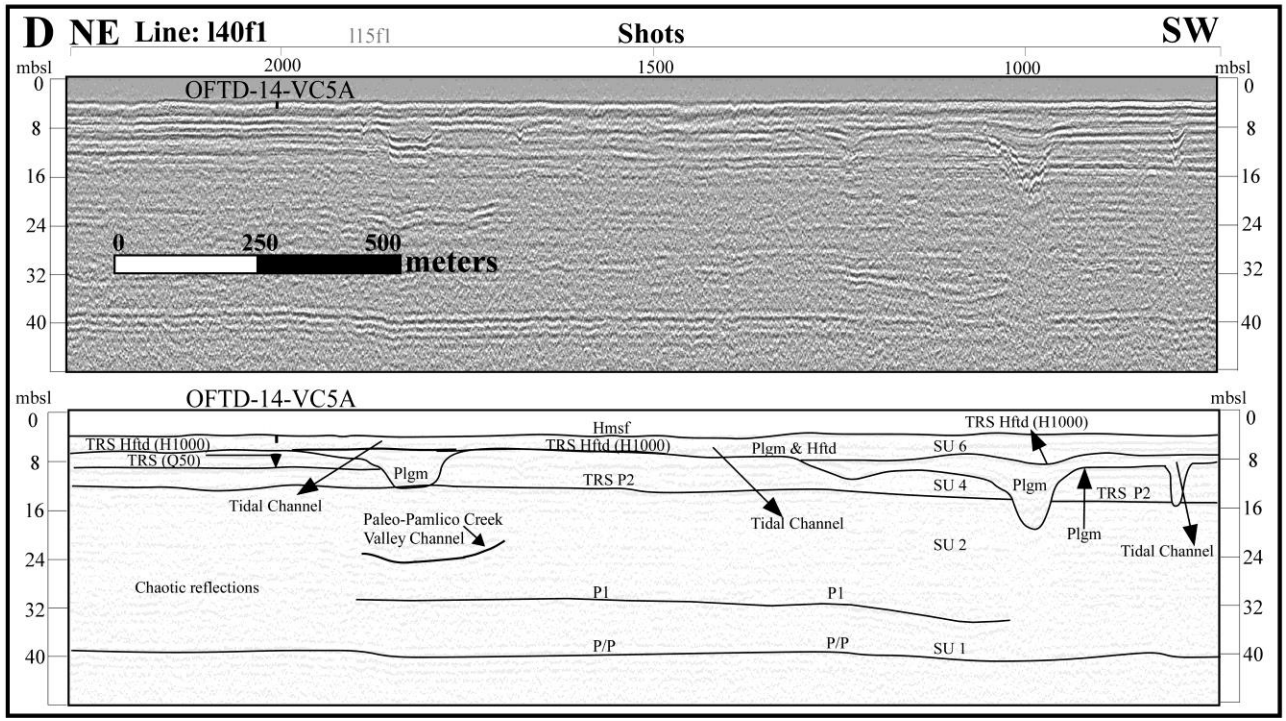
D NE Line: l40f1
l15f1
Shots
SW
mbsl
2000
1500
1000
OFTD-14-VC5A
0
250
500
meters
OFTD-14-VC5A
Hmsf
TRS Hftd (H1000)
TRS (Q50)
Plgm
Tidal Channel
Paleo-Pamlico Creek Valley Channel
Chaotic reflections
Plgm & Hftd
Tidal Channel
SU 6
SU 4
SU 2
SU 1
TRS P2
P1
P/P

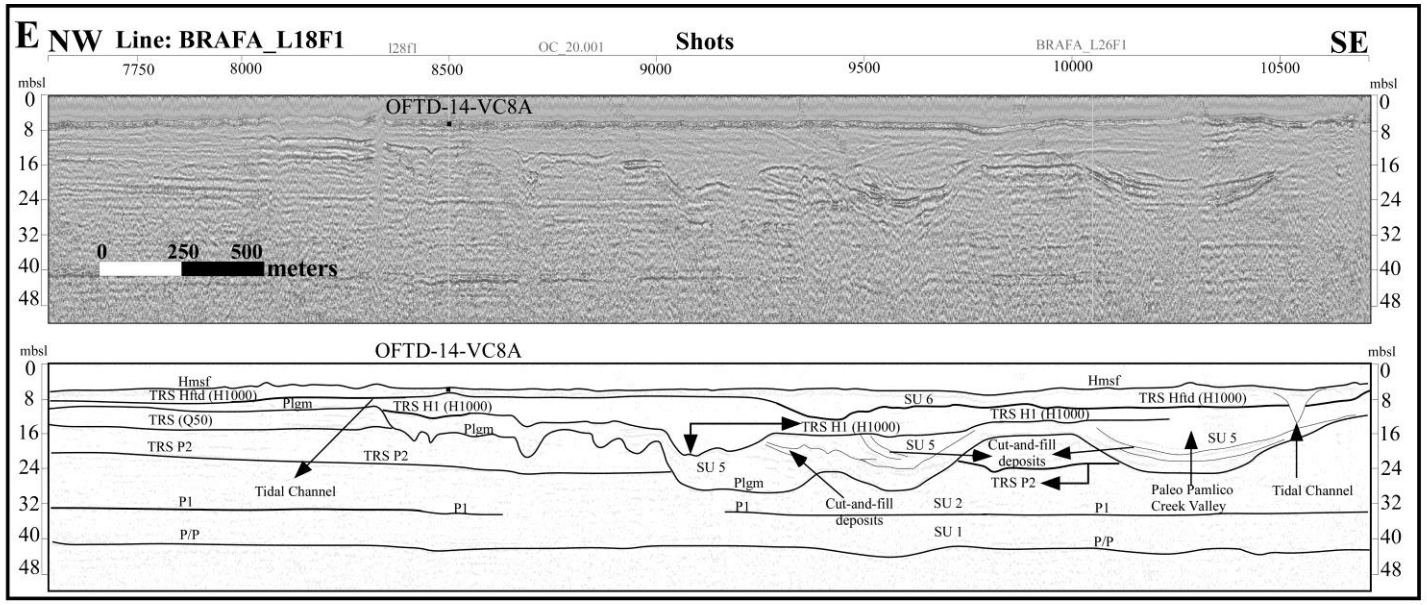
E NW Line: BRAFA_L18F1
l28f1
OC_20.001
Shots
BRAFA_L26F1
SE
7750
8000
8500
9000
9500
10000
10500
mbsl
OFTD-14-VC8A
0 250 500 meters
Hmsf
TRS Hftd (H1000)
Plgm
TRS H1 (H1000)
TRS (Q50)
TRS P2
P1
P/P
Tidal Channel
SU 6
SU 5
SU 2
SU 1
Cut-and-fill deposits
Paleo Pamlico Creek Valley

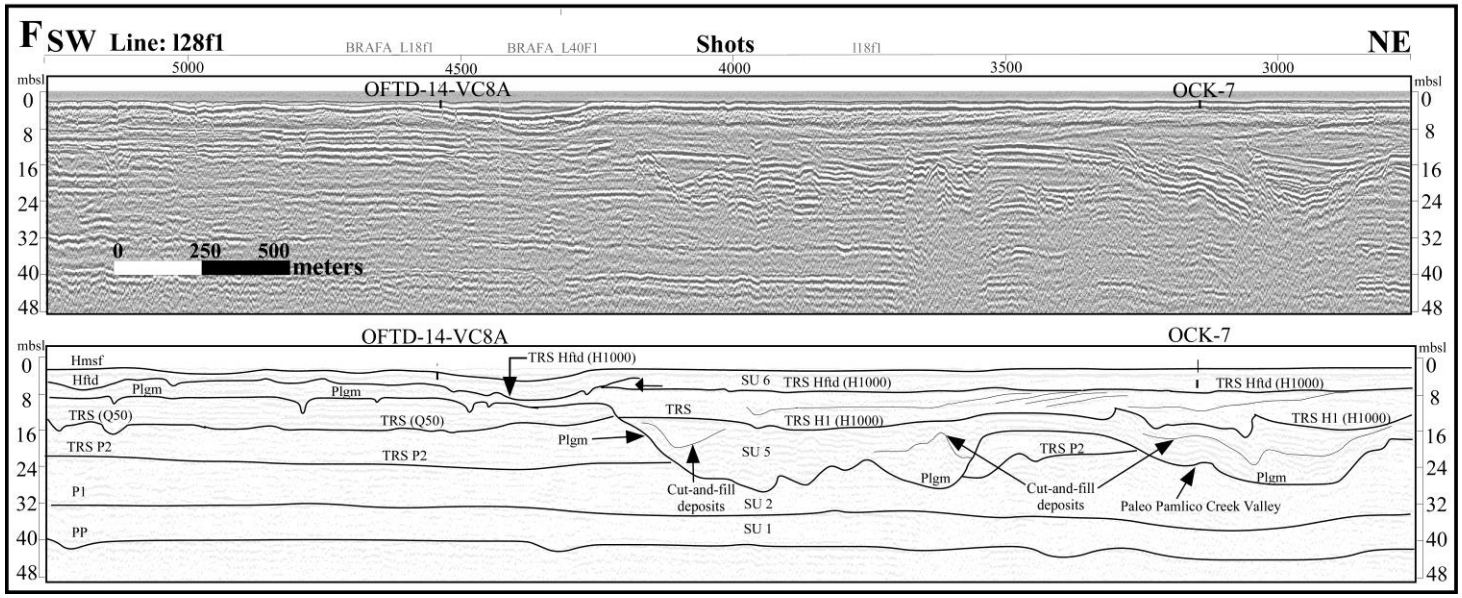
F SW Line: l28f1
BRAFA_L18f1
BRAFA_L40F1
Shots
l18f1
NE
5000
4500
4000
3500
3000
mbsl
OFTD-14-VC8A
OCK-7
0 250 500 meters
Hmsf
Hftd
TRS Hftd (H1000)
Plgm
TRS (Q50)
TRS
TRS H1 (H1000)
TRS P2
P1
PP
SU 6
SU 5
SU 2
SU 1
Cut-and-fill deposits
Paleo Pamlico Creek Valley

4.2.8 SU 4

Seismic Unit 4 is bounded by reflection P3 at the base and reflection Plgm at the top and ranges from ca. 10–30 m in thickness. The thickest part of this unit occurs within the fill of paleo-valleys (Fig. 5). Seismic facies include erosionally bounded packages that are internally composed of oblique and sigmoidal clinoforms as well as hummocky and chaotic reflectors with small amounts of sub-horizontal reflectors (Table 4).

4.2.9 Reflection Plgm

Seismic reflection Plgm occurs at depths ranging from ca. 1–24 mbsl and is medium-to-high amplitude, and semi-continuous. Mallinson et al. (2010a) defined reflection Q99 that correlates to Plgm and represents the boundary between Pleistocene and Holocene sediments and the LGM unconformity. Plgm is a subaerial unconformity, and represents the base of major incised paleo-valleys (Figs. 2, 4B, 5).

The gridded Plgm reflection shows the Pleistocene-Holocene Boundary to range in depth from ca. 1 –24 mbsl (Fig. 4B). The gridded map shows variable relief, averaging ca. 8–10 m. The shallowest portions occur on the distal OFTD region (Royal Shoal) and intermediate OFTD region, while the deepest portions occur within the proximal OFTD region and overlie the paleo Neuse/Tar River Valleys and the paleo-Pamlico Creek channel (Fig. 4B).

4.2.10 SU 5

Seismic Unit 5 is constrained by reflection Plgm at the bottom and reflection H1 at the top and ranges in thickness from ca. 4–16 m (Fig. 5; Table 4). Paleo-valley fill associated with the Pamlico Creek, Neuse, and Pamlico/Tar rivers correlates to SSU 5 (Mallinson et al., 2010a). The seismic facies are not laterally persistent and they include erosionally bounded packages that are internally composed of oblique and shingled reflectors with small amounts of sub-parallel reflectors. The sub-parallel reflectors and the associated horizontal bedding is interpreted as estuarine and shallow shelf sediments deposited during a transgression.

4.2.11 Reflection H1

The H1 reflection generally occurs from ca. 4–10 mbsl and is high amplitude, sub-horizontal, and semi-continuous (Table 4). It is interpreted to represent a bay ravinement surface which correlates to H_{1000} of Zaremba (2014) and Zaremba et al. (in review). The H1 reflection is locally attenuated by the presence of overlying peat deposits (e.g., the basal sediment in VC1) (Fig. 6A).

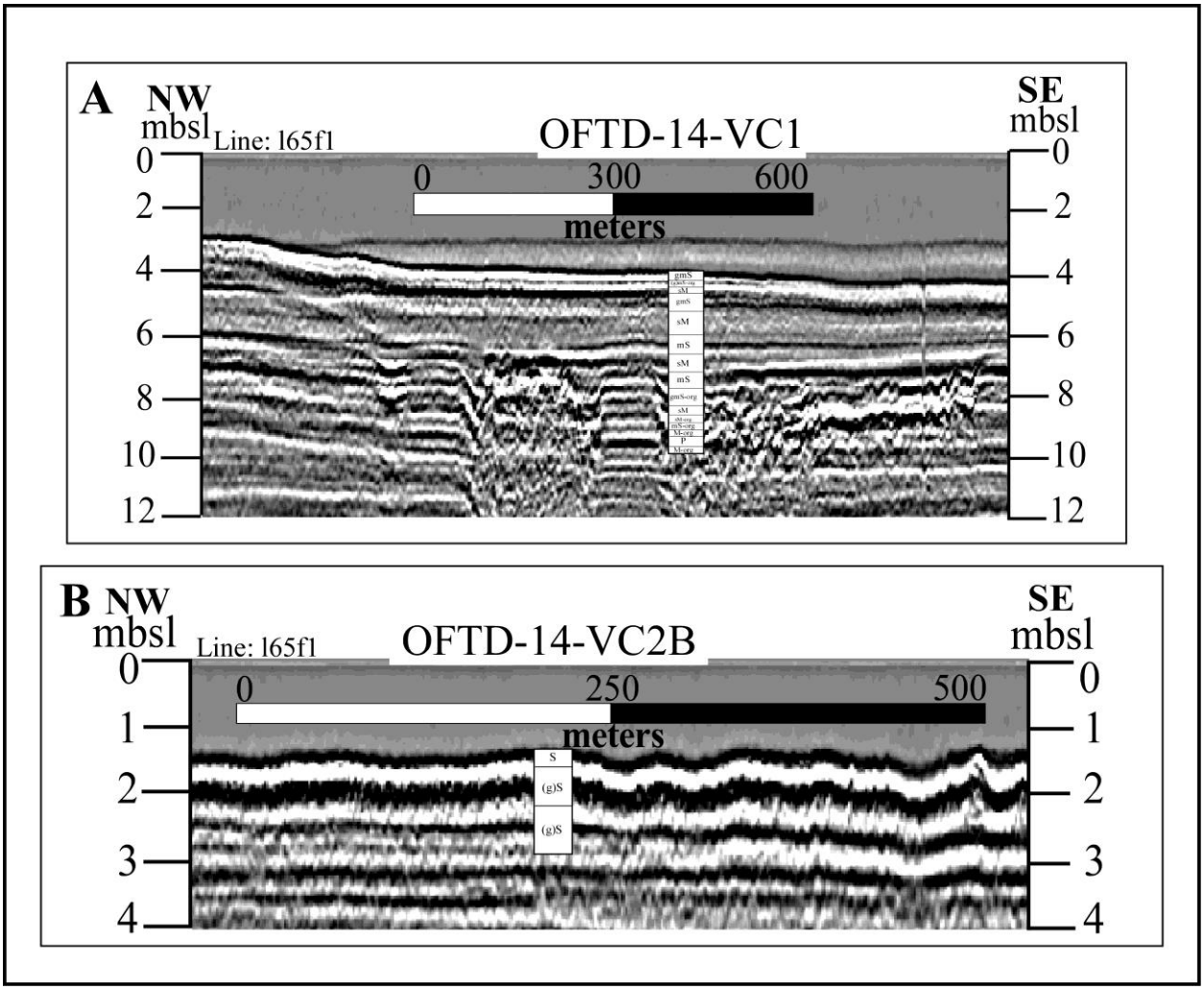

Figure 6. Correlations between geophysical data and associated lithological data in VC1 **(A)** and VC2B **(B)** core logs (Appendix A). See figure 1 for the location of cores.

4.2.12 SU 6

Seismic Unit 6 is constrained by reflections H1 at the bottom and Hmsf at the top, and includes a discontinuous reflection (Hftd) in the middle. The thickness ranges from ca. 0–10 m. Based on core data,

SU 6 is characterized by inlet and channel-fill (e.g., muddy sand and sandy mud estuarine sediments, and thick sand units that pinch out) partially controlled by, and associated with paleovalleys, interfluves, and the modern OFTD area (Table 4). Associated sedimentary units are defined in vibracores VC1, VC2B, VC3B, VC5A, and VC8A (Figs. 5, 6; Table 4; Appendix A). In some areas Holocene reflections are attenuated by peat such as the basal sedimentary unit of VC1 that occurs in SU 5 (Figs. 5A, 6A; Table 4). Of the five cores, four (VC2B, VC3B, VC5A, and VC8A) penetrated only to the upper portion of SU 6 (including Hftd and Hmsf reflections) (Figs. 5, 6B; Table 4; Appendix A).

4.2.13 Reflection Hftd

The Hftd reflection generally occurs at depths ranging from ca. 2–7 mbsl, is relatively discontinuous, medium-to-high-amplitude, and mimics the bathymetry of the modern seafloor rising up to ca. 2 mbsl in some areas (Figs. 5, 6, 14; Table 4). Based on the stratigraphic position of the Hftd reflection, and overlying sedimentary units and biofacies, the Hftd reflection represents the base of modern FTD deposits and is interpreted to represent a tidal ravinement surface which correlates to H_{1000} of Zaremba (2014) and Zaremba et al. (in review).

4.2.14 Reflection Hmsf

The Hmsf reflection occurs at varying depths throughout the OFTD (depending on the locations of paleovalleys and interstream divides) with the deepest closest to the inlet, and ranges from low-to-high amplitude. The Hmsf represents the modern seafloor (Fig. 5; Table 4).

4.3 Sedimentological Data

Patterns in grain size vary throughout the five vibracores (Tables 5, 6; Appendices A, B, C). Sediments are generally unimodal (Table 6), very well sorted to well sorted, very-fine to medium-grained quartz sand grains with varying amounts of mud, shells, shell fragments, gravel, mud mottling, laminations, and organics (Tables 5, 6; Appendices A, B, C). Fifteen lithofacies were identified throughout the five vibracores (Table 5). Gravelly muddy sand (gmS), gravelly sandy mud (gsM), sand

(S), muddy sand (mS), sandy mud (sM), and mud (M) are the more common lithofacies (Tables 5, 6; Appendices A, B, C).

Table 5. Description of the 15 lithofacies observed in vibracores.

Lithofacies	Code	Description and Sedimentary Features
Sand	S	Poorly to moderately sorted, very-fine to fine-grained sand; laminations, mottling, and shell fragments common
Gravelly sand	gS	Poorly to moderately sorted, very-fine to fine-grained sand with shells; mottling common
Slightly gravelly sand	(g)S	Moderately sorted, very-fine to fine-grained sand with shells; mottling common
Muddy sand	mS	Moderately sorted, very-fine to fine-grained sand with mud; mottling, laminations, and shell fragments common
Organic-rich muddy sand	mS-org	Moderately sorted, very-fine to fine grained sand with mud, wood, and charcoal debris; mottling, and shell fragments common
Gravelly muddy sand	gmS	Poorly to moderately sorted, very-fine to fine grained sand with mud; shells and shell fragments common
Organic-rich gravelly muddy sand	gmS-org	Poorly to moderately sorted, very-fine to fine grained sand with mud, shells and shell fragments; wood and charcoal debris common
Slightly gravelly muddy sand	(g)mS	Moderately sorted, very-fine to fine grained sand with mud; shells and shell fragments common
Mud	M	Mud with well sorted shells and shell fragments
Organic-rich mud	M-org	Mud with well sorted shells and shell fragments with wood and charcoal debris
Sandy Mud	sM	Mud with moderately sorted fine sand; laminations, mottling, and shell fragments common
Organic-rich sandy mud	sM-org	Mud with moderately sorted fine sand with wood and charcoal debris; mottling and shell fragments common
Organic-rich gravelly sandy mud	gsM-org	Mud with poorly to moderately sorted fine sand, shells, and shell fragments with wood and charcoal debris; mottling common
Slightly gravelly sandy mud	(g)sM	Mud with moderately sorted fine sand, shells, and shell fragments with wood and charcoal debris; mottling common
Peat	P	Peat with wood and charcoal debris

Table 6. Sediment grain size results using Gradistat. Mbsl- meters below sea level, and mbsf-meters below seafloor.

Core ID	mbsf	mbsl	Mean Φ	Mean	Sorting Φ	Sorting	Skewness Φ	Skewness	Kurtosis Φ	Kurtosis	Mode Φ	Median Φ
OFTD-14-VC2B	0.87–.090	2.07–2.10	2.08	fine sand	0.37	well sorted	-0.07	symmetrical	1.01	mesokurtic	2.24	2.12
OFTD-14-VC2B	1.62–1.65	2.82–2.85	2.26	fine sand	0.35	v. well sorted	0.04	symmetrical	1.42	leptokurtic	2.24	2.25
OFTD-14-VC3B	0.47–0.50	3.77–3.80	3.08	v. fine sand	0.32	v. well sorted	-0.28	coarse skewed	0.91	mesokurtic	3.24	3.14
OFTD-14-VC3B	1.09–1.12	4.39–4.42	3.11	v. fine sand	0.39	well sorted	-0.09	symmetrical	1.04	mesokurtic	3.24	3.16
OFTD-14-VC3B	1.79–1.82	5.09–5.12	2.99	fine sand	0.39	well sorted	-0.34	v. coarse skewed	0.92	mesokurtic	3.24	3.07
OFTD-14-VC3B	2.30–2.33	5.60–5.63	2.85	fine sand	0.39	well sorted	0.39	v. fine skewed	1.73	v. leptokurtic	2.74	2.81
OFTD-14-VC3B	2.89–2.91	6.19–6.21	2.81	fine sand	0.42	well sorted	-0.01	symmetrical	1.26	leptokurtic	2.74	2.78
OFTD-14-VC5A	0.50–0.52	2.0–2.02	2.32	fine sand	0.50	well sorted	0.09	symmetrical	1.14	leptokurtic	2.24	2.29
OFTD-14-VC5A	1.05–1.07	2.55–2.57	2.43	fine sand	0.49	well sorted	-0.13	coarse skewed	1.04	mesokurtic	2.74	2.45
OFTD-14-VC8A	1.37–1.40	4.37–4.40	2.37	fine sand	0.37	well sorted	0.25	fine skewed	1.30	leptokurtic	2.24	2.31
OFTD-14-VC8A	2.13–2.16	5.13–5.16	2.29	fine sand	0.34	v. well sorted	0.07	symmetrical	1.48	leptokurtic	2.24	2.26

4.4 Foraminiferal Assemblages

Fifty-five samples (22 surface, 33 down-core) were processed for foraminifera. Of these, 48 samples contained foraminifera and seven were barren (one surface, and six down-core). Three samples (two surface, one down-core) contained < 15 specimens. Forty-one taxa were identified (Appendices E, G).

4.4.1 Modern Foraminiferal Assemblages

The 22 surface samples (Fig. 1, Tables 7, 8; Appendix E) contained 37 foraminiferal taxa (Appendix E). Rotaliids dominated the assemblages (Table 7; Appendix E). The three most abundant species (defined by their average of ≥ 5%) were *Elphidium excavatum* (average 64%), *Ammonia parkinsoniana* (average 13%), and *Elphidium mexicanum* (average 5%) (Table 7; Appendix F). Secondary species (average of < 5% and ≥ 1%) comprised an average of 18% of assemblages (Tables 7, 8; Appendix F) and included *Elphidium galvestonense*, *Hanzawaia strattoni*, *Elphidium gunteri*, *Cibicides lobatulus*, and *Quinqueloculina seminula* (Appendix F). Rare species (average of < 1%) were represented by 27 benthic taxa and a few planktonic taxa (Appendix F).

Table 7. Foraminiferal characteristics of surficial samples listed by increasing distance from the inlet. Salinity values collected at time of sediment sampling.

Sample ID	# of foraminifera picked	# Live Specimens	# Dead Specimens	% Live	% Dead	% of Sample Picked	Species Richness (S)	Distance From Inlet (m)	No. Rotaliid Specimens	% Rotaliids	No. Miliolid Specimens	% Miliolids	No. Textulariid Specimens	% Textulariids	Calculated Number of Specimens in 60 mL	Salinity
OC-14-S16	112	1	111	1	99	38	17	3360	103	92	9	8			295	35
OC-14-S17	124	8	116	6	94	35	18	3496	116	94	7	6	1	1	354	38
OC-14-S1	151	4	147	3	97	8	13	3812	147	97	4	3			1888	28
OC-14-S7	116	16	100	14	86	100	12	4009	116	100					116	35
OC-14-S2	79	13	66	16	84	100	9	4528	78	99			1	1	79	27
OC-14-S3	93	9	84	10	90	100	10	5728	93	100					93	27
OC-14-S4	116	43	73	37	63	80	7	6559	116	100					145	27
OC-14-S21	124	24	100	19	81	5	10	6878	122	98			2	2	2480	25
OC-14-S5	136	46	90	34	66	100	6	7467	135	99	1	1			136	24
OC-14-S22	102	3	99	3	97	100	5	7625	102	100					102	24
OC-14-S11	109	45	64	41	59	21	7	7827	108	99	1	1			519	20
OC-14-S15	6		6		100	100	2	8420	6	100					6	20
OC-14-S8	15	1	14	7	93	100	4	8985	15	100					15	24
OC-14-S14	116	2	114	2	98	43	14	9007	110	95	5	4	1	1	270	18
OC-14-S12	113	15	98	13	87	27	6	9632	113	100					419	17
OC-14-S18	129	20	109	16	84	23	7	9731	129	100					561	23
OC-14-S6	107	36	71	34	66	90	9	9990	105	98	1	1	1	1	119	23
OC-14-S13	107	13	94	12	88	62	4	10171	107	100					173	17
OC-14-S10	11		11		100	100	3	10182	11	100					11	21
OC-14-S9	38	2	36	5	95	100	2	10899	38	100					38	23
OC-14-S19	118	15	103	13	87	10	6	12354	117	99			1	1	1180	23
OC-14-S20						100		13953								

Variations in modern foraminiferal assemblages as a function of distance from the inlet are shown in Figs. 8, 9. The distribution of each surface sample is related to the distance from the inlet and salinity (Figs. 7, 8, 9), salinity decreases further away from the inlet. Salinity measurements generally correlate with the biofacies distribution of each surface sample reflecting tidal influences (Fig. 9). Live specimens (average 14% of total specimens) were most abundant from 6 km–10 km from the inlet (Table 7). The number of specimens picked is relatively constant with an average of 96 for all samples with foraminifera present (Table 7; Appendix E). The number of calculated specimens in 60 mL of sediment varies greatly from 295–2480 with an average of 409 (Table 7; Appendix E).

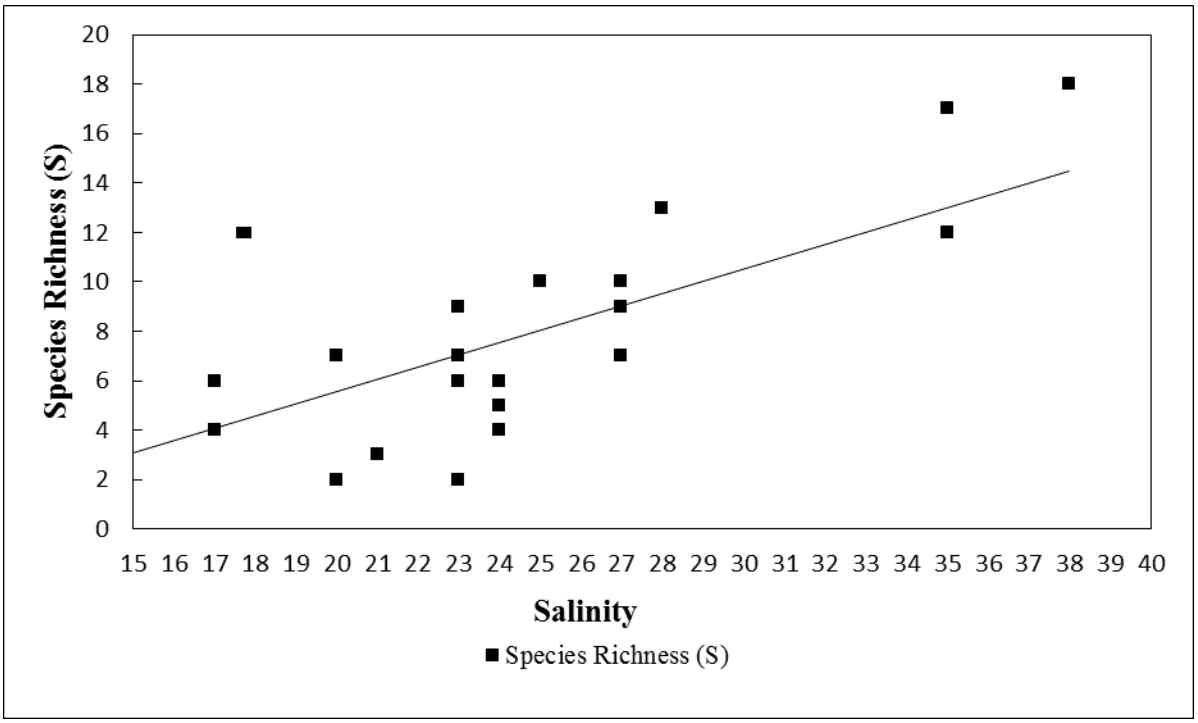

Figure 7. A plot of salinity values for 21 surface samples.

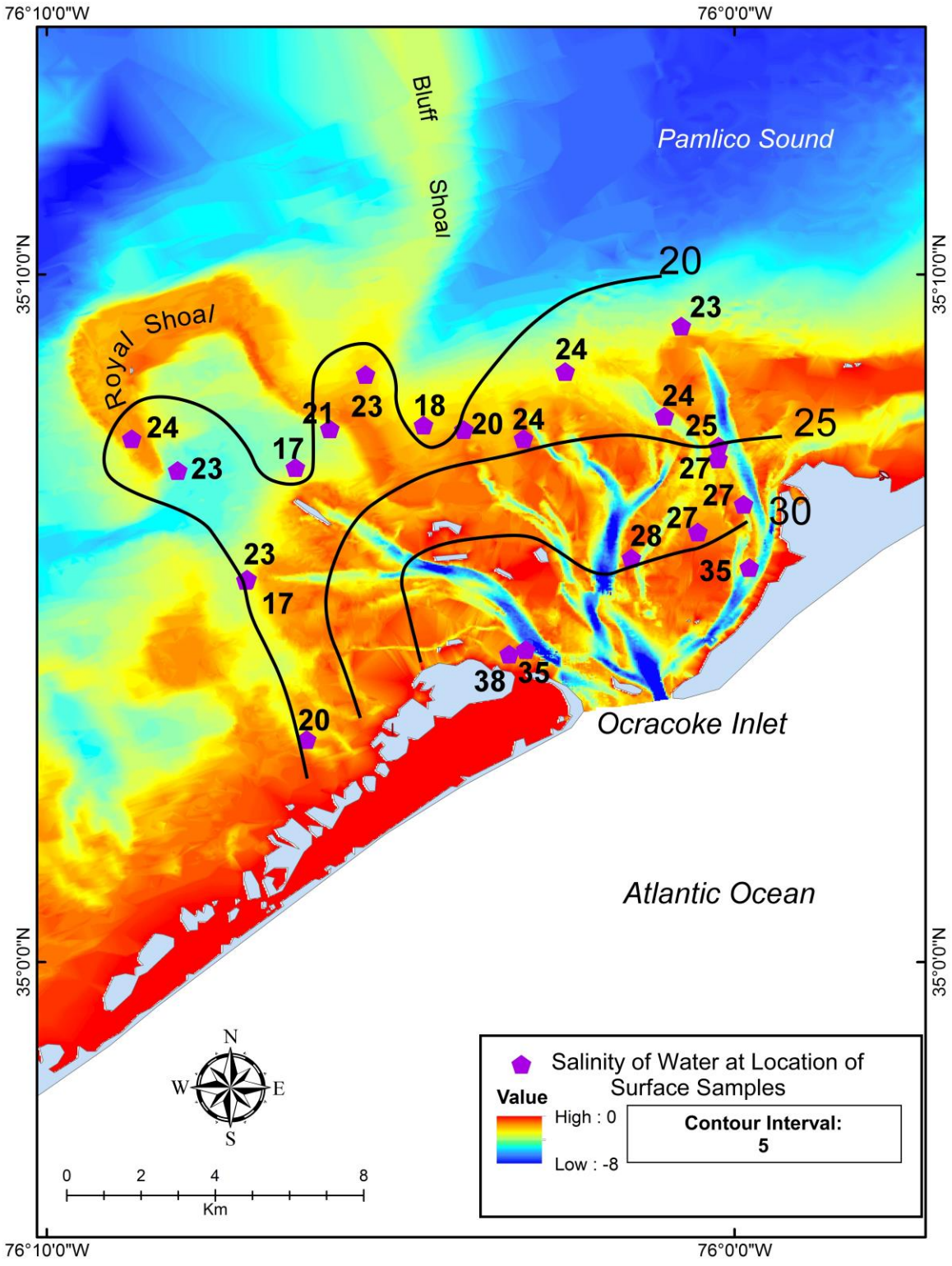

Figure 8. A contour map of the salinity at each surface sample location.

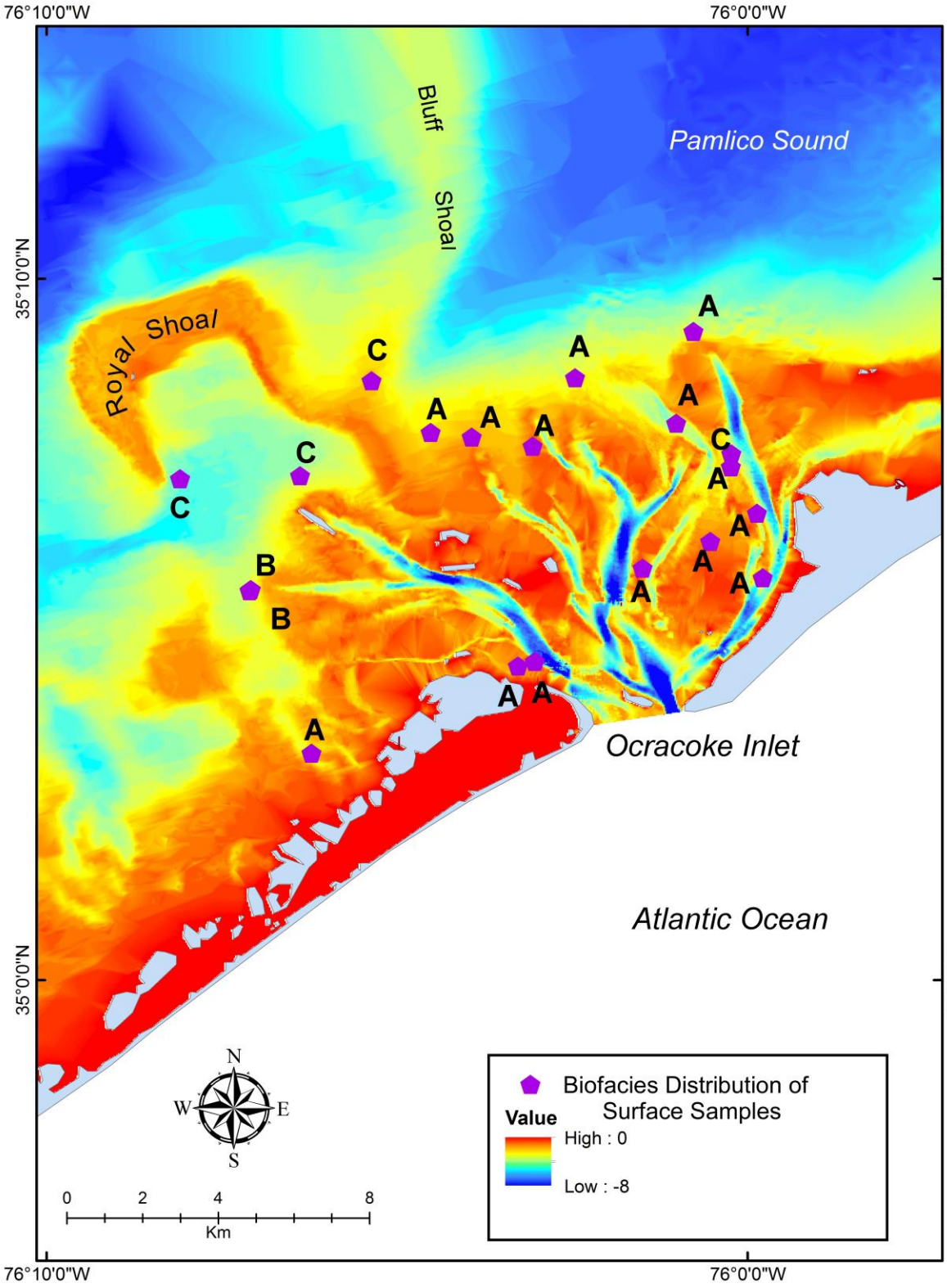

Figure 9. A biofacies distribution map of the surface samples included in the cluster analysis.

The relative abundance of *Elphidium excavatum* decreased slightly towards the inlet (Figs. 7, 8, 9; Tables 7, 8). *Ammonia parkinsoniana* clearly decreased in relative abundance towards the inlet (Figs. 7, 8, 9). Secondary species, characteristic of normal marine salinity conditions (Murray, 1969; Schnitker; 1971; Workman; 1981; Abbene et al., 2006; Foley, 2006; Vance et al., 2006) generally increased in relative abundance towards the inlet (Figs. 7, 8, 9; Tables 7, 8).

4.4.2 Cluster Analysis

The dendrogram resulting from a cluster analysis of 45 surface and down-core samples containing 28 species displays four biofacies (named A–D) (Fig. 10; Appendices I, J). Species richness was highest in Biofacies A and B (Table 8).

Table 8. Mean percent abundance of taxa in four biofacies defined by cluster analysis.

Biofacies A 16 samples, 27 taxa	**Mean %** **(Range %)**	**Biofacies B** 11 samples, 22 taxa	**Mean %** **(Range %)**	**Biofacies C** 15 samples, 9 taxa	**Mean %** **(Range %)**	**Biofacies D** 3 samples, 1 taxa	**Mean %**
Elphidium excavatum	67.10 (27–87)	*Elphidium excavatum*	56.18 (30–65)	*Elphidium excavatum*	86.72 (75–96)	*Elphidium excavatum*	100
Elphidium mexicanum	7.75 (2–48)	*Ammonia parkinsoniana*	24.95 (1–48)	*Ammonia parkinsoniana*	12.05 (3–22)		
Ammonia parkinsoniana	7.08 (6–10)	*Ammonia tepida*	5.80 (16-44)	*Elphidium galvestonense*	0.45 (1.9–4)		
Elphidium galvestonense	5.07 (1–17)	*Elphidium galvestonense*	3.47 (1–17)	*Hanzawaia strattoni*	0.11 (0.81-0.85)		
Hanzawaia strattoni	3.26 (1–9)	*Elphidium gunteri*	1.99 (1–26)	*Elphidium* sp.	0.11 (0–1.61)		
Elphidium gunteri	2.79 (1–25)	*Elphidium mexicanum*	1.72 (2–48)	*Elphidium mexicanum*	0.06 (0–0.93)		
Cibicides lobatulus	1.40 (1–7)	*Cibicides lobatulus*	1.06 (1–7)	*Ammonia tepida*	0.05 (0–0.85)		
Quinqueloculina seminula	0.77 (0.7–5)	*Nonionella atlantica*	0.91 (1–4)	*Buccella inusitata*	0.05 (0–0.81)		
Haynesina germanica	0.68 (0.6–3)	*Hanzawaia strattoni*	0.79 (1–9)	*Haynesina germanica*	0.05 (0–0.81)		
Nonionella atlantica	0.64 (0.8–4)	*Elphidium poeyanum*	0.56 (0.84–1.61)				
Elphidium sp.	0.38 (1–3)	*Haynesina germanica*	0.43 (0.76–2.59)				
Elphidium translucens	0.30 (0.8–2)	*Bolivina lowmani*	0.28 (0.7–2.3)				
Quinqueloculina sp.	0.27 (0.9–2)	*Elphidium* sp.	0.15 (0.78–0.88)				
Elphidium subarcticum	0.22 (0.8–1.08)	*Valvulineria* sp.	0.14 (0.76–0.78)				
Trifarina angulosa	0.18 (0.7–1.27)	*Quinqueloculina seminula*	0.14 (0.74–4.46)				
Quinqueloculina lamarckiana	0.17 (0.8–2)	*Guttulina lactea*	0.07 (0–0.66)				
Ammonia tepida	0.16 (0–2)	*Rosalina* sp.	0.07 (0–0.79)				
Elphidium poeyanum	0.15 (0.8–1.6)	*Buccella inusitata*	0.07 (0–0.79)				
Rosalina floridana	0.15 (0-2)	*Rosalina floridana*	0.07 (0–2.42)				
Buccella inusitata	0.15 (0.7–0.9)	*Elphidium subarcticum*	0.07 (0.66–1.08)				
Rosalina sp.	0.11 (0–1.79)	*Trifarina angulosa*	0.07 (0.72–1.27)				
Trochammina sp.	0.11 (0.8–0.93)	*Quinqueloculina jugosa*	0.07 (0–0.72)				
Miliolinella subrotunda	0.11 (0–1.72)						
Asterigerina carinata	0.10 (0.81–0.86)						
Quinqueloculina jugosa	0.10 (0.7–4.5)						
Valvulineria sp.	0.10 (0-0.84)						
Guttulina lactea	0.04 (0–0.66)						

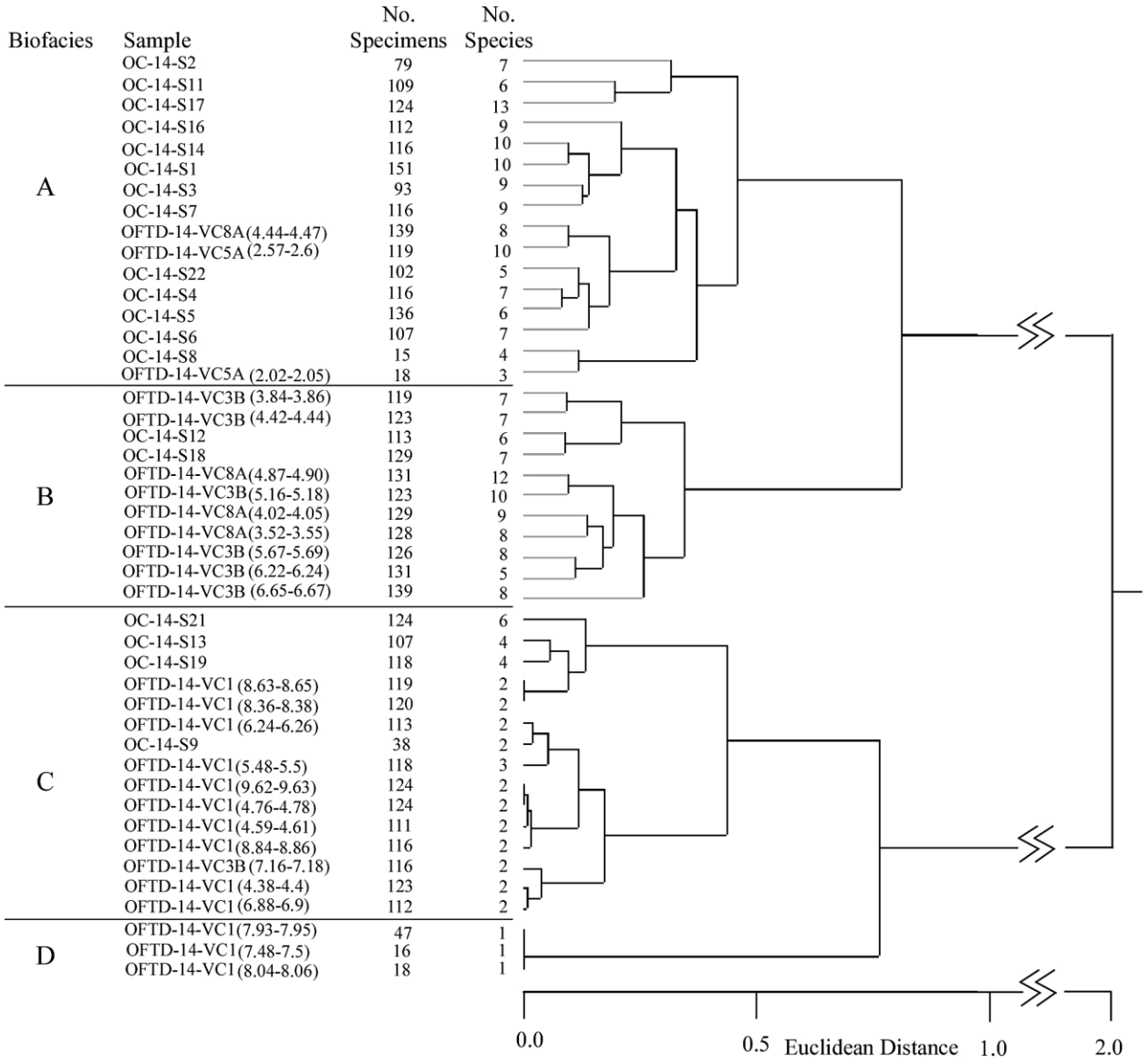

Figure 10. Dendrogram resulting from cluster analysis (Ward's Linkage, Euclidean distances) of surface and down-core foraminiferal assemblage data. Four biofacies we defined at Euclidean distance value of 0.5.

Biofacies A comprised 16 samples (12 surficial and four down-core) and 27 taxa (Fig. 10). The three most abundant species were *Elphidium excavatum* (67%), *Elphidium mexicanum* (8%), and *Ammonia parkinsoniana* (7%) (Tables 7, 8). This biofacies contained 21 rotaliid species, five miliolid species, and one textulariid species. All samples were collected near the proximal OFTD and from tidal channels within the intermediate OFTD (Fig. 1).

Biofacies B comprised 11 samples (two surficial, nine down-core) and 22 taxa (Fig. 10). The mean percent of the three most abundant species were *Elphidium excavatum* (56%), *Ammonia parkinsoniana* (25%), and *Ammonia tepida* (6%) (Tables 7, 8). This biofacies contained 19 rotaliid species and three miliolid species. Generally, samples within this biofacies were collected from the intermediate OFTD (Fig. 1).

The 15 samples and nine taxa of Biofacies C contained exclusively rotaliid species, with the two most abundant being *Elphidium excavatum* (mean 87%) and *Ammonia parkinsoniana* (mean12 %) (Tables 7, 8). Species richness is lower than in Biofacies A and B (Fig. 10). All samples within this biofacies were collected around the northwest area of the OFTD region, further from the mouth of the inlet (distal OFTD region, with a few samples in the intermediate OFTD) than samples comprising Biofacies A and B.

Few specimens (Fig. 10) and a single taxon, *Elphidium excavatum*, characterized Biofacies D (Table 8). All samples within this biofacies were from VC1 (Appendix A), collected within a channel at the end of the sandy, shallow, Royal Shoal (Fig.1) and located within a paleovalley. This core was furthest from the mouth of the inlet at the northwest end of the study area on the distal portion of the OFTD region.

4.5 Environmental Facies of the OFTD Area

Foraminiferal and lithological data have provided the information necessary to develop six environmental facies (EFs) (Table 9). These EFs were compared to previously documented foraminiferal and lithological data from the Pamlico Sound and surrounding areas (Abbene, 2006; Rosenberger, 2006; Hale, 2008; Foley, 2009; Metger, 2009; Pruitt et al., 2010; Peek et al., 2013). Below, EFs are discussed from VI to I, generally in terms of increasing salinity within the OFTD region. To describe the location of each EF within the OFTD region the following terms are used: (1) distal (farthest from the inlet), (2) intermediate, and (3) proximal (closest to inlet mouth).

Table 9. Environmental Facies descriptions and characteristics. Mbsl- meters below sea level, and mbsf-meters below seafloor.

EF	Lithologies & Associated Characteristics	Biofacies	Foraminiferal Species (listed decreasing in abundance)	Approximate Depth Range (mbsl)	Cores (VC) & Surface (S) Samples Present In (mbsl)	Cores (VC) & Surface Samples (S) that contain Planktonic Species (mbsl)	Location/ Presence of Foraminiferal Core (VC) & Surface (S) Samples	Barren Samples
I. High Energy Normal marine salinity FTD	Gravelly sand and sand: shells, mottling, mud burrows, & laminations	A	*Elphidium excavatum, Elphidium mexicanum, Ammonia parkinsoniana, Elphidium galvestonense, Hanzawaia strattoni, Elphidium gunteri, Cibicides lobatulus, Quinqueloculina seminula, Haynesina germanica, Nonionella atlantica, Elphidium* sp., *Elphidium translucens, Quinqueloculina* sp., *Elphidium subarcticum, Trifarina angulosa, Quinqueloculina lamarckiana, Ammonia tepida, Elphidium poeyanum, Rosalina floridina, Buccella inusitata, Rosalina* sp., *Trochammina* sp., *Miliolinella subrotunda, Asterigerina carinata, Quinqueloculina jugosa, Valvulineria* sp., *Guttulina lactea*	4.70–1.50; VC5A: 2.64–1.50; VC8A: 4.70–4.30	VC5A: (2), VC8A: (1); S (13): S1, S2, S3, S4, S5, S6, S7, S8, S11, S14, S16, S17, S22 (top of VC5A)	S14, S16, S17; VC5A (2.60–2.57)	Intermediate & Proximal OFTD	
II. Low Energy Normal marine salinity FTD	Gravelly muddy sand & muddy sand; shells, mottling, mud burrows, laminations, & charcoal & wood debris	B	*Elphidium excavatum, Ammonia parkinsoniana, Ammonia tepida, Elphidium galvestonenese, Elphidium gunteri, Elphidium mexicanum, Cibicides lobatulus, Nonionella atlantica, Hanzawaia strattoni, Elphidium poeyanum, Haynesina germanica, Bolivina lowmani, Elphidium* sp., *Valvulineria* sp., *Quinqueloculina seminula, Guttulina lactea, Rosalina* sp., *Buccella inusitata, Rosalina floridana, Elphidium subarcticum, Trifarina angulosa, Quinqueloculina jugosa*	6.70–3.0; VC3B: 6.70–3.30; VC8A: 5.30–3.30	VC3B: (6), VC8A: (3); S (2): S12, S18 (top of VC3B)	VC3B (4.44–4.42, 5.18–5.16, 5.69–5.67); VC8A (4.05–4.02, 4.90–4.87)	Intermediate OFTD	
III. High salinity estuarine	Sandy mud, muddy sand, & gravelly muddy sand; charcoal, wood, & shell fragments	C	*Elphidium excavatum, Ammonia parkinsoniana, Elphidium galvestonenese, Hanzawaia strattoni, Elphidium* sp., *Elphidium mexicanum, Ammonia tepida, Buccella inusitata, Haynesina germanica*	9.50–3.0; VC1: 9.50–4.0; VC3B: 7.40–6.70; VC8A: 3.30–3.0	VC1: (13), VC3B: (1); S (4): S9, S13, S19 (top of VC1), S21 (top of VC8A)	S19, S21	Distal OFTD; S21 exception-intermediate OFTD	
IV. Undetermined estuarine (mid–to high salinity)	Muddy sand with rare charcoal & wood debris	D	*Elphidium excavatum*	8.20–7.40; VC1	VC1: (3)		Distal OFTD	
V. Sand Flat/Shoal	Slightly gravelly sand, & sand; shells, shell fragments, mud mottling	N/A	*Elphidium excavatum, Ammonia parkinsoniana, Elphidium gunteri*	3.70–1.20; VC2B	VC2B: (2); S (2): S10, S15		Distal OFTD	VC2B: (2.88–2.85); S20 (top of VC2B)
VI. Freshwater Riverine Swamp Forest	Peat & Mud; charcoal & wood debris	N/A	Barren	9.60–9.50; VC1	VC1: (2)		Distal OFTD	VC1: (9.52–9.50, 9.60–9.58)

4.5.1 Environmental Facies VI: Riverine Freshwater Swamp Forest Environment

Environmental Facies VI (EF VI), present only in VC1, represents a riverine swamp forest and occurs from ca. 9.60–9.50 mbsl. Samples within EF VI are barren of foraminifera (Figs, 11, 12; Table 9; Appendices E, G). EF VI is characterized by freshwater peat and mud with charcoal and wood fragments (Appendix A; Table 5). The peat sample is dated at ca. 7200 cal yr BP (Table 2). EF VI overlies a major paleovalley (P3) below Royal Shoal, and represents the oldest Holocene deposits in the study area.

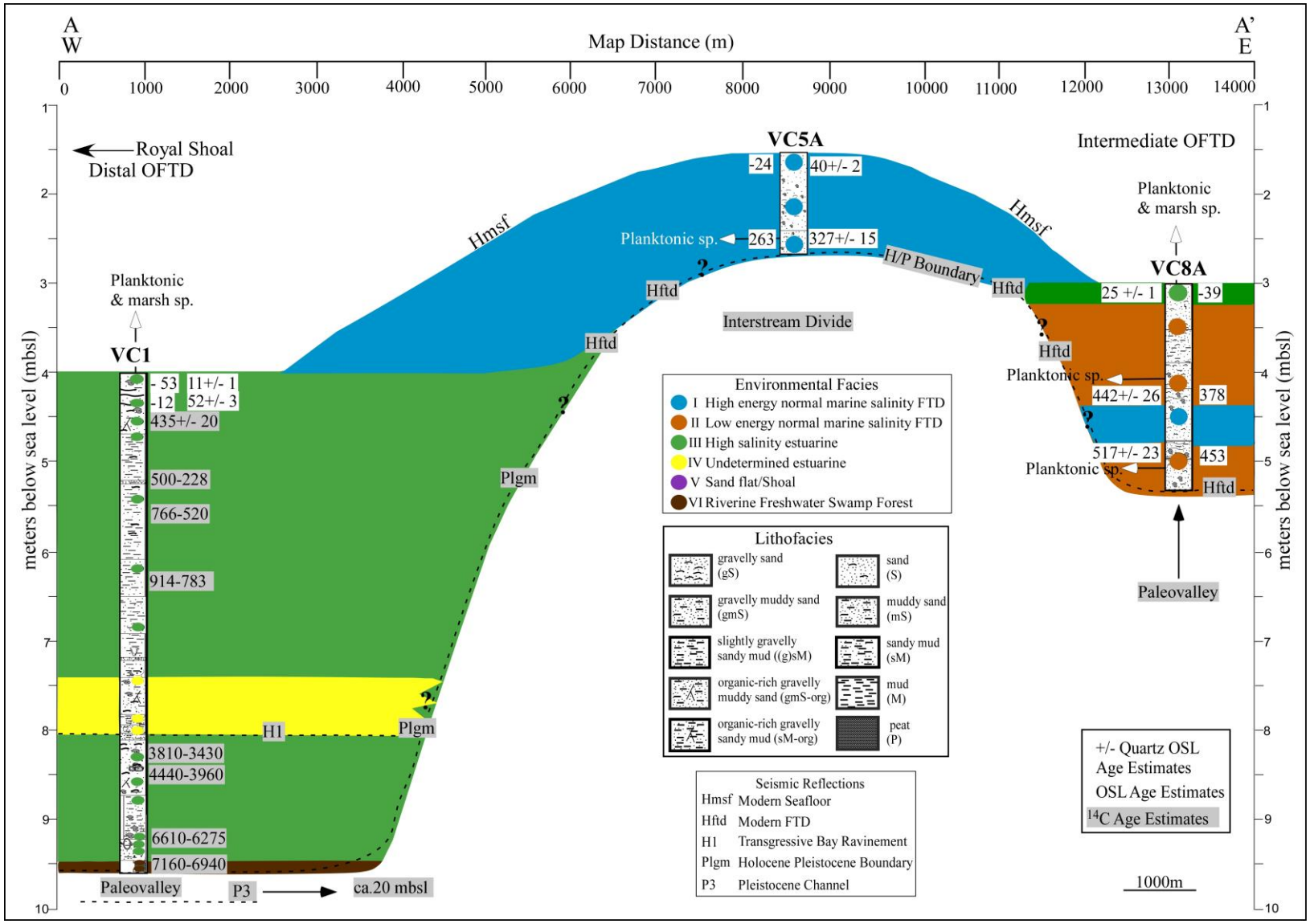

Figure 11. Transect A to A'. A shore-normal transect including cores VC1, VC5A, and VC8A.

4.5.2 Environmental Facies V: Sand Flat/Shoal Environment

Environmental Facies V (EF V) represents a sand flat/shoal environment. EF V is present in VC2B from ca. 3.70–1.20 mbsl and two surficial samples (S10, S15) (Figs. 8, 9, 10, 12; Tables 7, 9). Foraminiferal samples from EF V are barren or contain few specimens (≤ 15 specimens) and species (*Ammonia parkinsoniana, Elphidium excavatum,* and *Elphidium gunteri*) (Tables 7, 9; Appendices E, G). The absence or low abundance of foraminifera in these samples is likely the result of post mortem destruction in a mobile sand environment (Boltovskoy and Wright, 1976; Goldstein, 1995; Murray, 2006) (Appendices E, G). Typical lithofacies of EF V consist of moderately sorted, fine-to medium-grained slightly gravelly sand and massive, sand beds (Tables 5, 6). Shells, shell fragments, and mottling occur as common characteristics of the lithofacies (Tables 5, 6; Appendix A). EF V characterizes the distal area of the OFTD region, including Royal Shoal (Figs. 1, 12).

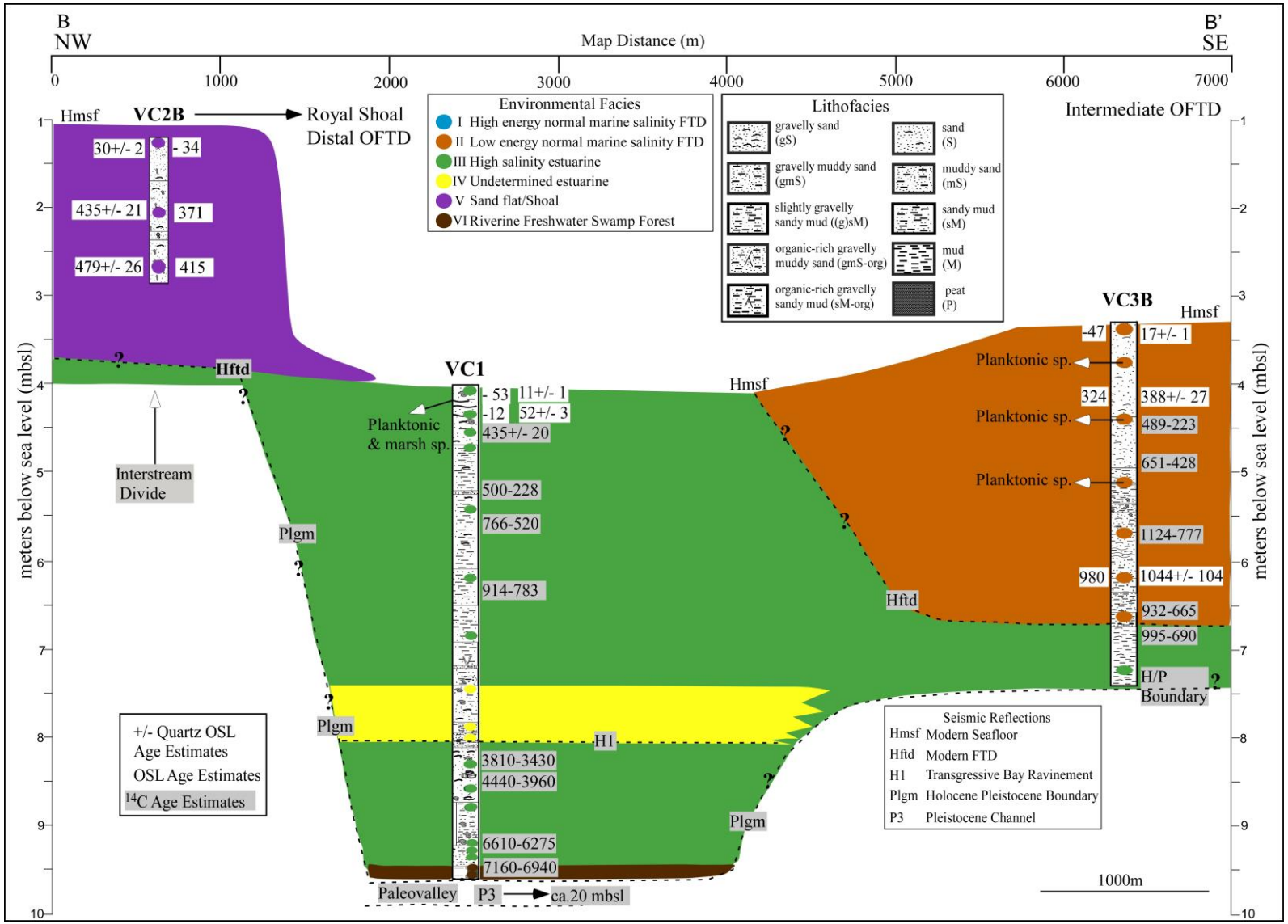

Figure 12. Transect B to B'. A shore-normal transect including cores VC2B, VC1, and VC3B.

4.5.3 Environmental Facies IV: Undetermined Estuarine Environment

Environmental Facies IV (EF IV) represents an undetermined estuarine environment, probably of mid- to high salinity given the presence of calcareous foraminifera (Metger, 2009; Grand Pre et al., 2011), and occurs from ca. 8.20–7.40 mbsl. All foraminiferal samples in EF IV are from VC1, (Figs. 11, 12; Table 9) and are characterized by Biofacies D (Fig. 10; Tables 8, 9; Appendix G) containing only *Elphidium excavatum*. EF IV is underlain and overlain by EF III and may represent a similar environment but with poorly preserved foraminifera. The typical lithology in EF IV is moderately sorted muddy sand with rare charcoal and wood debris (Tables 5, 9; Appendix A). Samples in EF IV are located within the distal OFTD region, including Royal Shoal, and overlie the base of a major paleovalley (P3) (Figs. 1, 11, 12; Table 9).

4.5.4 Environmental Facies III: High Salinity Estuarine

Environmental facies III (EF III) represents a high salinity estuarine environment. This EF III is recognized in three vibracores: VC1, VC3B, and VC8A, and four surficial samples: S9, S13, S19-top of VC1, and S21-top of VC8A (Figs. 11, 12, 13; Tables 7, 8, 9), and is characterized by Biofacies C (Fig. 10; Tables 7, 8, 9). This biofacies contains typical high salinity estuarine assemblages dominated by *Elphidium excavatum* (87 %) and *Ammonia parkinsoniana* (12 %) with secondary or rare species (depending on %) *Elphidium galvestonenese, Hanzawaia strattoni, Elphidium mexicanum, Buccella inusitata, and Haynesina germanica* (Tables 7, 9; Appendices E, G) (Grossman and Benson, 1967; Abbene et al., 2006; Foley, 2006; Hale, 2008; Pruitt, 2008; Metger, 2009; Pruitt et al., 2010; Grand Pre et al., 2011; Peek et al., 2013). Lithologies of EF III are dominantly sandy mud, muddy sand, and gravelly muddy sand (Table 5; Appendix A) with shells, shell fragments, organics, and mud mottling. EF III characterizes the distal OFTD area, including Royal Shoal, and occurs within the base of a major paleovalley (P3), with the exception of S21 (Figs. 1, 8, 9, 11, 12, 13; Table 9).

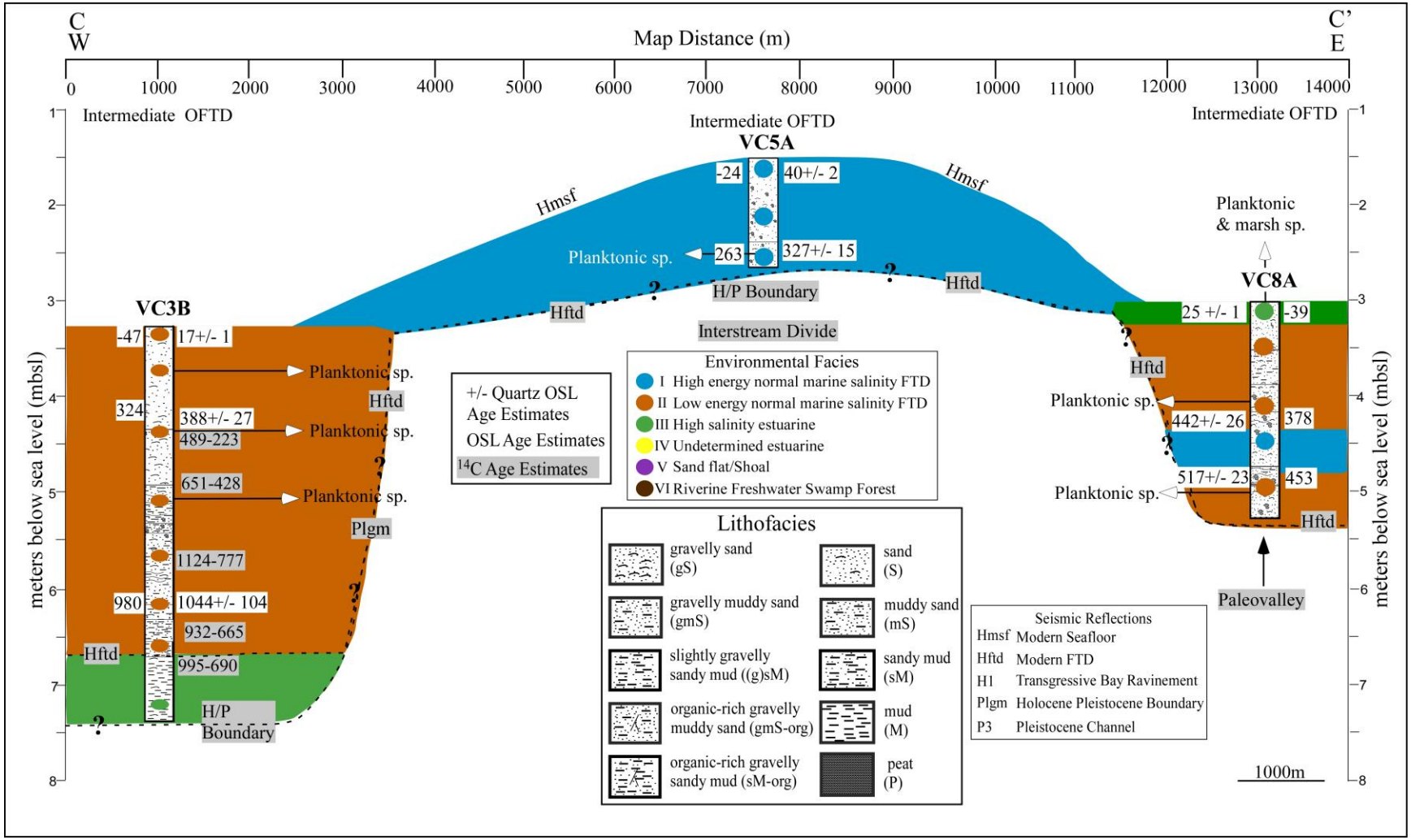

Figure 13. Transect C to C'. A shore-parallel transect including cores VC3B, VC5A, and VC8A.

4.5.5 Environmental Facies II: Normal Marine Salinity FTD (Low Energy) Environment

Environmental Facies II (EF II) represents low energy normal marine salinity FTD environments and occurs from ca. 6.70–3.00 mbsl (Figs. 11, 12, 13; Table 9). EF II is recognized in VC3B and VC8A and surficial samples S12 and S18 (top of VC3B). Biofacies B characterizes EF II (Fig. 10; Tables 6, 7, 9) and contains species characteristic of the inner continental shelf as well as FTD environments of North Carolina (Grossman and Benson, 1967; Schnitker, 1971; Workman, 1981; Abbene et al., 2006; Rosenberger, 2006; Hale, 2008; Metger, 2009; Smith et al., 2009; Grand Pre et al., 2011; Peek et al., 2013). Assemblages are more diverse than those of Biofacies C and slightly less than those of Biofacies A (Fig. 10; Tables 8, 9). Planktonic specimens are also present in EF II (Figs. 11, 12, 13; Table 9; Appendices E, G) and are indicative of normal marine salinity influences (Schnitker, 1971). Lithofacies of EF II are dominantly gravelly muddy sand and muddy sand. Shells, shell fragments, mottling, mud burrows, and heavy mineral laminations are common (Tables 5, 6, 9; Appendices A, B, C). EF II occurs within the west and east intermediate OFTD (Figs. 1, 11, 12, 13; Table 9).

4.5.6 Environmental Facies I: Normal Marine Salinity FTD (High Energy) Environment

Environmental Facies I (EF I) is similar to EF II but represents high energy normal marine salinity FTD environments (Table 9). EF I occurs from ca. 4.70–1.50 mbsl (Figs. 11, 13; Table 9) in VC5A and VC8A (Figs. 1, 11, 13; Table 9) and in the majority (13) of surficial samples (Tables 6, 7, 9). The assemblages of Biofacies A are typical of normal marine salinity FTDs of North Carolina (Fig. 10; Tables 7, 8) (Grossman and Benson, 1967; Schnitker, 1971; Workman, 1981; Abbene et al., 2006; Rosenberger, 2006; Culver et al., 2007; Hale, 2008; Metger, 2009; Smith et al., 2009; Grand Pre et al., 2011; Peek et al., 2013). EF I assemblages contain larger, more robust specimens than Biofacies B, indicating higher energy regimes. Planktonic species are also present in EF I and indicate an offshore, Gulf Stream provenance (Figs. 11, 13; Table 9; Appendices E, G). Lithofacies of EF I are characteristic of high energy regimes and are composed of gravelly sand with shells, mottling, mud burrows, and heavy mineral laminations (Tables 5, 6, 9; Appendices A, B, C). Generally, samples within EF I are located

within the northeastern and eastern intermediate OFTD. S16 and S17, grouped within EF I, are the only surface samples located within the proximal OFTD (Fig. 1; Tables 7, 9). EF I represents the modern distribution of OFTD foraminifera and lithologies (Figs. 1, 7, 8, 9, 13; Tables 6, 7, 9).

5.0 Discussion

Episodes of rapid climate change during the Quaternary are documented globally, and have had an effect on the Pamlico Sound region (Riggs et al., 1995; Abbene et al., 2006; Culver et al., 2007; Kemp et al., 2009; Mallinson et al., 2010a, 2010b, 2011; Grand Pre et al., 2011). Mallinson et al. (2010a) and Culver et al. (2011) reveal the geomorphology and the stratigraphy (e.g., interstream divides, relict inlets, relict drainage patterns) of the Pamlico Sound region. The evolution and modern morphology of this area is the result of the interaction between many geological processes acting on different time scales, among which sea-level oscillations, antecedent topography, sediment flux, and coastal oceanographic processes are the most significant. Although this study focuses primarily on the Holocene, the Pleistocene units and general stratigraphic framework are significant in their control on the modern morphology of this coastal system (Riggs et al., 1995; Mallinson et al., 2010a).

5.1 Pleistocene Geologic Evolution of the OFTD Area

Mallinson et al. (2010a) documented seven regionally continuous high amplitude reflections that defined six stratigraphic units in the Pleistocene strata underlying the Pamlico Sound region. Three of the seismic reflections from the OFTD area (Table 4) correlate to Pleistocene reflections defined by Mallinson et al. (2010a) but they occur in the study area at shallower depths as a result of the regional gradient and Quaternary thinning southward to the Cape Lookout High (Mallinson et al., 2010a; Thieler et al., 2014).

Four Pleistocene reflections are defined in this study: P1, P2, P3, and Plgm (Table 4). The P3 reflection (Fig. 4A) defines a prominent valley, that in the subsurface, meanders around Bluff Shoal (Pleistocene) and Royal Shoal (modern), from the northeast to the southwest (Figs. 1, 6B). P3 is deepest beneath the paleovalleys associated with the paleo-Neuse/Tar Rivers, and is the shallowest beneath the interstream divides (Figs. 4A, 5A, B, C). The valley-fill is characterized by steeply dipping clinoforms suggesting fluvial fill (SU 4) overlain by horizontally-bedded estuarine deposits (SU 4) (Figs. 4, 5A, B, C). The stratigraphic position of this paleovalley suggests that the P3 channel was incised during MIS 6,

and filled during MIS 5. The valley-fill is truncated by Q50 of Mallinson et al. (2010a) which is the TRS (Figs. 4A, 5, 6A; Table 4) associated with Termination II (the deglaciation and sea-level rise associated from MIS 6 to MIS 5) (Figs. 4, 5; Table 4).

The Plgm reflection defined in this study correlates to the Q99 reflection defined by Mallinson et al. (2010a) (Figs. 2, 4B, 5; Table 4). This reflection defines the paleo-drainage patterns of the paleo-Neuse/Tar River and Pamlico Creek and associated interstream divides, and represents a Pleistocene subaerial unconformity. The surface provided a platform upon which the Outer Banks barrier island system developed (Riggs et al., 1995; Mallinson et al., 2005; 2010a). The paleotopography that was flooded during the Holocene is identified from the transition of fluvial to more estuarine dominated environments which marks the Holocene evolution of the Pamlico Sound area.

5.2 Mid-to Late-Holocene Evolution of the OFTD Area

Data from this study provide for an understanding of the geologic response of this coastal system to sea-level rise and other processes since ca. 7200 cal yr BP (Fig. 14; Tables 2, 3). The correlation between litho-, bio-, and seismic facies is established by integrating EFs into constructed transects (Figs. 11, 12, 13) to interpret the modern and paleo-depositional environments of the OFTD region and Royal Shoal areas during the Holocene (Table 9). Five time intervals are discussed according to the distribution of EFs and their associated interpretations (Fig. 14). The longest core in this study, VC1, is the basis for much of the interpretation of the Holocene evolution between ca. 7200–1100 cal yr BP. All five cores (Appendix A) provide information on the past ca. 1100 years.

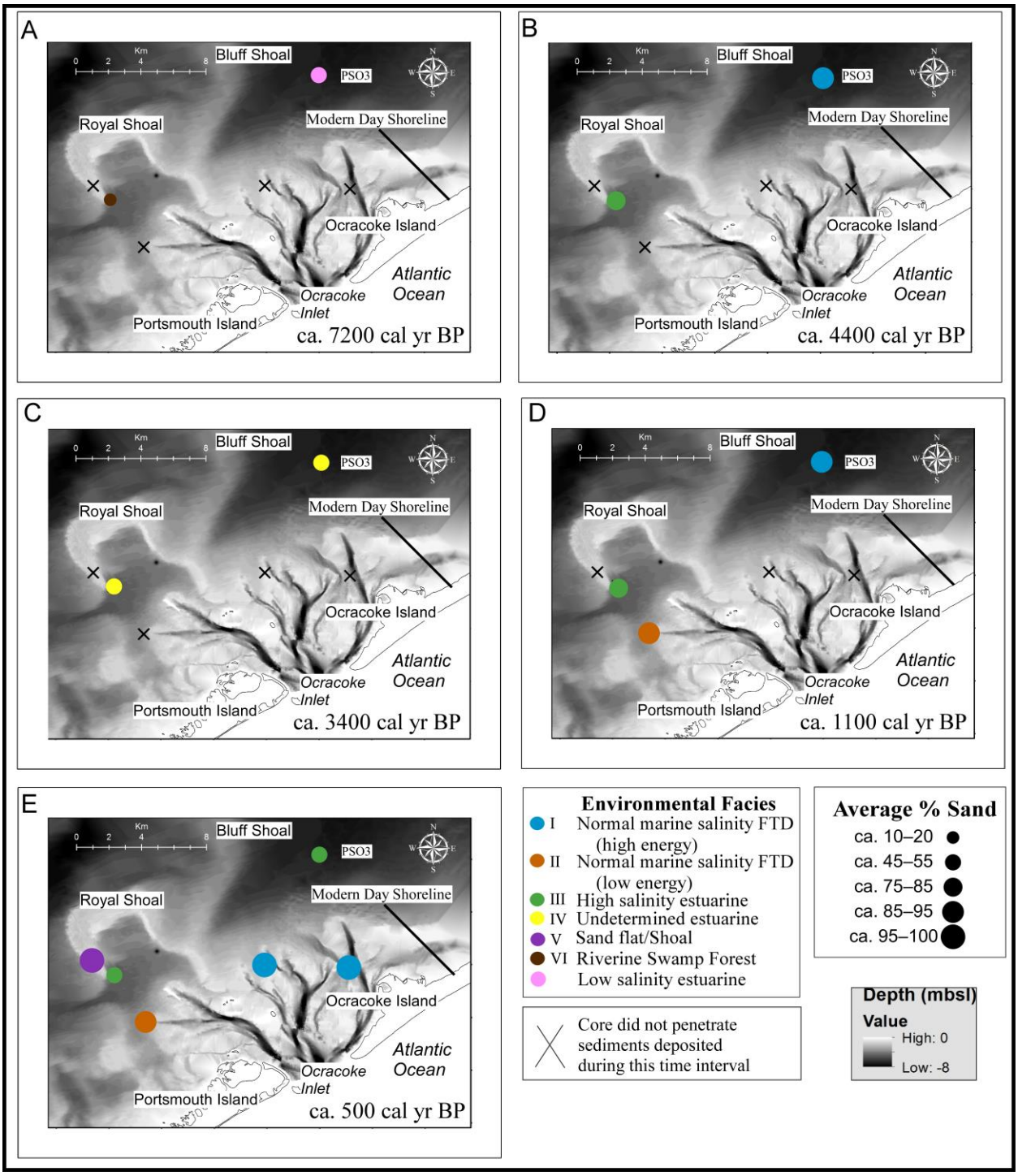

Figure 14. Five Holocene time intervals (A-E) show inferred paleoenvironmental reconstructions of the OFTD area (Culver et al., 2007; Grand Pre et al., 2011). The modern day shoreline is plotted for a geographic reference point for each time interval. Average % sand is illustrated in each time interval for each core as a size scaled circle. (A) Represents when estuarine conditions started to form from riverine swamp forest environments when paleo-valleys were flooded ca. 7200 cal yr B.P. (B) High salinity estuarine (VC1) and normal marine salinity waters (PS03) derived from northward migrating warm-core

filaments dominate the OFTD as a result of a segmentation of barriers destroyed around ca. 4500 cal yr BP. (C) Represents when barrier islands have rebuilt and undetermined estuarine (likely mid-to high salinity) conditions (VC1 and PS03) prevailed around ca. 3400 cal yr BP. (D) Around ca. 1100 cal yr BP the earliest record of normal salinity and FTD deposits are recorded (VC3B). High salinity estuarine conditions characterized VC1 sediments. Barrier island collapse during the MCA allowed for normal marine salinity waters to flow into the once estuarine conditions at the location of VC3B and PS03. (E) Around ca. 500 cal yr BP to present day Royal Shoal (VC2B) was active and associated sand flat and shoal environments resulted from sediments being eroded from the Pleistocene Bluff Shoal during the LIA. Ocracoke Inlet existed at this time allowing for normal salinity waters to influence FTD deposition (VC3B, VC5A, and VC8A). Barrier Island reformation allowed for normal marine salinity conditions to be replaced by estuarine conditions at the location of PS03, and estuarine conditions continued to characterize VC1 sediments.

5.2.1 7200 to 6900 cal yr BP

Rising sea level caused the initial flooding of the paleo-Pamlico Creek and Tar-Pamlico and Neuse River valleys creating drowned river estuaries ca. 7200 cal yr BP (Culver et al., 2007; Grand Pre et al., 2011). The westernmost core of this study (VC1) is located within the Neuse/Tar paleovalley and provides the longest Holocene record within the study area (Fig.1; Appendix A). The Holocene/Pleistocene Boundary (Plgm) is interpreted to occur between a fossiliferous blue clay and an overlying peat (Figs. 5, 6A) and mud sequence at ca. 9.60 mbsl. The peat, dated at ca. 7160–6940 cal yr BP, returned a $\delta^{13}C$ of -26.7 ‰ (Table 2) typical of terrestrial plant fragments (C3). The peat is interpreted as representing a freshwater riverine swamp forest depositional environment (EF VI) (Figs. 11, 12, 14A).

5.2.2 6900 to 4400 cal yr BP

Overlying the peat and mud is muddy sand with the surf clam *Mactra fragilis* that returned a radiocarbon age of 6610–6275 cal yr BP and a $\delta^{13}C$ of -5.1‰ (Figs. 11, 12; Tables 2, 9). *Mactra fragilis* has a reported salinity tolerance of 10–30 (Grabe et al., 1995). The $\delta^{13}C$ value suggests the influence of dissolved inorganic carbon (DIC) from organic sources in shell production (Mook, 1971). Such conditions are found today in the upper reaches of the estuaries where swamp forests provide substantial light carbon (^{12}C) to the local waters (Matson and Brinson, 1990; Corbett et al., 2007). The overlying unit is barren of foraminifera at the base, but grades upward into EF III, suggesting an upward increase in salinity. Thus the transition from freshwater swamp forest to mid-to high salinity estuarine at the site of

VC1 occurred between ca. 6900–6600 cal yr BP (Table 2). Lithofacies consist of interlaminated (mm) muddy sand and sandy mud with decreasing organic content (Figs. 11, 12; Tables 5, 9; Appendix A) suggesting tidal deposition. This is not inconsistent with previous studies documenting the initial flooding of paleovalleys ca. 7500 cal yr BP (Culver et al., 2007; Hale, 2008; Metger, 2009; Grand Pre et al., 2011).

5.2.3 4400 to 3400 cal yr BP

Continuation of mid-to high salinity estuarine conditions (EF III) are indicated in VC1 by an articulated oyster shell with an age estimate of 4440–3960 cal yr BP (Figs. 11, 12, 14B; Tables 2, 9) and a *Mulina lateralis* that returned an age estimate of 3810–3430 cal yr BP (Table 2). Lithofacies present during this time interval are generally characterized by gravelly muddy sand with organics (Table 5; Appendix A). The gravelly sand lithofacies suggests an increase in energy associated with the coeval large-scale segmentation of Ocracoke Island as described by Culver et al. (2007) and Grand Pre et al. (2011), or possibly due to rapid expansion of the estuary as interfluves were overtopped (Zaremba et al., in review). During this same time interval, normal marine salinity conditions existed at the PS03 and OCR 07 S202 locations to the east of the OFTD region (Figs. 1, 2) (Hale, 2008; Metger, 2009; Culver et al., 2007; Grand Pre et al., 2011). This eastward increase in salinity is consistent with the modern salinity distribution across the southern Pamlico Sound (Wells and Kim, 1989; Abbene et al., 2006). Foley (2006) did not record normal marine salinity units in central Pamlico Sound during this time, but did find high salinity estuarine environments very similar to EF III (Figs. 11, 12, 14B). Data from this study provide further evidence for higher salinity waters penetrating into the southern Pamlico Sound at ca. 4400 cal yr BP (Fig. 14B).

5.2.4 3400 to ca. 1100 cal yr BP

Sometime after ca. 3400 cal yr BP (Appendix A) EF III was replaced by EF IV, characterized by a monospecific assemblage of *Elphidium excavatum* occurring in sandy mud and muddy sand lithofacies (Fig. 14C; Tables 5, 7, 9). In core PS03 this facies was interpreted as representing decreasing energy and

salinity, as barrier islands reformed following the ca. 4000 cal yr BP incursion of marine waters into the Pamlico Sound (Culver et al., 2007; Grand Pre et al., 2011).

5.2.5 ca. 1100 to ca. 500 cal yr BP

EF III, characterized by muddy sand and sandy mud and Biofacies C, overlies EF IV in VC1 (Tables 5, 7, 9; Appendix A). This VC1 unit contains two ^{14}C age estimates ranging from 914–753 to 766–520 cal yr BP (Figs. 11, 12, 14D; Tables 2, 9; Appendix A). Correlative sediments in VC3B are characterized by EF II (normal marine salinity/FTD) and provide ages ranging from 995–690 to 651–428 cal yr BP (Figs. 12, 13, 14D; Tables 2, 3, 5, 6; Appendix A). These data indicate a return to high salinity conditions in the OFTD area at ca. 1100 cal yr BP (Fig. 14D). EF II represents the earliest cored FTD facies in the study area (Figs. 11, 12, 13, 14D; Tables 2, 3, 5, 9; Appendix A). This age is consistent with the ca. 1100 cal yr BP segmentation of the southern Outer Banks (Culver et al., 2007; Grand Pre et al., 2011) and formation of the Hatteras Flats (Peek et al., 2013). The depth of seismic reflection Hftd is consistent with the depth of the first occurrence of EF II in VC3B (Fig. 5C; Tables 4, 5, 9). This boundary is characterized by mud below and gravelly sandy mud above (Appendix A). The overlying unit coarsens upward to a gravelly sand (Appendix A). This ca. 1.5 m thick upward coarsening unit was deposited between ca. 1100 and ca. 800 cal yr BP and is interpreted as distal FTD grading upward to a slightly more proximal facies (Figs. 12, 13 14D; Tables 2, 3, 9; Appendix A).

It is clear that the first deposition of the FTD sediments occurred at ca. 1100 cal yr BP within the paleovalley area at the VC3B location (Fig. 14D). It is not clear whether this indicates the initial formation of Ocracoke Inlet, or if it indicates a transgression of inlet facies into the area. The timing is coeval with the formation of the Hatteras Flats (Peek et al., 2013) and is suggestive of a regional-scale process of inlet formation during the MCA.

5.2.6 ca. 500 cal yr BP to present day

EF I and II characterize the youngest/uppermost OFTD deposits (ca. 500 cal yr BP to present day) in cores VC3B, VC5A, and VC8A (Figs. 1, 11, 12, 13, 14E; Tables 2, 3, 9). Ocracoke Inlet existed at this time allowing for normal marine salinity waters to influence FTD deposition (cores VC3B, VC5A, and VC8A). Barrier island reformation allowed for normal salinity conditions to be replaced by high salinity estuarine conditions at the location of PS03 (Culver et al., 2007; Grand Pre et al., 2011). EF V characterizes Royal Shoal deposits in core VC2B. During the same interval, VC1 continues to be characterized by high salinity estuarine (EF III) environments. EF I, II, and V are characterized by gravelly sand and sand lithofacies (Tables 5, 6, 9; Appendices A, B, C) with shells, shell fragments, mud mottling, and heavy mineral laminations indicating high energy conditions. EF V is barren of foraminifera, and EF I and EF II contain typical FTD and shelf foraminifera (Figs. 10, 12; Tables 8, 9; Appendices E, G). Radiocarbon and OSL age estimates suggest that Royal Shoal is a modern shoal and began to form ca. 500 cal yr BP (Figs. 3, 11, 12, 13, 14E; Tables 2, 3). The coarse nature of the sediments and the absence of foraminifera suggest that the sediment source for Royal Shoal is the Pleistocene strata associated with Bluff Shoal, as opposed to sand advected through Ocracoke Inlet (Figs. 1, 2, 5, 6B, 12, 14E; Table 9; Appendices A, B, C).

6.0 Conclusions

Dynamic modern (and paleo) FTD deposits of the OFTD region located on the east coast of USA beneath the Outer Banks provide a platform for barrier islands to migrate landwards. OFTD and surrounding estuarine deposits in the Pamlico Sound are identified through the use of litho-, bio-, and seismic facies coupled with geochronological data. Using a multifaceted data analysis approach, as compared to a single methodology, provides precise historical records used for paleoenvironmental interpretations around the OFTD region. Four biofacies were identified from foraminiferal assemblages which aided in defining six environmental facies that characterize the OFTD region and surrounding Pamlico Sound estuarine paleodepositional environments.

At ca. 7200 cal yr BP rising sea level caused the initial flooding of the paleo-Pamlico Creek drainage system that was characterized by freshwater swamp environment (EF VI). Around ca. 6900–6600 cal yr BP the area transitioned to a high salinity estuarine environment (EF III) which was maintained until ca. 3400 cal yr BP. A lower energy mid-to high salinity estuarine environment (EF IV) occurred from ca. 3400–1100 cal yr BP.

Based on OSL age estimates the OFTD first occurred in the study area ca. 1100 cal yr BP (VC3B) and Royal Shoal was active ca. 500 cal yr BP (VC2B). This study demonstrates the utility of OSL dating within modern and paleo active inlet and FTD areas, as the data presented here has proven to be reliable in providing a geochronologic framework.

Environmental facies changes seen in the OFTD area generally corroborate changes seen in other regions of the Pamlico Sound. The first occurrence of FTD sediments at ca. 1100 cal yr BP is coeval with increased inlet activity and the formation of the Hatteras Flats (Peek et al., 2013), although it is not clear if this marks the initial formation of Ocracoke Inlet. Litho-, bio-, and seismic facies are similar which corroborates Peek et al. (2013) interpretation that the Hatteras Flats are coalesced FTDs. Royal Shoal is a modern shoal that began to form ca. 500 cal yr BP based on OSL age estimates. The sediments that

characterize Royal Shoal are derived from the Pleistocene Bluff Shoal during the LIA. The OFTD region probably existed to the south of the study area when estuarine deposits characterized the study area and migrated northwards as sea-level rose.

References

Abbene, I.J., Culver, S.J., Corbett, D.R., Buzas, M.A., Tully, L.S., 2006. Distribution of foraminifera in Pamlico Sound, North Carolina over the past century. Journal of Foraminiferal Research, 36, 136–151.

Adamiec, G., Aitken, M.J., 1998. Dose-rate conversion factors: update. Ancient TL 16, 37–50.

Aitken, M.J., 1998. An Introduction to Optical Dating: Oxford: Oxford University Press, 280 p.

Allen, T.R., Oertel, G.F., Gares, P.A., 2012. Mapping coastal morphodynamics with geospatial techniques, Cape Henry, Virginia, USA. Geomorphology, 137, 138–149.

Andersen, H.V., 1952. Buccella, a new genus of the rotaliid foraminifera: Journal of Washington Academy Science, 42, 143–151.

Applin, E.R., Ellisor, A.E., Kniker, H.T., 1925. Subsurface stratigraphy of the coastal plain of Texas and Louisiana: American Association of Petroleum Geologists, Bulletin, 9, 79–122.

Barbouti, A., Rastin, B., 1983. A study of the absolute intensity of muons at sea level and under various thicknesses of absorber. Journal of Physics G: Nuclear Physics 9, 1577–1595.

Bartlett, G.A., 1966. Distribution and abundance of foraminifera and theocamoebina in Miramichi River and Bay. Bedford Institute of Oceanography, 66–2, 1–104 p.

Blott, S.J., Pye, K., 2001. Grain size statistics program. Earth Surface Processes and Landforms, 26, 1237–1248.

Boothroyd, J.C., 1978. Mesotidal inlets and estuaries. In: R.A. Davis Jr. (eds.). Coastal Sedimentary Environments, Springer, New York, N.Y., 187–360.

Boltovskoy, E., Wright, R., 1976. Recent Foraminifera. The Hague: Dr. W. Junk b.v., 515 p.

Briffa, K.R., Barholin, T.S., Eckstein, D., Jones, P.D., Karlen, W., Schweingruber, F.H., Zetterberg, P., 1990. A 1400-year tree-ring record of summer temperatures in Fennoscandia. Nature, 346, 434–439.

Buzas, M.A., 1979. The measurement of species diversity. In: Lipps J.H., Berger, W.H., Buzas, M.A., Douglas, R.G., Ross, C.A. (eds.). Foraminiferal Ecology and Paleoecology. Society of Economic Paleontologists and Mineralogists, Short Course, 6, 3–10.

Buzas, M.A., 1990. Another look at confidence limits for species proportions. Journal of Paleontology, 64, 842–843.

Catuneanu, A., Steel, R.J., 2002. Transgressive deposits: a review of their variability. Earth Science Reviews, 62, 187–228.

Cronin, T., Willard, D., Karlsen, A., Ishman, S., Verardo, S., McGeehin, J., Kerhin, F., Holmes, C., Colman, S., Zimmerman, A., 2000. Climate variability in the eastern United States over the past millennium from Chesapeake Bay Sediments. Geology, 28, 3–6.

Cronin, T.M., Dwyer, G.S., Kamiya, T., Schwede, S., Willard, D.A., 2003. Medieval Warm Period, Little Ice Age and 20th century temperature variability from Chesapeake Bay. Global and Planetary Change, 36, 17–29.

Cole, W.S., 1931. The Pliocene and Pleistocene foraminifera of Florida: Florida State Geological Survey Bulletin, 6, 77 p.

Corbett, D., Vance, D., Letrick, E., Mallinson, D., Culver, S., 2007. Decadal-scale sediment dynamics and environmental change in the Albemarle estuarine system, North Carolina. Estuarine, Coastal, and Shelf Science, 71, 717-729.

Culver, S.J., Buzas, M.A., 1980. Distribution of recent benthic foraminifera off the North American Atlantic coast: Smithsonian Contributions to the Marine Sciences, 6, 512 p.

Culver, S.J., Buzas, M.A., 1981. Recent benthic foraminiferal provinces on the Atlantic continental margin of North America. Journal of Foraminiferal Research, 11, 217–240.

Culver, S.J., Woo, H.J., Oertel, G.F., Buzas, M.A., 1996. Foraminifera of coastal depositional environments, Virginia, U.S.A.: distribution and taphonomy. Palaios, 11, 459–486.

Culver, S.J., Ames, D.V., Corbett, R.D., Mallinson, D.J., Riggs, S.R., Smith, C.G., Vance, D.J., 2006. Foraminiferal and sedimentary record of late Holocene barrier island evolution, Pea Island, North Carolina: the role of storm overwash, inlet processes, and anthropogenic modification. Journal of Coastal Research, 22, 836–846.

Culver, S.J., Grand Pre, C.A., Mallinson, D.J., Riggs, S.R., Corbett, R.D., Foley, J., Hale, M., Metger, L., Ricardo, J., Rosenberger, J., Smith, C.G., Smith, C.W., Snyder, S.W., Twamley, D., 2007. Late Holocene barrier island collapse: Outer Banks, North Carolina, USA. The Sedimentary Record, 5, 4–8.

Culver, S.J., Farrell, K., Mallinson, D.J., Horton, B.P., Willard, D.A., Thieler, E.R., Riggs, S.R., Snyder, S.W., Wehmiller, J.F., Bernhardt, C.E., Hillier, C., 2008. Micropaleontologic record of late Pliocene and Quaternary paleoenvironments in the northern Albemarle Embayment, North Carolina, U.S.A. Palaeogeography, Palaeoclimatology, Palaeoecology, 264, 54–77.

Culver, S.J., Farrell, K., Mallinson, D.J., Horton, B.P., Willard, D.A., Thieler, E.R., Riggs, S.R., Snyder, S.W., Wehmiller, J.F., Bernhardt, C.E., Hillier, C., 2011. Micropaleontologic record of late Quaternary paleoenvironments in the central Albemarle Embayment, North Carolina, U.S.A. Palaeogeography, Palaeoclimatology, Palaeoecology, 305, 227–249.

Davis, R.A., Jr., Hine, A.C., Shinn, E.A., 1992. Holocene coastal development on the Florida peninsula. In: Fletcher, C.H., III, Wehmiller, J.F. (eds.). Quaternary Coasts of the United States: Marine and Lacustrine Systems. SEPM (Society for Sedimentary Geology) Special Publication, 48, 193–212 p.

Dolan, P.H., 1985. The Outer Banks of North Carolina. U.S. Geological Survey Professional Paper 1177-B. 103 p.

Engelhart, S.E., Horton, B.P., Kemp, A.C., 2011. Holocene sea level changes along the United States' Atlantic Coast. Oceanography, 24, 70–79.

Farrell, K.M., Harris, W.B., Mallinson, D.J., Culver, S.J., Riggs, S.R., Pierson, J., Self-Trail, J.M., Lautier, J.C., 2012. Standardizing texture and facies codes for a process-based classification of clastic sediment and rock. Journal of Sedimentary Research, 82, 364–378.

Farrell, K.M., Harris, W.B., Mallinson, D.J., Culver, S.J., Riggs, S.R., 2013. Graphic logging For interpreting process-generated stratigraphic sequences and aquifer/reservoir potential: with analog shelf to shoreface examples from the Atlantic coastal plain province, U.S.A. Journal of Sedimentary Research, 83, 723-745.

Fisher, J.J., 1962. Geomorphic Expression of Former Inlets Along the Outer Banks of North Carolina. Master's Thesis, University of North Carolina, 120 p.

Foley, J., 2006. Foraminiferal, sedimentological and geochemical indications of Holocene environmental change in Pamlico Sound, North Carolina. Master's Thesis, East Carolina University, 167 p.

Galbraith, R.F., Roberts, R.G., Laslett, G.M., Yoshida, H., Olley, J.M., 1999. Optical dating of single and multiple grains of quartz form Jinmium Rock Shelter, northern Australia: Part I, experimental design and statistical models, Archaeometry, 41, 339–364.

Godfrey, P.J., Godfrey, M.M., 1976. Barrier Island Ecology of Cape Lookout National Seashore and Vicinity, North Carolina. National Park Service Scientific Monograph Series, 9, 160 p.

Goldstein, S.T, Watkins, G.T., Kuhn, R.M., 1995. Microhabits of salt marsh foraminifera; St. Catherines Island, Georgia, USA. Marine Micropaleontology, 26, 17–29.

Grossman, S., Benson, R.H., 1967. Ecology of Rhizopodea and Ostracoda of southern Pamlico Sound region, North Carolina: Kansas University, Paleontology Contributions, 44, 1–90.

Grabe, S.A., Courtney, C.M., Lin, Z., Alberdi, D., Wilson, H.T. Jr., Blanchard, G., 1993. Environmental Monitoring and Assessment Program – Estuaries West Indian Province Sampling. Executive Summary: A Synoptic Survey of the Benthic Macroinvertebrates and Demersal Fishes of the Tampa Bay Estuarine System. Tampa Bay National Estuary Program Technical Publication, 3, 95–12.

Grand Pre, C.A., Culver, S.J., Mallinson, D.J., Farrell, K.M., Corbett, D.R., Horton, B.P., Hillier, C., Mallinson, D.J., Riggs, S.R., Snyder, S.W., Buzas, M.A., 2011. Rapid Holocene coastal change revealed by high-resolution micropaleontological analysis, Pamlico Sound, North Carolina, USA. Quaternary Research, 76, 319–334.

Hale, M., 2008. Late Holocene Back-Barrier Evolution of Ocracoke Island, Outer Banks, North Carolina. Master's Thesis, East Carolina University, 213 p.

Hayes, M.O., 1980. General morphology and sediment patterns in tidal inlets. Sedimentary Geology, 26, 139–156.

Horton, B.P., Peltier, W.R., Culver, S.J, Drummond, R., Engelhart, S.E, Kemp A.C., Mallinson D.J., Thieler, E.R., Ames D.V., Thomson, K.H., 2009. Holocene sea-level changes along the North Carolina coastline and their implications for glacial isostatic adjustment models. Quaternary Science Reviews, 28, 1725–1736.

Hubbard, D.K., Oertel, G., Nummedal, D., 1979. The role of waves and tidal currents in the development of tidal-inlet sedimentary structures and sand body geometry: examples from North Carolina, South Carolina, and Georgia: Journal of Sedimentary Petrology, 49, 1073–1092.

Karlson, A.W., Cronin, T.M., Ishman, S.E., Willard, D.A., Kerhin, R., Holmes, C.W., Marot, M., 2000. Historical trends in Chesapeake Bay dissolved oxygen based on benthic foraminifera from sediment cores. Estuaries, 23, 488–508.

Keigwin, L.D., 1996. The Little Ice Age and Medieval Warm Period in the Sargasso Sea. Science 274, 1504–1508.

Kemp, A.C., Horton, B.P., Culver, S.J., Corbett, D.R., Van de Plassche, O., Gehrels, W.R., Douglas, B.C., Parnell, A.C., 2009a. Timing and magnitude of recent accelerated sea-level rise (North Carolina, United States). Geology, 37, 1035–1038.

Kemp, A.C., Horton, B.P., Culver, S.J., 2009b. Distribution of modern salt-marsh foraminifera in the Albemarle-Pamlico estuarine system of North Carolina: implications for sea-level research. Marine Micropaleontology, 72, 222–238.

Kemp, A.C., Horton, B.P., Donnelly, J.P., Mann, M.E., Vermeer, M., Rahmstorf, S., 2011. Climate-related sea-level variations over the past two millennia. Proceedings of the National Academy of Sciences, 108, 11017–11022.

Kraft, J.C., Chrzastowski, M.J., Belknap, D.F., Toscano, M.A., Fletcher, C.H., III, 1987. The transgressive barrier-lagoon coast of Delaware: morphostratigraphy, sedimentary sequences and responses to relative rise in sea level. In: Nummendal, D., Pilkey, O.H., Howard, J.D (eds.). Sea-Level Fluctuation and Coastal Evolution. SEPM (Society for Sedimentary Geology) Special Publication, 41, 129–143.

Kornfeld, M.M., 1931. Recent littoral Foraminifera from Texas and Louisiana: Contributions from the Department of Geology of Stanford University, 1, 77–101.

Lamb, H.H., 1977. Climate: Present, Past and Future. Climatic History and the Future, 2, Methuen, London. 835 p.

Lian, O.B., Roberts, R.G., 2006. Dating the Quaternary: progress in luminescence dating of sediments. Quaternary Science Reviews, 25, 2449–2468.

Linnaeus, C., 1758, Systema Naturae. Ed. 10, Holmiae, Suecia [Sweden], impensis L. Salvii, 1, 824 p.

Luettich, R.A., Carr, S.D., Reynolds-Fleming, J.V., Fulcher, C.W., McNinch, J.E., 2002. Semi-diurnal seiching in a shallow, micro-tidal lagoonal estuary. Continental Shelf Research, 22, 1669–1681.

Mallinson, D.J., Riggs, S.R., Culver, S.J., Thieler, R., Foster, D., Corbett, D.R., Farrell, K., Wehmiller, J., 2005. Late Neogene and Quaternary evolution of the northern Albemarle Embayment (mid-Atlantic continental margin, USA). Marine Geology, 217, 97–117.

Mallinson, D.J., Burdette, K.E., Mahan, S.A., Brooks, G., 2008. Optically stimulated luminescence age controls on late Pleistocene and Holocene coastal lithosomes, North Carolina, USA. Quaternary Research, 69, 97–109.

Mallinson, D.J., Culver, S.J., Riggs, S.R., Thieler, E.R., Foster, D.S., Wehmiller, J.F., Farrell, K.M., Pierson, J., 2010a. Regional seismic stratigraphy and controls on the Quaternary evolution of the Cape Hatteras region of the Atlantic passive margin, USA. Marine Geology, 268, 16–33.

Mallinson, D.J., Smith, C.W., Culver, S.J., Riggs, S.R., Ames, D., 2010b. Geological characteristics and spatial distribution of paleo-inlet channels beneath the Outer Banks barrier islands, North Carolina, USA. Estuarine, Coastal, and Shelf Science, 88, 175–189.

Mallinson, D.J., Smith, C.W., Mahan, S., Culver, S.J., Peek, K., 2011. Barrier island response to late Holocene climate events, North Carolina, USA. Quaternary Research, 76, 46–57.

Madsen, A.T., Murray, A.S., 2009. Optically stimulated luminescence dating of young sediments: A review. Geomorphology, 109, 3–16.

Mann, M., Woodruff, J., Donnelly, J., Zhang, Z., 2009. Atlantic Hurricanes and climate over the past 1,500 years. Nature, 460, 880–883.

Marshall, N., 1951. Hydrography of North Carolina Marine Waters. In: H.F. Taylor and Associates, Survey of marine fishes of North Carolina: Chapel Hill, University of North Carolina Press, 76 p.

Matson, E.A., Brinson, M.M., 1990. Stable carbon isotopes and the C:N ratio in the estuaries of the Pamlico and Neuse Rivers, North Carolina. Journal of Limnography and Oceanography, 35, 1290–1300.

Mann, M., Woodruff, J., Donnelly, J., Zhang, Z., 2009. Atlantic Hurricanes and climate over the past 1,500 years. Nature, 460, 880–883.

Mello, J.F., Buzas, M.A., 1968. An application of cluster analysis as a method of determining biofacies. Journal of Paleontology, 42, 747–758.

Metger, L, 2009. Holocene Paleoenvironmental Change in Southern Pamlico Sound, North Carolina. Master's Thesis, East Carolina University, 178 p.

Montagu, G. 1803. Testacea Britannica, or Natural History of British Shells, Marine, Land, and Fresh-water, Including the Most Minute. J.S. Hollis, Romsey, England, 3, 660 p.

Mook, W.G., 1971. Paleotemperatures and chlorinities from stable carbon and oxygen isotopes in shell carbonate. Palaeogeography, Palaeoclimatology, Palaeoecology, 9, 245–263.

Moran, K.L., Mallinson, D.J., Culver, S.J., Leorri, E., Mulligan, R.P. Late Holocene evolution of Currituck Sound, North Carolina, USA: environmental change driven by sea-level rise, storms, and barrier island morphology. Journal of Coastal Research, in review.

Moslow, T.F., Heron, S.D., Jr., 1978. Relict inlets: preservation and occurrence in the Holocene stratigraphy of southern Core Banks, North Carolina. Journal of Sedimentary Petrology, 48, 1275–1286.

Moslow, T.F., Tye, R.S., 1985. Recognition and characterization of Holocene tidal inlet sequences. Marine Geology, 63, 129–151.

Munsterman, D., Kerstholt, S., 1996. Sodium polytungstate, a new non-toxic alternative to bromoform in heavy liquid separation. Review of Palaeobotany and Palynology, 91, 417–422.

Murray, J.W., 1969. Recent foraminifers from the Atlantic continental shelf of the United States. Micropaleontology, 15, 401–419.

Murray, J.W., 1982. Benthic foraminifera: the variability of living, dead or total assemblages in the interpretation of paleoecology. Journal of Micropaleontology, 1, 137–140.

Murray, J.W., 1991. Ecology and Paleoecology of Benthic Foraminifera. Longman, Harlow, 397 p.

Murray, J.W., 2006. Ecology and Applications of Benthic Foraminifera. Cambridge University Press, New York, 426 p.

Murray, A.S., Wintle, A.G, 2000. Luminescence dating of quartz using an improved single-aliquot regenerative-dose protocol. Radiation Measurements, 32, 57–73.

Murray, A.S., Wintle, A.G, 2003. The single-aliquot regenerative-dose protocol: potential for improvements in reliability. Radiation Measurements, 37, 377–381.

Nathan, R.P., Thomas, P.J., Jain, M., Murray, A.S., Rhodes, E.J., 2003. Environmental does rate heterogeneity of beta radiation and its implications for luminescence dating: Monte Carlo modelling and experimental validation. Radiation Measurements, 37, 305–313.

d'Orbigny, A.D., 1839a. Foraminiferes. In: de la Sagra, R., Histoire Physique, Politique et Naturelle de l'lle de Cuba, 8. A. Bertrand: Paris, 224 p.

d'Orbigny, A.D., 1839b. Voyage dans l' Amerique Meridionale–Foraminiferes, 5. P. Bertrand: Paris and Strasbourg, 86 p.

d' Orbigny, A., 1846. Foraminiferes Fossils du Basin Tertiaire de Vienne (Autriche), 7, 38. Gide de Comp: Paris, 318 p.

Olley, J., Caitcheon, G, Murray, A., 1998. The distribution of apparent dose as determined by Optically Stimulated Luminescence in small aliquots of fluvial quartz: Implications for dating young sediments. Quaternary Geology, 17, 1033–1040.

Peltier, W.R., 1999. Global sea level rise and glacial isostatic adjustment. Global and Planetary Change, 20, 93–133.

Peltier, W.R., 2002. On eustatic sea level history: last glacial maximum to Holocene. Quaternary Science Reviews, 21, 377–396.

Peek, K.M., Mallinson, D.J., Culver, S.J., Mahan, S.A., 2013. Holocene geologic development of the Cape Hatteras region, Outer Banks, North Carolina, USA. Journal of Coastal Research, 175–189.

Phleger, F.B, Parker, F.L., 1951. Ecology of Foraminifera, Northwest Gulf of Mexico, Part II: Foraminiferal Species: Geological Society of America Memoir, 46, 64 p.

Porter, H.J., Houser, L., 1997. Seashells of North Carolina. North Carolina Sea Grant College Program, (UNC-SG-97-03), Raleigh, NC, 132 p.

Pietrafesa, L.J., Janowitz, G.S., Chao, T.Y., Weisberg, R.H., Askari, F., Noble, 1986. The Physical Oceanography of Pamlico Sound: UNC SeaGrant Publication No. UNC-WP-86-5.

Prescott, J.R., Stephan, L.G., 1982. The contribution of cosmic radiation to the environmental dose for thermoluminescence dating. Proceedings of the Second Specialist Seminar on Thermoluminescence Dating, 6. Council of Europe, Strasbourg, 17–25.

Pruitt, R.J., 2008. Foraminiferal Evidence for Recent Paleoenvironmental Change in Core Sound, North Carolina: Master's Thesis, East Carolina University, Greenville, NC, 190 p.

Pruitt, R.J., Culver, S.J., Buzas, M.A., Corbett, D.R., Horton, B.P., Mallinson, D.J., 2010. Modern Foraminiferal Distribution and Recent Environmental Change in Core Sound, North Carolina, USA. Journal of Foraminiferal Research, 40, 344–365.

Rhodes, E.J., 2011. Optically Stimulated Luminescence Dating of Sediments over the Past 200,000 Years. Annual Review of Earth and Planetary Sciences, 39, 461–488.

Rink, W.J., Forrest, B., 2005. Dating Evidence for the Accretion History of Beach Ridges on Cape Canaveral and Merritt Island, Florida, USA. Journal of Coastal Research, 21, 1000–1009.

Riggs, S.R., York, L.L., Wehmiller, J.F., Snyder, S.W., 1992. Depositional patterns resulting from high frequency Quaternary sea-level fluctuations in northeastern North Carolina: Quaternary Coasts of the United States: Marine and Lacustrine Systems. SEPM (Society for Sedimentary Geology) Special Publications, 48, 141–153.

Riggs, S.R., Cleary, W.J., Synder, S.W., 1995. Influence of inherited geologic framework on barrier shoreface morphology and dynamics. Marine Geology, 126, 213–234.

Riggs, S.R., Ames, D.V., 2003. Drowning the North Carolina Coast: Sea-Level Rise and Estuarine Dynamics: North Carolina Sea Grant College Program, Publication No. UNC-SG-03-04, Raleigh, NC, 152 p.

Riggs, S.R., Ames, D.V., Culver, S.J., Mallinson, D.J., 2011. The Battle for North Carolina's Coast: Evolutionary History, Present Crisis, and Vision for the Future. Chapel Hill: University of North Carolina Press, 142 p.

Robinson, M.M., McBride, R.A., 2003. Old Currituck Inlet, VA/NC: inlet history documented by foraminiferal evidence (Part II). Proceedings Coastal Sediments 03, ASCE Press, 14.

Robinson, M.M., McBride, R.A., 2006. Benthic foraminifera from a relict flood tidal delta along the Virginia/North Carolina Outer Banks. Micropaleontology, 52, 67–80.

Robinson, M.M., McBride, R.A., 2008. Anatomy of a shoreface sand ridge revisited using foraminifera: False Cape Shoals, Virginia/North Carolina inner shelf. Continental Shelf Research, 28, 2428–2441.

Rodnight, H., Duller, G.A., Wintle, A.G., Tooth, S., 2006. Assessing the reproducibility and accuracy of optical dating of fluvial deposits. Quaternary Geochronology, 2, 109–120.

Rosenberger, J.E., 2006. Late Holocene Back-Barrier Development of Portsmouth Island, Outer Banks, North Carolina: Master's Thesis, East Carolina University, Greenville, NC, 185 p.

Schnitker, D., 1971. Distribution of foraminifera on the North Carolina continental shelf: Tulane Studies in Geology and Paleontology, 8, 169–215.

Scott, D.B., Medioli, F.S., 1977. Quantitative studies of marsh foraminiferal distributions in Nova Scotia and comparison with those in other parts of the world: implications for sea level studies: Cushman Foundation for Foraminiferal Research Special Publication, 17, 1–58 p.

Scott, D.B., Medioli, F.S., 1980. Living vs. total foraminifera populations: their relative usefulness in paleoecology. Journal of Paleontology, 54, 814–831.

Scott, D.B., Medioli, F.S., Schafer, C.T., 2001. Monitoring in Coastal Environments Using Foraminifera and Theocamoebian Indicators: Cambridge University Press, Cambridge, 177 p.

Smith, C.G., 2004. Late Holocene Geologic Development of Pea Island and Avon–Buxton Area, Outer Banks, North Carolina: Master's Thesis, East Carolina University, 260 p.

Smith, C.W., 2006. Lithologic, Geophysical, and Paleoenvironmental Framework of Relict Inlet Channel-Fill and Adjacent Facies: North Carolina Outer Banks: Master's Thesis, East Carolina University, 296 p.

Smith, C.G., Culver, S.J., Riggs, S.R., Ames, D., Corbett, D.R., Mallinson, D., 2008. Geospatial analysis of barrier island width of two segments of the Outer Banks, North Carolina, USA: anthropogenic curtailment of natural self-sustaining processes. Journal of Coastal Research, 24, 70–83.

Smith, C.G., Culver, S.J., Mallinson, D.J., Riggs, S.R., Corbett, D.R., 2009. Recognizing former flood-tide deltas in the Holocene stratigraphic record from the Outer Banks, North Carolina, USA. Stratigraphy, 6, 61–78.

Stahle, D.W, Cleaveland, M.K., Blanton, D.B., Therrell, M.D., Gay, D.A., 1998. The Lost Colony and Jamestown droughts. Science, 280, 564–56.

Stuiver, M., Reimer, P., 1993. Extended ^{14}C data base and revised CALIB 3.0 ^{14}C Age calibration program. Radiocarbon, 35, 215–230.

Thieler, E.R. and Ashton, A.D., 2011. 'Cape Capture.' Geologic data and modeling results suggest the Holocene loss of a Carolina Cape. Geology, 39, 339–342.

Thieler, E.R., Foster, D.S., Himmelstoss, E.A., Mallinson, D.J., 2014. Geologic framework of the northern North Carolina, USA inner continental shelf and its influence on coastal evolution. Marine Geology, 348, 113–130.

Trouet, V., Esper, J., Graham, N.E., Baker, A., Scource, J.D., Frank, D.C., 2009. Persistent positive North Atlantic oscillation mode dominated the Medieval Climate Anomaly. Science, 324, 78–80.

Terquem, O., 1875. Essai sur le classement des animaux qui vivent sur la plage et dans les environs de Dunquerque: Paris, Fasc. 1, 1–54 p.

Thomas, D.H., 2008. Native American landscapes of St. Catherines Islands, Georgia II. The data. American Museum of Natural History, 88, 343–831.

Twamley, D.F., 2006. Holocene Geological Development of the Hatteras Village Area, Outer Banks, North Carolina: Master's Thesis, East Carolina University, Greenville, North Carolina, 157 p.

Vance, D.J., Culver, S.J., Corbett, D.R., Buzas, M.A., 2006. Foraminifera in the Albemarle estuarine system, North Carolina: distribution and recent environmental change. Journal of Foraminiferal Research, 36, 15–33.

Walker, G., and Jacob, E., 1798. In: Adams, G. (eds.). Essays on the Microscope. Containing a practical description of the most improved microscopes; a general history of insects. A description of 383 animalicula etc. 2nd edition with considerable additions and improvements by K. Kanmacher: Dillion and Keating, London, 712 p.

Walton, W.R., 1955. Ecology of living benthonic foraminifera, Todos Santos Bay, Baja California. Journal of Paleontology, 29, 952–1018.

Williamson, W.C., 1858. On Recent Foraminifera of Great Britain: Ray Society (London) Publication, 107 p.

Wells, J.T., Kim, S.Y., 1989. Sedimentation in the Albemarle-Pamlico lagoonal system: synthesis and hypothesis. In: Ward, L.G., and Ashley, G.M., (eds.). Physical Processes and Sedimentology of Siliclastic-Dominated Lagoonal Systems. Marine Geology, 88, 263–284.

Woo, H.J., Culver, S.J., and Oertel, G.F., 1997. Benthic foraminiferal communities of a barrier-lagoon system, Virginia, U.S.A. Journal of Coastal Research, 13, 1192–1200.

Workman, R. R. Jr., 1981. Foraminiferal Assemblages of the Nearshore Inner Continental Shelf, Nags Head and Wilmington Areas, North Carolina: Master's Thesis, East Carolina University, 161 p.

Wintle, A.G., Murray, A.S., 2006. A review of quartz optically stimulated luminescence characteristics and their relevance in single-aliquot regenerative dating protocols. Radiation Measurements, 41, 369–391.

Zaremba, N.J., 2014. Holocene Stratigraphy and Paleoenvironmental Change of Pamlico Sound, North Carolina, USA: Master's Thesis, East Carolina University, Greenville, NC, 109 p.

Zaremba, N.J., Mallinson, D.J., Leorri, E., Culver, S.J., Riggs, S.R., Mulligan, R.P., Horsman, E. Controls on the stratigraphic record and paleoenvironmental change within Holocene estuarine system: Pamlico Sound, North Carolina, USA. Marine Geology, in review.

Appendix A: OFTD core logs

The core log key explains how grain size samples are displayed as triangles and foraminiferal samples are displayed with stars, presented in mbsf (meters below sea floor) and mbsl (meters below sea level). The key also shows how lithofacies are represented in core logs. Percent sand data (Appendix B) from foraminiferal and grain size samples that were wet sieved are displayed in core logs. Associated lithofacies, biofacies, and environmental facies interpretations are also shown. OSL and ^{14}C age estimates and their locations are presented with arrows at the associated depth. OSL ages are reported in cal yr BP (bottom of arrow) as well as quartz years (top of arrow). Radiocarbon ages are reported in cal yr BP (top of arrow).

CORE LOG KEY

Lithofacies Key

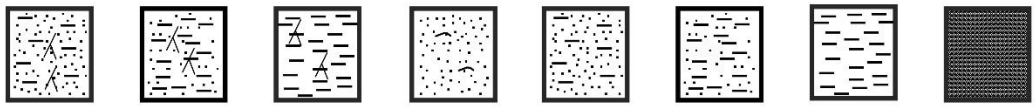

organic-rich muddy sand (mS-org) | organic-rich sandy mud (sM-org) | organic-rich mud (M-org) | sand (S) | muddy sand (mS) | sandy mud (sM) | mud (M) | peat (P)

organic-rich gravelly muddy sand (gmS-org) | organic-rich gravelly sandy mud (gsM-org) | slightly gravelly sand ((g)S) | gravelly sand (gS) | gravelly muddy sand (gmS) | slightly gravelly sandy mud ((g)sM) | slightly gravelly muddy sand ((g)mS)

Sedimentary Features Key

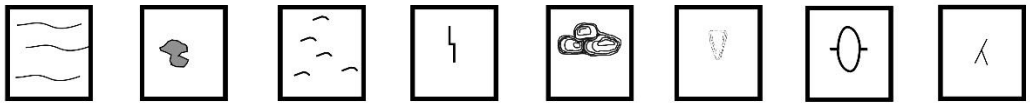

laminations | mottled mud spots | shell fragments | worm tube | oyster clump | angel wing | surf clam | organics

Sample Key

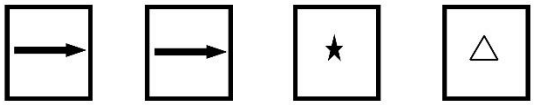

OSL Sample | Radiocarbon ^{14}C Sample (cal yr BP) | Foraminiferal Sample | Grain Size Sample

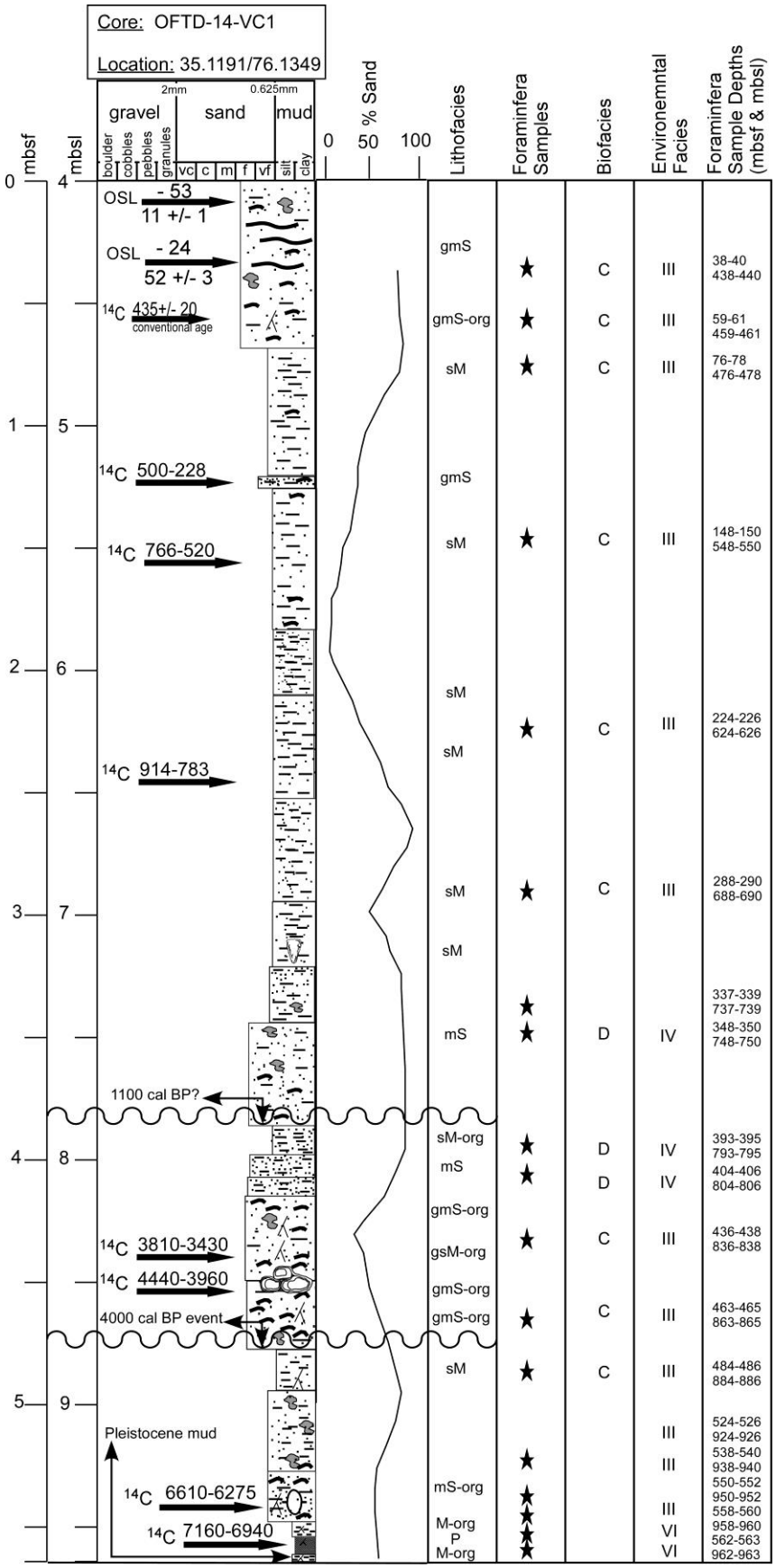
Core: OFTD-14-VC1
Location: 35.1191/76.1349
2mm
0.625mm
gravel
sand
mud
boulder
cobbles
pebbles
granules
vc
c
m
f
vf
silt
clay
0
50
100
% Sand
mbsf
mbsl
Lithofacies
Foraminfera Samples
Biofacies
Environemntal Facies
Foraminfera Sample Depths (mbsf & mbsl)
OSL - 53
11 +/- 1
OSL - 24
52 +/- 3
14C 435+/- 20
conventional age
14C 500-228
14C 766-520
14C 914-783
1100 cal BP?
14C 3810-3430
14C 4440-3960
4000 cal BP event
Pleistocene mud
14C 6610-6275
14C 7160-6940
gmS
gmS-org
sM
gmS
sM
sM
sM
sM
mS
sM-org
mS
gmS-org
gsM-org
gmS-org
gmS-org
sM
mS-org
M-org
P
M-org
C
D
III
IV
VI
38-40
438-440
59-61
459-461
76-78
476-478
148-150
548-550
224-226
624-626
288-290
688-690
337-339
737-739
348-350
748-750
393-395
793-795
404-406
804-806
436-438
836-838
463-465
863-865
484-486
884-886
524-526
924-926
538-540
938-940
550-552
950-952
558-560
958-960
562-563
962-963

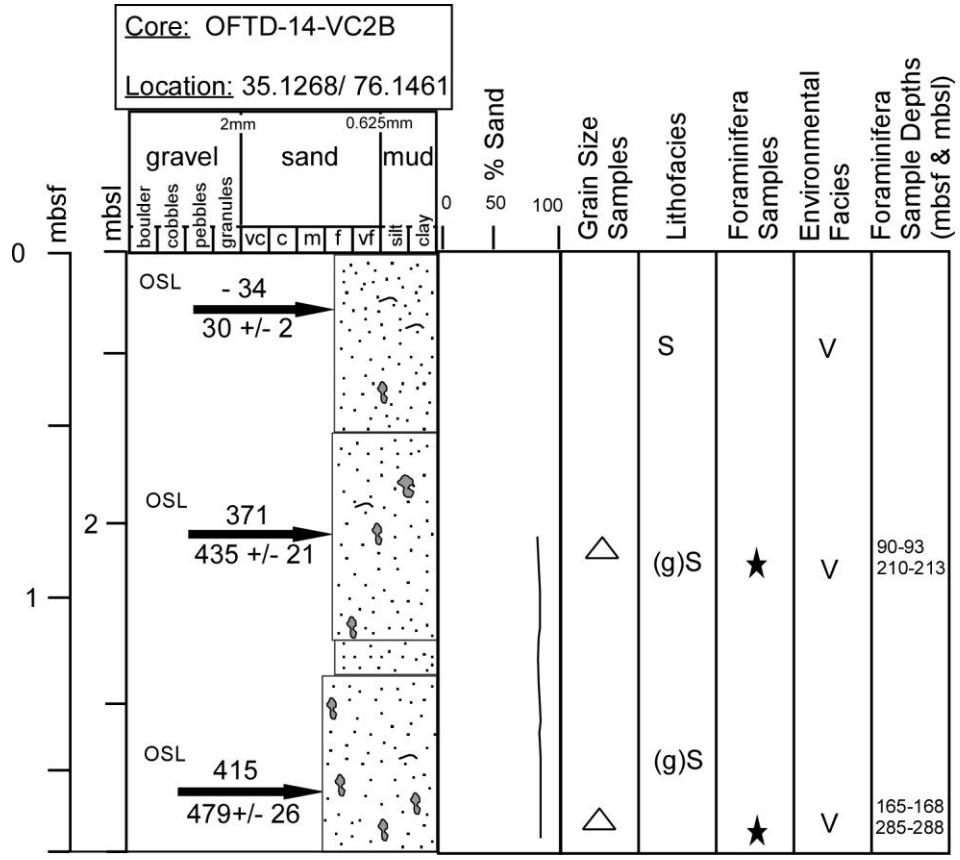
Core: OFTD-14-VC2B
Location: 35.1268/ 76.1461
2mm
0.625mm
gravel
sand
mud
boulder
cobbles
pebbles
granules
vc
c
m
f
vf
silt
clay
0
50
100
% Sand
mbsf
mbsl
0
1
2
OSL
- 34
30 +/- 2
OSL
371
435 +/- 21
OSL
415
479+/- 26
Grain Size Samples
Lithofacies
S
(g)S
(g)S
Foraminifera Samples
Environmental Facies
V
V
V
Foraminifera Sample Depths (mbsf & mbsl)
90-93
210-213
165-168
285-288

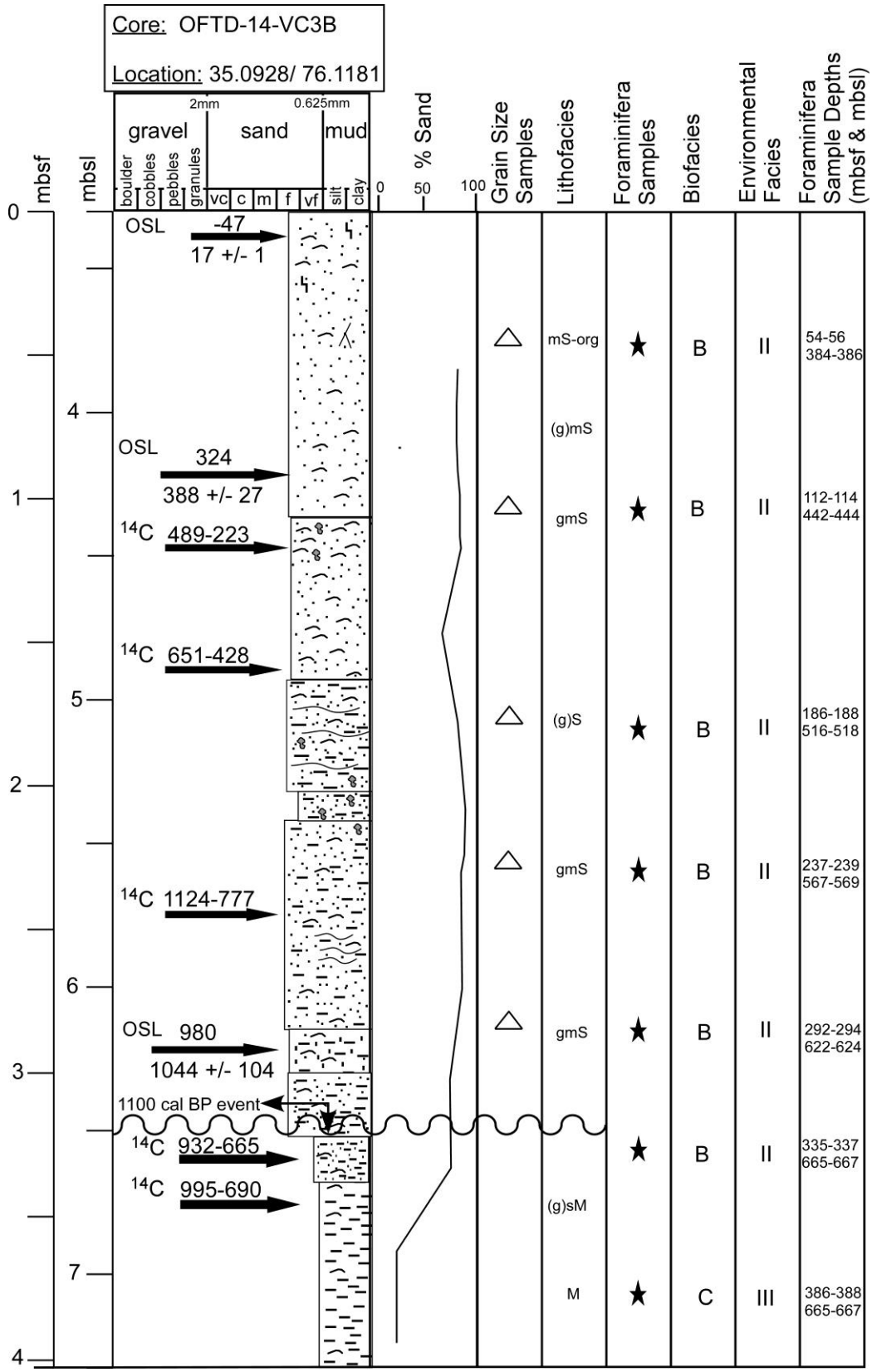
Core: OFTD-14-VC3B
Location: 35.0928/ 76.1181
2mm
0.625mm
gravel
sand
mud
boulder
cobbles
pebbles
granules
vc
c
m
f
vf
silt
clay
mbsf
mbsl
% Sand
0
50
100
Grain Size Samples
Lithofacies
Foraminifera Samples
Biofacies
Environmental Facies
Foraminifera Sample Depths (mbsf & mbsl)
OSL -47
17 +/- 1
OSL 324
388 +/- 27
14C 489-223
14C 651-428
14C 1124-777
OSL 980
1044 +/- 104
1100 cal BP event
14C 932-665
14C 995-690
mS-org
(g)mS
gmS
(g)S
gmS
gmS
(g)sM
M
B
B
B
B
B
C
II
II
II
II
II
III
54-56
384-386
112-114
442-444
186-188
516-518
237-239
567-569
292-294
622-624
335-337
665-667
386-388
665-667

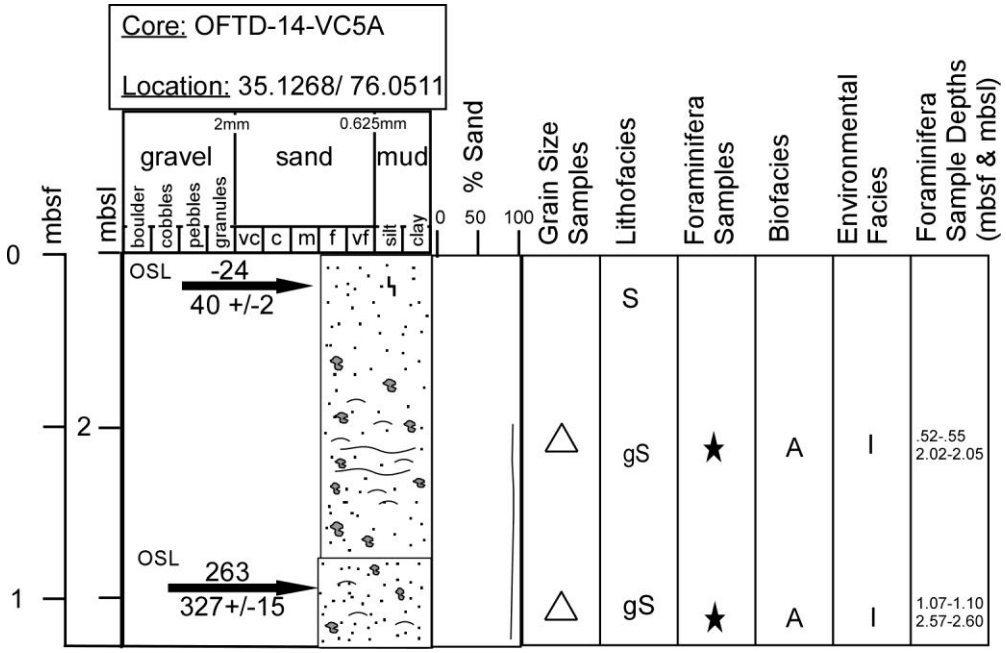
Core: OFTD-14-VC5A
Location: 35.1268/ 76.0511
2mm
0.625mm
gravel
sand
mud
boulder
cobbles
pebbles
granules
vc
c
m
f
vf
silt
clay
mbsf
mbsl
0
50
100
% Sand
Grain Size Samples
Lithofacies
Foraminifera Samples
Biofacies
Environmental Facies
Foraminifera Sample Depths (mbsf & mbsl)
OSL
-24
40 +/-2
OSL
263
327+/-15
S
gS
gS
A
A
I
I
.52-.55
2.02-2.05
1.07-1.10
2.57-2.60
0
1
2

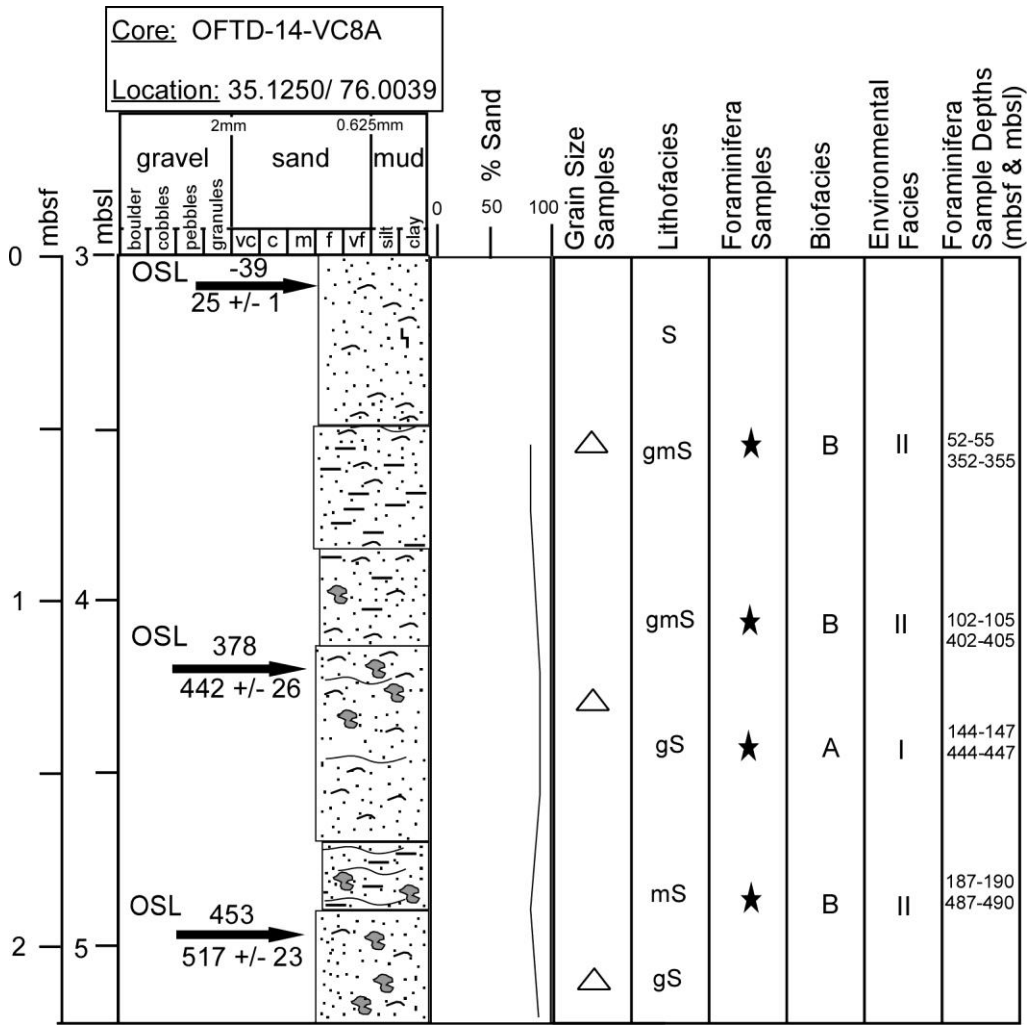
Core: OFTD-14-VC8A
Location: 35.1250/ 76.0039
2mm
0.625mm
gravel
sand
mud
boulder
cobbles
pebbles
granules
vc
c
m
f
vf
silt
clay
0
50
100
% Sand
mbsf
mbsl
0
1
2
3
4
5
OSL -39
25 +/- 1
OSL 378
442 +/- 26
OSL 453
517 +/- 23
Grain Size Samples
Lithofacies
S
gmS
gmS
gS
mS
gS
Foraminifera Samples
Biofacies
B
B
A
B
Environmental Facies
II
II
I
II
Foraminifera Sample Depths (mbsf & mbsl)
52-55
352-355
102-105
402-405
144-147
444-447
187-190
487-490

Appendix B: Gradistat results for vibracores

Weight percentages and statistics were calculated using GRADISTAT software (Blott and Pye, 2001) to determine sorting, skewness, mean, mode, median, and kurtosis grain-size data. Reported in Φ.

Core ID	mbsf	mbsl	MEAN Φ	SORTING Φ	SKEWNESS Φ	KURTOSIS Φ	MODE Φ	MEDIAN Φ
OFTD-14-VC2B	0.87-0.90	2.07-2.10	2.08	0.37	-0.07	1.01	2.24	2.12
OFTD-14-VC2B	1.62-1.65	2.82-2.85	2.26	0.35	0.04	1.42	2.24	2.25
OFTD-14-VC3B	0.47-0.50	3.87-3.90	3.08	0.32	-0.28	0.91	3.24	3.14
OFTD-14-VC3B	1.09-1.12	4.39-4.42	3.11	0.39	-0.09	1.04	3.24	3.16
OFTD-14-VC3B	1.79-1.82	5.09-5.12	2.99	0.39	-0.34	0.92	3.24	3.07
OFTD-14-VC3B	2.30-2.33	5.60-5.63	2.85	0.39	0.39	1.73	2.74	2.81
OFTD-14-VC3B	2.89-2.91	6.19-6.21	2.81	0.42	-0.01	1.26	2.74	2.78
OFTD-14-VC5A	0.50-0.52	2.0-2.02	2.32	0.50	0.09	1.14	2.24	2.29
OFTD-14-VC5A	1.05-1.07	2.55-2.57	2.43	0.49	-0.13	1.04	2.74	2.45
OFTD-14-VC8A	1.37-1.40	4.37-4.40	2.37	0.37	0.25	1.30	2.24	2.31
OFTD-14-VC8A	2.13-2.16	5.13-5.16	2.29	0.34	0.07	1.48	2.24	2.26

Appendix C: Percent gravel, sand, and mud for wet sieved foraminifera and grain size samples

Illustrates the Core ID, meters below sea floor (mbsf), meters below sea level (mbsl), weight before sieving (g), > 710 µm (g) fraction, > 63 µm (g) fraction, weight after sieving (g), gravel (%), sand (%), and mud (%) for each foraminifera and grain size sample.

Core	mbsf	mbsl	Weight before sieving (g)	> 710 µm (g)	63-710 µm (g)	Weight after sieving (g)	Gravel (%)	Sand (%)	Mud (%)
OFTD-14-VC1	0.38-0.30	4.38-4.40	32.93	0.02	18.96	18.98	0.06	57.58	42.36
OFTD-14-VC1	0.59-0.61	4.59-4.61	43.29	0.02	27.11	27.13	0.05	62.62	37.33
OFTD-14-VC1	0.76-0.78	4.76-4.78	37.05	0.01	10.12	10.13	0.03	27.31	72.66
OFTD-14-VC1	1.48-1.50	5.48-5.50	26.63	0.07	5.80	5.87	0.26	21.78	77.96
OFTD-14-VC1	2.24-2.26	6.24-6.26	24.56	0.01	1.83	1.84	0.04	7.45	92.51
OFTD-14-VC1	2.88-2.90	6.88-6.90	25.74	0.02	1.96	1.98	0.08	7.61	92.31
OFTD-14-VC1	3.37-3.39	7.37-7.39	25.77	0.01	11.96	11.97	0.04	46.41	53.55
OFTD-14-VC1	3.48-3.50	7.48-7.50	41.76	0.04	32.05	32.09	0.10	76.75	23.16
OFTD-14-VC1	3.93-3.95	7.93-7.95	33.84	0.01	13.60	13.61	0.03	40.19	59.78
OFTD-14-VC1	4.04-4.06	8.04-8.06	39.64	0.05	28.40	28.45	0.13	71.64	28.23
OFTD-14-VC1	4.36-4.38	8.36-8.38	52.97	0.51	39.01	39.52	0.96	73.65	25.39
OFTD-14-VC1	4.63-4.65	8.63-8.65	48.20	0.86	36.49	37.35	1.78	75.71	22.51
OFTD-14-VC1	4.84-4.86	8.84-8.86	32.38	0.04	7.95	7.99	0.12	24.55	75.32
OFTD-14-VC1	5.24-5.26	9.24-9.26	45.65	0.03	22.09	22.12	0.07	48.39	51.54
OFTD-14-VC1	5.38-5.40	9.38-9.40	53.53	0.27	38.28	38.55	0.50	71.51	27.98
OFTD-14-VC1	5.50-5.52	9.50-9.52	40.08	0.27	19.80	20.07	0.67	49.40	49.93
OFTD-14-VC1	5.62-5.63	9.62-9.63	18.53	0.03	9.32	9.35	0.16	50.30	49.54
OFTD-14-VC2	0.87-0.90	2.07-2.10	101.49	0.02	100.25	100.26	0.02	98.77	1.21
OFTD-14-VC2	0.90-0.93	2.10-2.13	69.50	0.01	68.50	68.50	0.01	98.56	1.43
OFTD-14-VC2	1.62-1.65	2.82-2.85	92.56	0.05	89.82	89.86	0.05	97.03	2.92
OFTD-14-VC2	1.65-1.68	2.85-2.88	86.49	0.03	83.48	83.51	0.04	96.51	3.45
OFTD-14-VC3B	0.47-0.50	3.77-3.80	60.68	0.01	52.93	52.94	0.02	87.22	12.76
OFTD-14-VC3B	0.54-0.56	3.84-3.86	46.31	0.06	39.23	39.29	0.14	84.70	15.17
OFTD-14-VC3B	1.09-1.12	4.39-4.42	77.63	0.06	69.28	69.34	0.08	89.25	10.68
OFTD-14-VC3B	1.12-1.14	4.42-4.44	66.22	0.81	48.64	49.45	1.22	73.45	25.33
OFTD-14-VC3B	1.79-1.82	5.09-5.12	74.70	0.05	67.95	68.00	0.07	90.97	8.96
OFTD-14-VC3B	1.86-1.88	5.16-5.18	63.36	0.04	60.26	60.30	0.06	95.11	4.83
OFTD-14-VC3B	2.30-2.33	5.60-5.63	62.98	0.06	57.11	57.17	0.10	90.68	9.22
OFTD-14-VC3B	2.37-2.39	5.67-5.69	66.46	0.03	60.80	60.83	0.04	91.48	8.48
OFTD-14-VC3B	2.89-2.91	6.19-6.21	88.41	0.66	67.74	68.40	0.75	76.62	22.64
OFTD-14-VC3B	2.92-2.94	6.22-6.24	58.08	0.04	44.16	44.20	0.07	76.04	23.89
OFTD-14-VC3B	3.35-3.37	6.65-6.67	39.94	0.03	4.32	4.35	0.07	10.82	89.11
OFTD-14-VC3B	3.86-3.88	7.16-7.18	40.57	0.01	1.91	1.92	0.02	4.71	95.27
OFTD-14-VC5A	0.50-0.52	2.00-2.02	58.42	0.09	57.43	57.52	0.15	98.30	1.54
OFTD-14-VC5A	0.52-0.55	2.02-2.05	59.28	0.11	57.91	58.02	0.19	97.69	2.12
OFTD-14-VC5A	1.05-1.07	2.55-2.57	51.49	0.23	50.47	50.70	0.45	98.03	1.53
OFTD-14-VC5A	1.07-1.10	2.57-2.50	65.43	0.04	63.89	63.93	0.06	97.65	2.29
OFTD-14-VC8A	0.52-0.55	3.52-3.55	68.15	0.24	63.88	61.24	0.35	89.51	10.14
OFTD-14-VC8A	1.02-1.05	4.02-4.05	75.41	0.05	71.74	68.86	0.07	91.26	8.68
OFTD-14-VC8A	1.37-1.40	4.37-4.40	70.59	0.04	72.04	69.25	0.06	98.05	1.90
OFTD-14-VC8A	1.44-1.47	4.44-4.47	68.64	0.04	70.74	67.99	0.06	98.99	0.95
OFTD-14-VC8A	1.87-1.90	4.87-4.80	66.84	0.02	63.28	60.55	0.03	90.56	9.41
OFTD-14-VC8A	2.13-2.16	5.13-5.16	66.37	0.22	68.13	65.54	0.33	98.41	1.26

Appendix D: Original References for foraminiferal taxa

Alphabetical list of foraminiferal species with references to original publications.

Ammonia parkinsoniana (d'Orbigny): *Rosalina parkinsoniana* d'Orbigny, 1839b, p. 99, pl. 4, figs. 25-27.

Ammonia tepida (Cushman): *Rotalia beccarii* (Linneaus) var. *tepida* Cushman, 1926, p. 79, pl. 1. Figs 25-27.

Asterigerina carinata d'Orbigny: *Asterigerina carinata* d'Orbigny, 1839b, p. 118, pl. 5, fig. 25, pl. 6, figs. 1,2.

Bolivina lowmani Phleger and Parker: *Bolivina lowmani* Phleger and Parker, 1951, pt. 2, p. 13, pl. 6, figs. 20a, b, 21.

Buccella inusitata Andersen: *Buccella inusitata* Andersen, 1952, p. 148, figs. 10,11.

Cibicides lobatulus (Walker and Jacob): *Nautilus lobatulus* Walker and Jacob, 1798, p. 642, pl. 14, fig. 36.

Elphidium excavatum (Terquem): *Polystomella excavata* Terquem, 1875, p. 25, pl. 2, figs. 2 a-f.

Elphidium galvestonense (Kornfeld): *Elphidium gunteri* (Cole) var. *galvestonensis* Kornfeld, 1931, p. 87, pl. 15, figs. 1a, b, 2a, b, 3a, b.

Elphidium gunteri Cole: *Elphidium gunteri* Cole 1931, p. 34, pl. 4, figs. 9,10.

Elphidium mexicanum (Kornfeld): *Elphidium incertum* (Williamson) var. *mexicanum* Kornfeld, 1931, p. 89, pl. 16, figs. 1a, b, 2a, b.

Elphidium poeyanum (d'Orbigny): *Polystomella poeyana* d'Orbigny 1839b, p. 55, figs. 25, 26.

Elphidium subarcticum Cushman: *Elphidium subarcticum* Cushman, 1944, p. 27, pl. 3, figs. 34, 35.

Elphidium translucens Natland: *Elphidium translucens* Natland, 1938, p. 144, pl. 5, figs. 3,4.

Guttulina lactea (Walker and Jacob): *Serpula lactea* Walker and Jacob, 1798, p. 634, pl. 14, fig. 4.

Hanzawaia strattoni (Applin): *Truncatulina americana* (Cushman) var. *strattoni* Applin et al., 1925, p. 99, pl. 3, fig. 3.

Haynesina germanica (Ehrenberg): *Nonionina germanica* (Ehrenberg), 1841, p. 23, pl. 2, figs. 1a-g.

Miliolinella subrotunda (Montagu, 1803): *Vermiculum subrotunda* Montagu, 1803, p, 521.

Nonionella atlantica Cushman: *Nonionella atlantica* Cushman, 1947, p. 90, pl. 20, figs. 4, 5.

Quinqueloculina jugosa Cushman: *Quinqueloculina seminulum* (Linnaeus) var. *jugosa* Cushman, 1944, p. 13, pl. 2, fig. 15.

Quinqueloculina lamarckiana d'Orbigny: *Quinqueloculina lamarckiana* d'Orbigny, 1839a, p. 189, pl. 11, figs. 14-15.

Quinqueloculina seminula (Linnaeus): *Serpula seminulum* Linnaeus, 1758, p. 786.

Rosalina floridana (Cushman): *Discorbis floridanus* Cushman, 1922, pg. 39, pl. 5, figs 11, 12.

Textularia cf. *T. gramen* d'Orbigny, *Textularia gramen* d'Orbigny, 1846, p. 248, pl. 15, figs. 4-6.

Trifarina angulosa (Williamson): *Uvigerina angulosa* Williamson, 1858, p. 67, pl. 5, fig. 140.

Appendix E: Surface Sample Foraminiferal Census Data

Sample OC-14-S20 was barren

.

	OC-14- Surface Samples																				
Taxon ↓ Sample →	S1	S2	S3	S4	S5	S6	S7	S8	S9	S10	S11	S12	S13	S14	S15	S16	S17	S18	S19	S21	S22
Ammonia parkinsoniana	14	5	9	9	8	4	5	1	5	5	8	36	18	10	2	10	8	37	21	18	9
Ammotium salsum		1																			
Asterigerina carinata														2							
Bolivina lowmani																			1		
Buccella inusitata														1		2					
Cibicides lobatulus	2				1									2		5	5				
Elphidium excavatum	102	21	66	94	118	92	74	12	33	5	59	67	86	76	4	51	70	81	93	93	73
Elphidium galvestonense	5	9	5	1	2	2	10	1			2	7	2	7		11	4	2	1	5	1
Elphidium gunteri	13	1	2	2	1	1	8							7		8	3		1	1	5
Elphidium mexicanum	7	38	5	7	6	2	5				9	1	1	4		7	7	4			14
Elphidium poeyanum																	2				
Elphidium sp.	1		1	2								1				3				2	
Elphidium sp. A							1														
Elphidium subarcticum	1		1				1							1							
Elphidium translucens	1						1							1			3				
Eponides repandus																1					
Globigerinoides sp.		1																			
Guttulina lactea														1							
Hanzawaia strattoni		2	1			3				1	28	1		1			9	3			
Haplophragmoides wilberti																1					
Haynesina germanica		1	2				4	1								1	1				
Indeterminate rotaliid														1							
Miliolinella subrotunda																2					
Nonionella atlantica	2		1				3							1		4	1				
Planktonic sp.	1					1					1					2					
Planulina sp.																1					
Quinqueloculina jugosa						1											1				
Quinqueloculina lamarckiana																1	1			1	
Quinqueloculina seminula	1			1		1	3				2			1			2			1	
Quinqueloculina sp.																2	1		1	1	
Rosalina floridana																	3	1			
Rosalina sp.							1										1				
Siphotrochammina lobata																				1	
Textularia earlandi																				1	
Trifarina angulosa																		1			
Trochammina "squamata"	1																				
Trochammina sp.																	2				
Total Foraminifera picked	151	79	93	116	136	107	116	15	38	11	109	113	107	116	6	112	124	129	118	124	102
No. rotaliid specimens	147	78	93	116	135	105	116	15	38	11	108	113	107	110	6	103	116	129	117	122	102
No. miliolid specimens	4				1	1					1			5		9	7				
No. textulariid specimens		1				1								1			1		1	2	

Appendix F: Surface Sample Foraminiferal Percent Abundance Data

Sample OC-14-S20 was barren.

OC-14- Surface Samples

Taxon % ↓ Sample →	S1	S2	S3	S4	S5	S6	S7	S8	S9	S10	S11	S12	S13	S14	S15	S16	S17	S18	S19	S21	S22	Average
Ammonia parkinsoniana	9	6	10	8	6	4	4	7	13	45	7	32	17	9	33	9	6	29	18	15	9	13
Ammotium salsum																				1		
Asterigerina carinata							1										1					
Bolivina lowmani																		1				
Buccella inusitata																1	1			1		
Cibicides lobatulus		1	2				3	7								1	1					1
Elphidium excavatum	68	27	71	81	87	86	64	80	87	45	54	59	80	66	67	46	56	63	79	75	72	64
Elphidium galvestonense	3	11	5	1	1	2	9	7			2	6	2	6		10	3	2	1	4	1	3
Elphidium gunteri		3	1			3				9	26	1		1			7	2				2
Elphidium mexicanum	5	48	5	6	4	2	4				8	1	1	3		6	6	3			14	5
Elphidium poeyanum																	2					
Elphidium sp.	1		1	2								1				3				2		
Elphidium sp. A																1						
Elphidium subarcticum	1		1				1							1								
Elphidium translucens	1						1							1			2					
Eponides repandus							1															
Globigerinoides sp.														1								
Guttulina lactea	1																					
Hanzawaia strattoni	9	1	2	2	1	1	7							6		7	2		1	1	5	2
Haplophragmoides wilberti		1																				
Haynesina germanica	1			1		1	3				2			1			2			1		
Indeterminate rotaliid																1						
Miliolinella subrotunda														2								
Nonionella atlantica	1		1				3							1		4	1					
Planktonic sp.																2	1		1	1		
Planulina sp.																1						
Quinqueloculina jugosa																	2					
Quinqueloculina lamarckiana														1		2						
Quinqueloculina seminula	1				1									2		4	4					1
Quinqueloculina sp.	1					1					1					2						
Rosalina floridana																	2	1				
Rosalina sp.																2						
Siphotrochammina lobata																				1		
Textularia earlandi																			1			
Trifarina angulosa		1																				
Trochammina "squamata"														1								
Trochammina sp.						1											1					
Total %	100	100	100	100	100	100	100	100	100	100	100	100	100	100	100	100	100	100	100	100	100	
% rotaliid specimens	97	99	100	100	99	98	100	100	100	100	99	100	100	95	100	92	94	100	99	98	100	
% miliolid specimens	3				1	1					1			4		8	6					
% textulariid specimens		1				1								1			1		1	2		

Appendix G: Down-Core Foraminiferal Census Data

	OFTD-14-Vibracores																																					
CORE	VC1	VC1	VC1	VC1	VC1	VC1	VC1	VC1	VC1	VC1	VC1	VC1	VC1	VC1	VC1	VC1	VC1	VC1	VC1	VC2B	VC2B	VC3B	VC3B	VC3B	VC3B	VC3B	VC3B	VC3B	VC5A	VC5A	VC8A	VC8A	VC8A	VC8A	VC8A	VC8A	VC8A	VC8A
Taxon ↓ Sample ID (mbsf) →	.38-.4	.59-.61	.76-.78	1.48-1.5	2.24-2.26	2.88-2.9	3.37-3.39	3.48-3.5	3.93-3.95	4.04-4.06	4.36-4.38	4.63-4.65	4.84-4.86	5.24-5.26	5.38-5.4	5.5-5.52	5.58-5.6	5.62-5.63	.90-.93	1.65-1.68	.54-.56	1.12-1.14	1.86-1.88	2.37-2.39	2.92-2.94	3.35-3.37	3.86-3.88	.52-.55	1.07-1.10	.52-.55	1.02-1.05	1.44-1.47	1.87-1.90						
Taxon ↓ Sample ID (mbsl) →	4.38-4.4	4.59-4.61	4.76-4.78	5.48-5.5	6.24-6.26	6.88-6.9	7.37-7.39	7.48-7.5	7.93-7.95	8.04-8.06	8.36-8.38	8.63-8.65	8.84-8.86	9.24-9.26	9.38-9.4	9.5-9.52	9.58-9.6	9.62-9.63	2.1-2.13	2.85-2.88	3.84-3.86	4.42-4.44	5.16-5.18	5.67-5.69	6.22-6.24	6.65-6.67	7.16-7.18	2.02-2.05	2.57-2.6	3.52-3.55	4.02-4.05	4.44-4.47	4.87-4.90						
Ammobaculites sp.		1																																				
Ammonia parkinsoniana	5	9	11	13	17	4					27	27	9					11	1		20	35	23	26	37	61	7		12	25	25	13	24						
Ammonia tepida				1																	7	6	6	10	13	27			3	8	1		5					
Bolivina lowmani																															3							
Buccella inusitata																															1	1						
Cassidulina subglobosa																													1									
Cibicides lobatulus																							5	2		2		1	1		2	1	4					
Elphidium excavatum	118	101	113	104	96	108		16	47	18	93	92	107					113			72	59	69	79	71	41	109	14	80	83	84	101	72					
Elphidium galvestonense																					17	17	1					3	1	1		3	1					
Elphidium gunteri																						1	5	3	9	1			1	2	1	5	2					
Elphidium mexicanum																					1	3	3			1			9	4	5	6	2					
Elphidium poeyanum																					1	1	1		1	3			1				1					
Elphidium sp.																														1								
Elphidium subarcticum																																	1					
Globigerinoides sp.																							2	1														
Guttulina lactea																							1															
Hanzawaia strattoni																					1		4	1					6			6	5					
Haynesina germanica																								1					1	3	1	1	1					
Nonionella atlantica																							3	1		2					3		4					
Planktonic sp.																						1		1					1		3		5					
Quinqueloculina jugosa																										1												
Quinqueloculina seminula																																	2					
Rosalina sp.																								1														
Trifarina angulosa																													1			1	1					
Valvulineria sp.																													1	1		1	1					
Total Foraminfera picked	123	111	124	118	113	112		16	47	18	120	119	116					124	1		119	123	123	126	131	139	116	18	119	128	129	139	131					
Calculated # of Specimens in 60 g	7172	4923	12852	17015	8834	2089		167	83	27	4350	4740	1720					64242	1		22200	446	4193	5119	24359	15033	686	18	29	4025	3695	1086	4201					
No. rotaliid specimens	123	110	124	118	113	112		16	47	18	120	119	116					124	1		119	123	122	126	131	138	116	18	119	128	129	139	129					
No. miliolid specimens																							1			1							2					
No. textulariid specimens		1																																				

Appendix H: Down-Core Foraminiferal Percent Abundance Data

	OFTD-14-Vibracores																																
CORE	VC1	VC1	VC1	VC1	VC1	VC1	VC1	VC1	VC1	VC1	VC1	VC1	VC1	VC1	VC1	VC1	VC1	VC1	VC2B	VC2B	VC3B	VC3B	VC3B	VC3B	VC3B	VC3B	VC3B	VC5A	VC5A	VC8A	VC8A	VC8A	VC8A
Taxon %-↓ Sample ID (mbsf) →	.38-.4	.59-.61	.76-.78	1.48-1.5	2.24-2.26	2.88-2.9	3.37-3.39	3.48-3.5	3.93-3.95	4.04-4.06	4.36-4.38	4.63-4.65	4.84-4.86	5.24-5.26	5.38-5.4	5.5-5.52	5.58-5.6	5.62-5.63	.90-.93	1.65-1.68	.54-.56	1.12-1.14	1.86-1.88	2.37-2.39	2.92-2.94	3.35-3.37	3.86-3.88	.52-.55	1.07-1.10	.52-.55	1.02-1.05	1.44-1.47	1.87-1.90
Taxon % ↓ Sample ID (mbsl) →	4.38-4.4	4.59-4.61	4.76-4.78	5.48-5.5	6.24-6.26	6.88-6.9	7.37-7.39	7.48-7.5	7.93-7.95	8.04-8.06	8.36-8.38	8.63-8.65	8.84-8.86	9.24-9.26	9.38-9.4	9.5-9.52	9.58-9.6	9.62-9.63	2.1-2.13	2.85-2.88	3.84-3.86	4.42-4.44	5.16-5.18	5.67-5.69	6.22-6.24	6.65-6.67	7.16-7.18	2.02-2.05	2.57-2.6	3.52-3.55	4.02-4.05	4.44-4.47	4.87-4.90
Ammobaculites sp.		1																															
Ammonia parkinsoniana	4	8	9	11	15	4					23	23	8					9	100		17	28	19	21	28	44	6		10	20	19	9	18
Ammonia tepida				1																	6	5	5	8	10	19			3	6	1		4
Bolivina lowmani																															2		
Buccella inusitata																															1	1	
Cassidulina subglobosa																													1				
Cibicides lobatulus																							4	2		1		6	1		2	1	3
Elphidium excavatum	96	91	91	88	85	96		100	100	100	78	77	92					91			61	48	56	63	54	29	94	78	67	65	65	73	55
Elphidium galvestonense																					14	14	1					17	1	1		2	1
Elphidium gunteri																						1	4	2	7	1			1	2	1	4	2
Elphidium mexicanum																					1	2	2			1			8	3	4	4	2
Elphidium poeyanum																					1	1	1		1	2			1				1
Elphidium sp.																														1			
Elphidium subarcticum																																	1
Globigerinoides sp.																							2	1									
Guttulina lactea																							1										
Hanzawaia strattoni																					1		3	1					5			4	4
Haynesina germanica																								1					1	2	1	1	1
Nonionella atlantica																							2	1		1					2		3
Planktonic sp.																						1		1					1		2		4
Quinqueloculina jugosa																										1							
Quinqueloculina seminula																																	2
Rosalina sp.																								1									
Trifarina angulosa																													1			1	1
Valvulineria sp.																													1	1		1	1
Total %	100	100	100	100	100	100		100	100	100	100	100	100					100	100		100	100	100	100	100	100	100	100	100	100	100	100	100
% rotaliid specimens	100	99	100	100	100	100		100	100	100	100	100	100					100	100		100	100	99	100	100	99	100	100	100	100	100	100	98
% miliolid specimens																							1			1							2
% textulariid specimens		1																															

Appendix I: Percent abundance data of foraminiferal assemblages of samples included in the cluster analysis

Percent abundance data of 45 samples (only those with ≥ 15 total specimens) and twenty-eight species (benthic species that contain more than one specimen in the entire study) included in the cluster analysis. Samples that begin with an S are OC-14 surficial samples, and samples that begin with a VC are OFTD-14 vibracore samples.

Taxon ↓ Sample ID→	S1	S2	S3	S4	S5	S6	S7	S8	S9	S11	S12	S13	S14	S16	S17	S18	S19	S21	S22
Ammonia parkinsoniana	9.27	6.33	9.68	7.76	5.88	3.74	4.31	6.67	13.16	7.34	31.86	16.82	8.62	8.93	6.45	28.68	17.80	14.52	8.82
Ammonia tepida																			
Asterigerina carinata							0.86								0.81				
Bolivina lowmani																0.78			
Buccella inusitata														0.89	0.81			0.81	
Cibicides lobatulus		1.27	2.15				3.45	6.67						0.89	0.81				
Elphidium excavatum	67.55	26.58	70.97	81.03	86.76	85.98	63.79	80.00	86.84	54.13	59.29	80.37	65.52	45.54	56.45	62.79	78.81	75.00	71.57
Elphidium galvestonense	3.31	11.39	5.38	0.86	1.47	1.87	8.62	6.67		1.83	6.19	1.87	6.03	9.82	3.23	1.55	0.85	4.03	0.98
Elphidium gunteri		2.53	1.08			2.80				25.69	0.88		0.86		7.26	2.33			
Elphidium mexicanum	4.64	48.10	5.38	6.03	4.41	1.87	4.31			8.26	0.88	0.93	3.45	6.25	5.65	3.10			13.73
Elphidium poeyanum															1.61				
Elphidium sp.	0.66		1.08	1.72							0.88			2.68				1.61	
Elphidium subarcticum	0.66		1.08				0.86						0.86						
Elphidium translucens	0.66						0.86						0.86		2.42				
Guttulina lactea	0.66																		
Hanzawaia strattoni	8.61	1.27	2.15	1.72	0.74	0.93	6.90						6.03	7.14	2.42		0.85	0.81	4.90
Haynesina germanica	0.66			0.86		0.93	2.59			1.83			0.86		1.61			0.81	
Miliolinella subrotunda													1.72						
Nonionella atlantica	1.32		1.08				2.59						0.86	3.57	0.81				
Quinqueloculina jugosa															1.61				
Quinqueloculina lamarckiana													0.86	1.79					
Quinqueloculina seminula	1.32				0.74								1.72	4.46	4.03				
Quinqueloculina sp.	0.66					0.93				0.92				1.79					
Rosalina floridana															2.42	0.78			
Rosalina sp.														1.79					
Trifarina angulosa		1.27																	
Trochammina sp.						0.93									0.81				
Valvulineria sp.																			

Core	VC1	VC1	VC1	VC1	VC1	VC1	VC1	VC1	VC1	VC1	VC1	VC1	VC1	VC3B	VC3B	VC3B	VC3B	VC3B	VC3B	VC3B	VC5A	VC5A	VC8A	VC8A	VC8A	VC8A
Taxon ↓ Sample ID (mbsf) →	.38-.4	.59-.61	.76-.78	1.48-1.5	2.24-2.26	2.88-2.9	3.48-3.5	3.93-3.95	4.04-4.06	4.36-4.38	4.63-4.65	4.84-4.86	5.62-5.63	.54-.56	1.12-1.14	1.86-1.88	2.37-2.39	2.92-2.94	3.35-3.37	3.86-3.88	.52-.55	1.07-1.10	.52-.55	1.02-1.05	1.44-1.47	1.87-1.90
Taxon ↓ Sample ID (mbsl) →	4.38-4.4	4.59-4.61	4.76-4.78	5.48-5.5	6.24-6.26	6.88-6.9	7.48-7.5	7.93-7.95	8.04-8.06	8.36-8.38	8.63-8.65	8.84-8.86	9.62-9.63	3.84-3.86	4.42-4.44	5.16-5.18	5.67-5.69	6.22-6.24	6.65-6.67	7.16-7.18	2.02-2.05	2.57-2.6	3.52-3.55	4.02-4.05	4.44-4.47	4.87-4.90
Ammonia parkinsoniana	4.07	8.11	8.87	11.02	15.04	3.57				22.50	22.69	7.76	8.87	16.81	28.46	18.70	20.63	28.24	43.88	6.03		10.08	19.53	19.38	9.35	18.32
Ammonia tepida				0.85										5.88	4.88	4.88	7.94	9.92	19.42			2.52	6.25	0.78		3.82
Asterigerina carinata																										
Bolivina lowmani																								2.33		
Buccella inusitata																								0.78	0.72	
Cibicides lobatulus																4.07	1.59		1.44		5.56	0.84		1.55	0.72	3.05
Elphidium excavatum	95.93	90.99	91.13	88.14	84.96	96.43	100.00	100.00	100.00	77.50	77.31	92.24	91.13	60.50	47.97	56.10	62.70	54.20	29.50	93.97	77.78	67.23	64.84	65.12	72.66	54.96
Elphidium galvestonense														14.29	13.82	0.81					16.67	0.84	0.78		2.16	0.76
Elphidium gunteri															0.81	4.07	2.38	6.87	0.72			0.84	1.56	0.78	3.60	1.53
Elphidium mexicanum														0.84	2.44	2.44			0.72			7.56	3.13	3.88	4.32	1.53
Elphidium poeyanum														0.84	0.81	0.81		0.76	2.16			0.84				0.76
Elphidium sp.																							0.78			
Elphidium subarcticum																										0.76
Elphidium translucens																										
Guttulina lactea																0.81										
Hanzawaia strattoni														0.84		3.25	0.79					5.04			4.32	3.82
Haynesina germanica																	0.79					0.84	2.34	0.78	0.72	0.76
Miliolinella subrotunda																										
Nonionella atlantica																2.44	0.79		1.44					2.33		3.05
Quinqueloculina jugosa																			0.72							
Quinqueloculina lamarckiana																										
Quinqueloculina seminula																										1.53
Quinqueloculina sp.																										
Rosalina floridana																										
Rosalina sp.																	0.79									
Trifarina angulosa																						0.84			0.72	0.76
Trochammina sp.																										
Valvulineria sp.																						0.84	0.78		0.72	0.76

Appendix J: Transformed percent abundance data of foraminiferal assemblages of samples included in the cluster analysis

Transformed abundance data of 45 samples (only those with ≥ 15 total specimens) and twenty-eight species (benthic species that contain more than one specimen in the entire study) included in the cluster analysis. Samples that begin with an S are OC-14 surficial samples, and samples that begin with a VC are OFTD-14 vibracore samples.

Taxon ↓ Sample ID→	S1	S2	S3	S4	S5	S6	S7	S8	S9	S11	S12	S13	S14	S16	S17	S18	S19	S21	S22
Ammonia parkinsoniana	0.62	0.51	0.63	0.56	0.49	0.39	0.42	0.52	0.74	0.55	1.20	0.85	0.60	0.61	0.51	1.13	0.87	0.78	0.60
Ammonia tepida																			
Asterigerina carinata							0.19								0.18				
Bolivina lowmani																0.18			
Buccella inusitata														0.19	0.18			0.18	
Cibicides lobatulus		0.23	0.29				0.37	0.52						0.19	0.18				
Elphidium excavatum	1.93	1.08	2.00	2.24	2.40	2.37	1.85	2.21	2.40	1.65	1.76	2.22	1.89	1.48	1.70	1.83	2.18	2.09	2.02
Elphidium galvestonense	0.37	0.69	0.47	0.19	0.24	0.27	0.60	0.52		0.27	0.50	0.27	0.50	0.64	0.36	0.25	0.18	0.40	0.20
Elphidium gunteri		0.32	0.21			0.34				1.06	0.19		0.19		0.55	0.31			
Elphidium mexicanum	0.43	1.53	0.47	0.50	0.42	0.27	0.42			0.58	0.19	0.19	0.37	0.51	0.48	0.35			0.76
Elphidium poeyanum															0.25				
Elphidium sp.	0.16		0.21	0.26							0.19			0.33				0.25	
Elphidium subarcticum	0.16		0.21				0.19						0.19						
Elphidium translucens	0.16						0.19						0.19		0.31				
Guttulina lactea	0.16																		
Hanzawaia strattoni	0.60	0.23	0.29	0.26	0.17	0.19	0.53						0.50	0.54	0.31		0.18	0.18	0.45
Haynesina germanica	0.16			0.19		0.19	0.32			0.27			0.19		0.25			0.18	
Miliolinella subrotunda													0.26						
Nonionella atlantica	0.23		0.21				0.32						0.19	0.38	0.18				
Quinqueloculina jugosa															0.25				
Quinqueloculina lamarckiana													0.19	0.27					
Quinqueloculina seminula	0.23				0.17								0.26	0.43	0.40				
Quinqueloculina sp.	0.16					0.19				0.19				0.27					
Rosalina floridana															0.31	0.18			
Rosalina sp.														0.27					
Trifarina angulosa		0.23																	
Trochammina sp.						0.19									0.18				
Valvulineria sp.																			

Core	VC1	VC1	VC1	VC1	VC1	VC1	VC1	VC1	VC1	VC1	VC1	VC1	VC1	VC1	VC3B	VC3B	VC3B	VC3B	VC3B	VC3B	VC3B	VC5A	VC5A	VC8A	VC8A	VC8A	VC8A
Taxon -↓ Sample ID (mbsf) →	.38-.4	.59-.61	.76-.78	1.48-1.5	2.24-2.26	2.88-2.9	3.48-3.5	3.93-3.95	4.04-4.06	4.36-4.38	4.63-4.65	4.84-4.86	5.62-5.63	.54-.56	1.12-1.14	1.86-1.88	2.37-2.39	2.92-2.94	3.35-3.37	3.86-3.88	.52-.55	1.07-1.10	.52-.55	1.02-1.05	1.44-1.47	1.87-1.90
Taxon ↓ Sample ID (mbsl) →	4.38-4.4	4.59-4.61	4.76-4.78	5.48-5.5	6.24-6.26	6.88-6.9	7.48-7.5	7.93-7.95	8.04-8.06	8.36-8.38	8.63-8.65	8.84-8.86	9.62-9.63	3.84-3.86	4.42-4.44	5.16-5.18	5.67-5.69	6.22-6.24	6.65-6.67	7.16-7.18	2.02-2.05	2.57-2.6	3.52-3.55	4.02-4.05	4.44-4.47	4.87-4.90
Ammonia parkinsoniana	0.41	0.58	0.60	0.68	0.80	0.38				0.99	0.99	0.56	0.60	0.84	1.13	0.89	0.94	1.12	1.45	0.50		0.65	0.92	0.91	0.62	0.88
Ammonia tepida				0.18										0.49	0.45	0.45	0.57	0.64	0.91			0.32	0.51	0.18		0.39
Asterigerina carinata																										
Bolivina lowmani																								0.31		
Buccella inusitata																								0.18	0.17	
Cibicides lobatulus																0.41	0.25		0.24		0.48	0.18		0.25	0.17	0.35
Elphidium excavatum	2.74	2.53	2.54	2.44	2.34	2.76	3.14	3.14	3.14	2.15	2.15	2.58	2.54	1.78	1.53	1.69	1.83	1.65	1.15	2.65	2.16	1.92	1.87	1.88	2.04	1.67
Elphidium galvestonense														0.78	0.76	0.18					0.84	0.18	0.18		0.29	0.17
Elphidium gunteri															0.18	0.41	0.31	0.53	0.17			0.18	0.25	0.18	0.38	0.25
Elphidium mexicanum														0.18	0.31	0.31			0.17			0.56	0.36	0.40	0.42	0.25
Elphidium poeyanum														0.18	0.18	0.18		0.17	0.29			0.18				0.17
Elphidium sp.																							0.18			
Elphidium subarcticum																										0.17
Elphidium translucens																										
Guttulina lactea																0.18										
Hanzawaia strattoni														0.18		0.36	0.18					0.45			0.42	0.39
Haynesina germanica																	0.18					0.18	0.31	0.18	0.17	0.17
Miliolinella subrotunda																										
Nonionella atlantica																0.31	0.18		0.24					0.31		0.35
Quinqueloculina jugosa																			0.17							
Quinqueloculina lamarckiana																										
Quinqueloculina seminula																										0.25
Quinqueloculina sp.																										
Rosalina floridana																										
Rosalina sp.																	0.18									
Trifarina angulosa																						0.18			0.17	0.17
Trochammina sp.																										
Valvulineria sp.																						0.18	0.18		0.17	0.17